

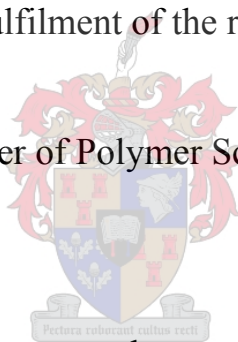
# Synthesis and Characterization of Graft and Block Copolymers using Hydroboration

by

Abd-Almonam Baleg

Thesis presented in partial fulfilment of the requirements for the degree of

Master of Polymer Science



at the

University of Stellenbosch

Study Leader:

Dr P.E. Mallon

Co-study Leader:

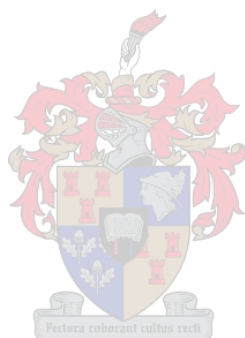
Dr A.J.P. van Zyl

Stellenbosch

December 2006

## Declaration

I, the undersigned, hereby declare that the work contained in this thesis is my own original work and that I have not previously in its entirety or in part submitted it at any university for a degree.

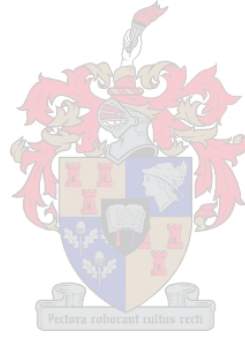


Signature

Date

إهداء

إهداء إلى من زرع فيّ تلمس العلم وحب البحث..... إلى روح والدي الطاهرة



## Abstract

Graft and block copolymers were synthesized using multifunctional and monofunctional macroinitiators to produce the copolymers. The process involved hydroboration of commercially available unsaturated rubbers and chain-end unsaturated macromonomers with 9-borabicyclo [3.3.1] nonane (9-BBN). The resulting secondary alkyl 9-BBN moieties in the starting materials were subsequently exposed to oxygen in the presence of free radical polymerizable monomers to facilitate the formation of graft and block copolymers.

This research was initiated by first studying the hydroboration of a model compound, 2-hexene, in order to determine the optimal conditions for the graft reactions. The model compound was subsequently used as a macroinitiator to initiate the polymerization of methylmethacrylate (MMA). The same borane chemistry was extended to the synthesis of polystyrene (PS) block copolymers. Chain-end unsaturated PS macromonomers, synthesized by anionic polymerization, were effectively hydroborated and then polymerized to produce PS-b-PMMA block copolymers.

The synthesis of polyolefin graft copolymers was subsequently achieved by hydroboration. Several commercial rubbers with different levels of unsaturated segments were efficiently grafted with vinyl monomers MMA and styrene (St) following the “graft from” approach. The grafted reactions were carried out under various reaction conditions to determine the effect of the following factors: concentration of oxygen, amount of borane and monomer concentration. By controlling these factors, different graft densities were achieved with high graft efficiencies. All reactions produced mixed products including unreacted (non-functional) macroinitiator, homopolymer, graft copolymer and in case of the highly unsaturated polymer a crosslinked gel.

Finally, the chemical compositions as well as the molar mass distribution of the graft copolymers were fully characterized by different chromatographic techniques. <sup>1</sup>H-NMR and FTIR were also used to confirm the structure of these copolymers. Gradient HPLC was developed and extensively used to characterize the graft copolymers.

## Opsomming

Ent- en blok-kopolimere is gesintetiseer deur gebruik te maak van multifunksionele en monofunksionele makroafsetters. Die proses behels die hidroboring van kommersiële onversadigde elastomere en makromonome met onversadigde endgroepe met 9-borabisikliese [3.3.1] nonaan (9-BBN). Die sekondere alkiel 9-BBN groeperings, in die reaksieprodukte wat verkry is, is dan blootgestel aan suurstof in die teenwoordigheid van 'n monomeer, wat deur 'n vrye radikaal meganisme polimerisaarbaar is, om ent- en blok-kopolimere te vorm.

Eerstens is die hidroboring van die 2-hekseen as modelverbinding bestudeer, om sodoende die optimale toestande vir die uiteindelijke reaksie te bepaal. Daarna is die modelverbinding gebruik as makroafsetter vir die polimerisasie van metiel metakrilaat (MMA). Soortgelyke boraanchemie is gebruik vir die sintese van polistireen (PS) blok-kopolimere. PS makromonome met onversadigde endgroepe, berei d.m.v. anioniesepolimerisasie, is daarna suksesvol gehidroboreer, en gepolimeriseer om PS-b-PMMA blok-kopolimere te berei.

Die sintese van poli(olefien) ent-kopolimere is ook bereik deur hidroboring. Verskeie kommersiële elastomere met verskillende vlakke van onversadiging is effektief geënt met viniel monomere, MMA en stireen (St), deur gebruik te maak van die “ent-vanaf” tegniek. Die reaksies is uitgevoer onder 'n verskeidenheid verskillende reaksietoestande om die uitwerking van die volgende faktore te bepaal: suurstof konsentrasie, die hoeveelheid van die boraanverbinding, en monomeer konsentrasie. Deur hierdie faktore te beheer is fraksies van verskillende ent-digthede behaal, met hoë ent-effektiwiteite. Alle reaksies het 'n mengsel van produkte opgelewer, insluitend (nie-funksionele) makroafsetters, homopolimeer, ent-kopolimere, asook kruisgebinde gels (in die geval van hoogs-onversadigde polimere).

Die chemiese samestelling, asook die verspreiding van molekulêre massa van die kopolimere, is ten volle gekarakteriseer m.b.v. verskeie chromatografiese tegnieke. <sup>1</sup>H-NMR en FTIR spektroskopie is ook gebruik om die struktuur van die kopolimere vas te stel. 'n Gradient-HPLC tegniek is ontwikkel en suksesvol gebruik om die kopolimere te karakteriseer.

## Acknowledgements

Firstly, I would like to thank and acknowledge the institution that has made this project possible; The Libyan International Centre for Macromolecules Chemistry and Technology, without whose generous sponsorship this would not have been possible.

*I would like to take this opportunity to thank the following people for their contributions to this project:*

Dr P.E. Mallon, my promoter, for his knowledge, input, motivation and encouragement during this study.

My co-promoter, Dr A.J.P. van Zyl, for his fruitful advice, encouragement and guidance during this study.

Dr M.J.Hurdall for her assistance with the grammatical corrections of my thesis.

I would like to thank all my friends and colleagues for sharing their talents and expertise with me.

On a more personal note, I would like to thank my parents and my family for giving me the opportunity to further my studies and helping me to achieve my goals.

My South African host family, Anthonissen family Carel and Christine, thank you so much for the enjoyable time that we spent together and for helping me with English.

Finally and most importantly, I thank my wife, Amani, with all my heart, for her love, support and patience. She will always be my inspiration and encouragement.

## Table of contents

<b>Chapter 1</b> .....	<b>1</b>
<b>Introduction and objectives</b> .....	<b>1</b>
1.1 Introduction .....	1
1.2 Objectives .....	2
1.3 Layout of the thesis .....	3
1.4 References .....	4
<b>Chapter 2</b> .....	<b>5</b>
<b>Historical and theoretical background</b> .....	<b>5</b>
<b>2.1 Boranes in organic chemistry</b> .....	<b>5</b>
2.1.1 Introduction.....	5
2.1.2 Boranes – a first glance.....	5
2.1.3 Historical overview of hydroboration.....	5
2.1.4 Borane reagents for organic synthesis .....	8
2.1.4.1 Borane-tetrahydrofuran complex (BTHF) .....	11
2.1.4.2 Dimethylsulfide borane (DMSB) .....	12
2.1.4.3 Diethylaniline borane (DEANB).....	13
2.1.4.4 <i>tert</i> -Butylamine borane (TBAB) .....	13
2.1.4.5 Morpholine borane (MPB).....	14
2.1.4.6 Dimethylamine borane (DMAB) .....	14
2.1.4.7 Triethylamine borane (TEAB) .....	15
2.1.4.8 Pyridine borane (PYB).....	15
2.1.4.9 9-Borabicyclo [3.3.1] nonane (9-BBN).....	15
2.1.4.10 Borane-methyl sulfide (BMS).....	16
2.1.4.11 Borane-1,4-thioxane.....	16
2.1.4.12 Bis (2-methoxyethyl)sulfide.....	16
<b>2.2 The theory of hydroboration</b> .....	<b>17</b>
2.2.1 Introduction.....	17
2.2.2 Hydroboration.....	17
2.2.2.1 Oxidation.....	18
2.2.3 Hydroboration of alkenes .....	18
2.2.4 Mechanism of hydroboration.....	18
2.2.5 Initiation .....	19
2.2.6 Isomerization of organoboranes.....	20
2.2.7 Reactions of organoboranes.....	21
2.2.7.1 Reaction with alkaline hydrogen peroxide.....	21
2.2.7.2 Reaction with oxygen.....	22

2.2.8 9-Borabicyclo [3.3.1] nonane (9-BBN) .....	23
2.2.8.1 Stability of 9-BBN .....	24
2.2.8.2 Reactions of 9-BBN with hydroxyl compounds .....	25
2.2.8.3 Effect of structure on olefin hydroboration by 9-BBN .....	25
2.2.9 Hydroboration of hindered olefins.....	30
2.2.10 Reduction.....	31
2.2.10.1 Reduction with alkylboranes.....	31
2.3 Theory and overview of the polymerization processes and polymer architectures used in this study .....	32
2.3.1 Graft copolymers .....	32
2.3.2 Block copolymers .....	32
2.3.3 Anionic polymerization .....	33
2.3.4 Butyl rubber (polyisobutylene-co-isoprene) (PIB-co-PIP).....	33
2.3.5 Polyisoprene (PIP) .....	34
2.3.6 Ethylene propylene rubbers (EPDM) .....	34
2.4 References .....	36
<b>Chapter 3 .....</b>	<b>39</b>
<b>Synthesis of graft and block copolymers .....</b>	<b>39</b>
3.1 Introduction .....	39
3.2 Materials.....	40
3.2.1 Purifications of solvents .....	40
3.2.2 Purification of monomers .....	41
3.3 Experimental conditions.....	41
3.4 Experimental reaction procedures .....	41
3.4.1 Synthesis of (2-hexenyl-9-BBN) .....	41
3.4.2 Synthesis of poly(methyl methacrylate-2-hexyl).....	41
3.4.3 Synthesis of vinyl-terminated polystyrene macromonomers .....	42
3.4.4 Synthesis of PS-b-PMMA .....	43
3.4.5 Hydroboration reaction of butyl rubber with 9-BBN .....	44
3.4.6 Synthesis of methylmethacrylate grafted butyl rubber.....	45
3.4.7 Hydroboration reaction of polyisoprene.....	46
3.4.8 Synthesis of graft copolymer of polyisoprene rubber with methylmethacrylate ((PIP-co-PIP)-g-PMMA) .....	46
3.4.9 Hydroboration reaction of EPDM rubber with 9-BBN .....	47
3.4.10 Synthesis of graft copolymer of ethylene propylene rubber with methylmethacrylate EPDM-g-PMMA.....	47
3.4.11 Synthesis of graft copolymer of ethylene propylene rubber with polystyrene EPDM-g-PS .....	48
3.5 Soxhlet extraction of insoluble polymer fractions .....	48
3.6 Crosslink density .....	49



3.7 Characterization.....	50
3.7.1 Nuclear magnetic resonance (NMR) spectroscopy .....	50
3.7.2 High-performance liquid chromatography (HPLC) .....	50
3.7.2.1 Mobile phase .....	51
3.7.3 Size-exclusion chromatography (SEC).....	53
3.7.4 Fourier-transform infrared (FTIR) spectroscopy .....	53
3.8 References .....	54
<b>Chapter 4 .....</b>	<b>55</b>
<b>Results and discussion .....</b>	<b>55</b>
4.1 Introduction .....	55
4.2 Copolymerization of methyl methacrylate with 2-hexenyl-9-BBN in a continuous reaction .....	55
4.2.1 2-Hexenyl-9-BBN.....	55
4.2.2 Characterization of polymethylmethacrylate made via 2-hexenyl-9- BBN macroinitiator .....	56
4.3 Block copolymer of polystyrene with methyl methacrylate (PS-b-PMMA) .58	
4.3.1 Synthesis and characterization of polystyrene macromonomer .....	58
4.3.2 Characterization of PS-b-PMMA by proton nuclear magnetic resonance spectroscopy ( <sup>1</sup> H-NMR).....	59
4.3.3 Characterization of block copolymer PS-b-PMMA by Fourier- transform infrared spectroscopy (FTIR).....	62
4.3.4 Characterization of PS-b-PMMA block copolymers by size-exclusion chromatography (SEC).....	65
4.3.5 Characterization of block copolymers with high-performance liquid chromatography (HPLC) at the critical point of both polystyrene and methyl methacrylate.....	67
4.4 Methylmethacrylate grafted poly(isobutylene-co-isoprene) .....	70
4.4.1 Preparation.....	70
4.4.2 Characterization of (PIB-co-PIP)-g-PMMA graft copolymers by proton nuclear magnetic resonance spectroscopy ( <sup>1</sup> H-NMR).....	70
4.4.3 Characterization of (PIB-co-PIP)-g-PMMA graft copolymers by Fourier-transform infrared spectroscopy (FTIR).....	73
4.4.4 Characterization of (PIB-co-PIP)-g-PMMA graft copolymers by size- exclusion chromatography (SEC).....	75
4.4.5 Characterization of (PIB-co-PIP)-g-PMMA graft copolymers by high- performance liquid chromatography (HPLC).....	77
4.5 Graft copolymer of polyisoprene rubber with methylmethacrylate .....	80
4.5.1 Preparation.....	80
4.5.2 Characterization of PIP-g-PMMA graft copolymers by proton nuclear magnetic resonance spectroscopy ( <sup>1</sup> H-NMR) .....	80
4.5.3 Characterization of PIP-g-PMMA graft copolymers by Fourier- transform infrared spectroscopy (FTIR).....	83

4.5.4 Characterization of PIP-g-PMMA graft copolymers by size-exclusion chromatography (SEC) .....	85
4.5.5 Characterization of PIP-g-PMMA graft copolymers with high-performance liquid chromatography (HPLC).....	87
4.6 EPDM rubber grafted with methylmethacrylate and styrene .....	88
4.6.1 Characterization of EPDM-g-PMMA and EPDM-g-PS graft copolymers by proton nuclear magnetic resonance spectroscopy ..	89
4.6.1.1 EPDM-g-PMMA .....	89
4.6.1.2 EPDM-g-PS .....	91
4.6.2 Characterization of EPDM-g-PMMA and EPDM-g-PS graft copolymers by Fourier-transform infrared spectroscopy (FTIR) ..	93
4.6.2.1 EPDM-g-PMMA .....	93
4.6.2.2 EPDM-g-PS.....	95
4.6.3 Characterization of EPDM-g-PMMA and EPDM-g-PS graft copolymers by size-exclusion chromatography (SEC).....	97
4.6.3.1 EPDM-g-PMMA .....	98
4.6.3.2 EPDM-g-PS.....	99
4.6.4 Characterization of EPDM-g-PMMA and EPDM-g-PS graft copolymers by high-performance liquid chromatography .....	99
4.6.4.1 Separation of EPDM-g-PMMA graft copolymer with HPLC	100
4.6.4.2 Separation of EPDM-g-PS graft copolymer with HPLC .....	102
4.7 References .....	104
<b>Chapter 5 .....</b>	<b>105</b>
<b>Conclusions and recommendations .....</b>	<b>105</b>
5.1 Conclusions .....	105
5.2 Recommendations .....	107

## List of Figures

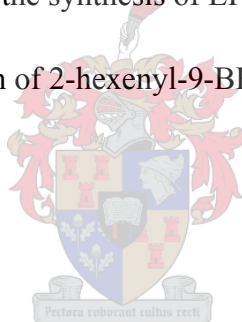
Figure 3.1: Conventional Soxhlet extraction apparatus.....	49
Figure 3.2: Gradient profile for the HPLC separation of the graft products; stationary phase: Nucleosil CN 100 Å, eluent: THF/(i-octane or cyclohexane). .....	52
Figure 4.1: <sup>1</sup> H-NMR spectra of 2-hexene (a) before hydroboration, (b) after hydroboration, and (c) PMMA-2-hexenyl, in CDCl <sub>3</sub> solvent.....	57
Figure 4.2: <sup>1</sup> H-NMR spectrum of styrene macromonomer terminated by allylchlorodimethylsilane, in CDCl <sub>3</sub> solvent.....	59
Figure 4.3: <sup>1</sup> H-NMR spectra of PS macromonomer (a) before hydroboration, (b) after hydroboration, and (c) PS-b-PMMA, in CDCl <sub>3</sub> solvent.....	61
Figure 4.4: FTIR spectra of (a) PMMA, (b) extracted PS-b-PMMA copolymer (run #2) and (c) vinyl-terminated PS (peak assignments given in Table 4.2)....	63
Figure 4.5: (a) Comparison of the normalized RI & UV signals of the product before extraction and (b) comparison of the normalized RI & UV signals of product after extraction. ....	66
Figure 4.6: Chromatogram showing the critical point of adsorption of polystyrene standards. Mobile phase composition: ACN-THF (50.2-49.8), flow rate 0.5 ml/min, and the highest molar mass polystyrene 100000 g/mol. ....	67
Figure 4.7: Typical example of a chromatogram of PS-b-PMMA at the critical point of polystyrene (Stationary phase Nucleosil C18 and symmetry C18, mobile phase 49.8:50.2% by volume CAN:THF, flow 0.5 ml/min, samples dissolved in 50:50% by volume CAN:THF). ....	68
Figure 4.8: Elution curves of PS-b-PMMA and a PMMA standard at the critical point of polymethylmethacrylate. (Stationary phase column system of silica gel Si-300 and Si-100, mobile phase 70:30% by volume MEK-Cyclohexane, flow 0.5 ml/min, samples were dissolved in 70:30% by volume MEK-Cyclohexane). ....	69
Figure 4.9: <sup>1</sup> H-NMR spectra of PIB-co-PIP, #2 in Table 4.4, (a) before hydroboration, (b) after hydroboration, and (c) (PIB-co-PIP)-g-PMMA copolymer, in CDCl <sub>3</sub> solvent. ....	71
Figure 4.10: FTIR spectra of (a) PMMA, (b) (PIB-co-PIP)-g-PMMA run #2 in Table 4.4, and (c) PIB-co-PIP starting material (peak assignments are given in Table 4.5). ....	74
Figure 4.11: Comparison of the normalized RI & UV signals of (a) PIB-co-PIP homopolymer and (b) PMMA with the normalized RI and UV signals of (c) (PIB-co-PIP)-g-PMMA copolymer. ....	76
Figure 4.12: Gradient HPLC chromatograms of (a) PIB-co-PIP starting material, (b) PMMA standard and (c) graft product (PIB-co-PIP)-g-PMMA. (Stationary phase: Nucleosil CN 100Å; eluent: THF/Cyclohexane; detectors: ELSD and UV at 235 nm). The gradient was started at 1:99 (v/v) (THF:Cyclohexane), held constant for 2 mins, changed linearly to 34:66 (THF:Cyclohexane) within 8 mins, held constant for 10 min, and changed linearly to 100:0 (THF:Cyclohexane) within 3 min, held constant for 5 min. The flow rate was 0.5 ml/min. ....	79

Figure 4.13: <sup>1</sup> H-NMR spectra of PIP (a) before hydroboration, (b) after hydroboration, and (c) PIP-g-PMMA copolymer, in CDCl <sub>3</sub> solvent.....	81
Figure 4.14: FTIR spectra of (a) PMMA, (b) PIP-g-PMMA and (c) PIP. (Peak assignments given in Table 4.8).....	84
Figure 4.15: Comparison of the normalized RI signal of PIP with the normalized RI and UV signals of the PIP-g-PMMA copolymer.....	86
Figure 4.16: Gradient HPLC chromatogram of the PIP-g-PMMA graft product. (Stationary phase: Nucleosil CN 100Å, eluent: THF/i-octane; detectors: ELSD and UV at 239 nm. The gradient was started at 99:1 (v/v) (THF:i-octane), held constant for 1 min, changed linearly to 34:66 (THF:i-octane), within 2 mins, held constant for 10 mins, and changed linearly to 100:0 (THF:i-octane), within 2 mins. ELSD and UV detectors were used).....	88
Figure 4.17: <sup>1</sup> H-NMR spectra of EPDM (a) before hydroboration, (b) after hydroboration, and (c) EPDM-g-PMMA copolymer, in CDCl <sub>3</sub> solvent. ...	91
Figure 4.18: <sup>1</sup> H-NMR spectra of EPDM (a) before hydroboration, (b) after hydroboration, and (c) EPDM-g-PS copolymer, in CDCl <sub>3</sub> solvent.....	92
Figure 4.19: FTIR spectra of (a) PMMA, (b) EPDM-g-PMMA and (c) EPDM (peaks explained in Table 4.11). ....	94
Figure 4.20: FTIR spectra of (a) PMMA, (b) EPDM-g-PMMA after extraction, and (c) EPDM starting material (peak assignments given in Table 4.12). ....	97
Figure 4.21: Comparison of the normalized RI signal of EPDM with the normalized RI and UV signals of the EPDM-g-PMMA copolymer.....	98
Figure 4.22: Comparison of the normalized RI signal of EPDM with the normalized RI and UV signals of the EPDM-g-PS copolymers after extraction. ....	99
Figure 4.23: Gradient HPLC chromatogram of the graft product and starting materials. (Stationary phase: Nucleosil CN 100Å; eluent: THF/i-octane; detector: ELSD). ....	100
Figure 4.24: Gradient HPLC chromatogram of the extracted graft product. (Stationary phase: Nucleosil CN 100Å; eluent: THF/i-octane; detector: ELSD).....	101
Figure 4.25: EPDM starting materials analyzed by gradient HPLC. (Stationary phase: Nucleosil CN 100Å; eluent: THF/i-octane; detector: ELSD).....	101
Figure 4.26: PMMA standards analyzed by gradient HPLC. (Stationary phase: Nucleosil CN 100Å; eluent: THF/i-octane; detector: ELSD).....	102
Figure 4.27: Gradient HPLC chromatogram of the EPDM-g-PS graft product. (Stationary phase: Nucleosil C <sub>18</sub> 300+500 Å; eluent: THF/i-octane; detectors: ELSD The gradient was started at 99:1 (v/v) (THF:i-octane), held constant for 1 min, changed linearly to 34:66 (THF:i-octane) within 5 mins, held constant for 10 mins, and changed linearly to 100:0 (THF:i-octane) within 2 mins). ....	103
Figure 4.28: Gradient HPLC chromatogram of the extracted EPDM-g-PS graft product. (Stationary phase: Nucleosil C <sub>18</sub> 300+500 Å; eluent: THF/i-octane; detector: ELSD).....	103

## List of Schemes

Scheme 2.1 Preparation of organoboranes by the reaction of dialkylzincs with trialkoxyboranes.....	5
Scheme 2.2 Formation of sodium tetrahydroborate and diborane.....	6
Scheme 2.3 Reaction of ethylene with diborane.....	6
Scheme 2.4 Addition of boranes to alkenes to yield organoboranes.....	6
Scheme 2.5 Hydroboration and oxidation of an alkene with BTHF.....	12
Scheme 2.6 Reduction of an amide using BTHF.....	12
Scheme 2.7 Hydroboration and oxidation by DMSB.....	12
Scheme 2.8 Ketone reduction using chiral oxazaborolidine catalysts.....	13
Scheme 2.9 Ketone reduction with DEANB.....	13
Scheme 2.10 Formation of a benzazepine.....	14
Scheme 2.11 Epoxide ring-opening using MPB with BF <sub>3</sub> .....	14
Scheme 2.12 Reaction of allyloxycarbonyl group for the protection of amines.....	14
Scheme 2.13 Reductive amination with TEAB.....	15
Scheme 2.14 Reductions of oximes with PYB.....	15
Scheme 2.15 Formation of erythro-β-hydroxy sulfones.....	15
Scheme 2.16 The hydroboration reaction.....	17
Scheme 2.17 General hydroxylation reactions of organoboranes.....	18
Scheme 2.18 Mechanism of hydroxylation showing formation of a four-centered transition state.....	19
Scheme 2.19 Mechanism of autoxidation of boranes.....	20
Scheme 2.20 Reaction scheme for the isomerization of organoboranes.....	20
Scheme 2.21 Oxidation via hydroboration.....	21
Scheme 2.22 Oxidation reactions of hydroborated compounds with H <sub>2</sub> O <sub>2</sub> and NaOH.....	21
Scheme 2.23 Reaction of organoboranes with oxygen.....	22
Scheme 2.24 Formation of alkyl hydroperoxides.....	22
Scheme 2.25 Hydroboration of alkenes to form alcohols.....	22
Scheme 2.26 Reaction scheme for the organoboration with oxygen.....	22
Scheme 2.27 Treatment of oxidation intermediate with hydrogen peroxide.....	23
Scheme 2.28 Formation of 9-BBN.....	23
Scheme 2.29 Hydroboration of cyclic olefins with 9-BBN.....	23
Scheme 2.30 Hydroboration of terminal olefins with 9-BBN.....	24
Scheme 2.31 Hydroboration of cis-4-methyl-2-pentene.....	24
Scheme 2.32 Hydroboration of 1-alkenes with 9-BBN or Sia <sub>2</sub> BH.....	26
Scheme 2.33 Hydroboration of 3,3-dimethyl-1-butene with 9-BBN or Sia <sub>2</sub> BH.....	26
Scheme 2.34 Hydroboration of cis-2-pentene.....	27
Scheme 2.35 Hydroboration of branched internal olefin.....	27
Scheme 2.36 Hydroboration with 9-BBN.....	27
Scheme 2.37 Hydroboration of 2,5-dimethyl-3-hexene.....	28

Scheme 2.38 Reaction rates for cis and trans alkenes for both 9-BBN and Sia <sub>2</sub> BH. ...	28
Scheme 2.39 Reaction rates for cis and trans alkene isomers containing highly branched alkyl groups. ....	29
Scheme 2.40 Hydroboration of cyclic olefins with 9-BBN or Sia <sub>2</sub> BH. ....	29
Scheme 2.41 Hydroboration of cyclohexene with 9-BBN or Sia <sub>2</sub> BH. ....	30
Scheme 2.42 Formation of dicyclohexylborane. ....	31
Scheme 2.43 Reduction with alkylboranes. ....	31
Scheme 2.44 Structure representation of graft copolymers. ....	32
Scheme 2.45 Structure of polyisobutylene-co-isoprene. ....	33
Scheme 2.46 Structure of polyisoprene. ....	34
Scheme 2.47 Structure of EPDM. ....	35
Scheme 3.1 Reaction scheme for the synthesis of 2-hexenyl-PMMA. ....	42
Scheme 3.2 Synthesis of allylchloro-dimethylsilane-polystyrene macromonomers via anionic polymerization. ....	43
Scheme 3.3 Reaction scheme of the synthesis of PS-b-PMMA. ....	44
Scheme 3.4 Reaction scheme for the polymerization of butyl rubber. ....	45
Scheme 3.5 Reaction scheme of the synthesis of polyisoprene-g-PMMA. ....	47
Scheme 3.6 Reaction scheme for the synthesis of EPDM-g-PMMA/PS. ....	48
Scheme 4.1: Reaction mechanism of 2-hexenyl-9-BBN. ....	56



## List of Tables

Table 2.1: Examples of boron reagents for organic synthesis .....	9
Table 3.1: Anionic polymerisation reaction compositions for the synthesis of PS macromonomer using n-butyllithium as initiator and allylchloro-dimethylsilane as termination agent.....	43
Table 4.1: Reaction conditions used in the synthesis of the PS-b-PMMA block copolymer, using hydroborated polystyrene macromonomer .....	62
Table 4.2: Characteristic infrared peaks in spectra of PS, extracted PS-b-PMMA, and PMMA homopolymer.....	64
Table 4.3: Molar mass and polydispersity of the components of PS-b-PMMA block copolymers, as determined by SEC chromatography .....	66
Table 4.4: Different reaction conditions used during the ‘graft-from’ approach to prepare (PIB-co-PIP)-g-PMMA, using hydroborated poly(isobutylene-co-isoprene).....	72
Table 4.5: Characteristic infrared peaks of PIB-co-PIP, (PIB-co-PIP)-g-PMMA and PMMA .....	73
Table 4.6: Molar mass and polydispersities of the components of (PIB-co-PIP)-g-PMMA graft copolymers, as determined by SEC chromatography .....	77
Table 4.7: Different reaction conditions used during the ‘graft-from’ approach to prepare PIP-g-PMMA, using hydroborated polyisoprene .....	82
Table 4.8: Characteristic infrared peaks of PIP, PIP-g-PMMA and PMMA.....	85
Table 4.9: Different reaction conditions used during the ‘graft-from’ approach to prepare EPDM-g-PMMA.....	90
Table 4.10: Different reaction conditions used during the ‘graft-from’ approach to prepare EPDM-g-PS, using hydroborated EPDM .....	93
Table 4.11: Characteristic infrared peaks of EPDM, EPDM-g-PMMA and PMMA homopolymer .....	95
Table 4.12: Characteristic infrared peaks of EPDM, EPDM-g-PMMA and PMMA homopolymer .....	96



## List of abbreviations and symbols

ACN	Acetonitrile
B	Boron
B <sub>2</sub> H <sub>6</sub>	Diborane dimer
9-BBN	9-Borabicyclo[3,3.1]nonane
B-H	Boron-hydrogen
BMS	Borane-methyl sulphide
BOC	Butyloxycarbonyl protecting group
BTHF	Borane-tetrahydrofuran complex
BuLi	Butyllithium
CBZ	Carbobenzoxy group
CCD	Chemical composition distribution
CDCl <sub>3</sub>	Chloroform-d
CN	Cyanopropyl sorbent
Cs <sub>2</sub> B <sub>12</sub> H <sub>12</sub>	Cesium dodecahydrododecaborate methanolate
DBBT	Dibutylboron triflate
DCBCL	Dicyclohexylchloroborane
DEANB	Diethylaniline borane
Diglyme	diethylene glycol dimethyl ether
DIMB	Diisopropoxymethylborane
DMAB	Dimethylamine borane
DMA <sub>4</sub> B <sub>2</sub>	Tetrakis(dimethylamino) diboron
DMSB	Dimethylsulphide borane
ELSD	Evaporative light scattering detector
EMA	Ethyl methacrylate
EPDM	Ethylene propylene-5-ethylidene-2-norbornene rubbers
EPM	Ethylene propylene rubber
FTIR	Fourier-transform infrared spectroscopy
<sup>1</sup> H-NMR	Proton nuclear magnetic resonance spectroscopy
HPLC	High performance liquid chromatography
IP	Polyisoprene
K <sub>2</sub> B <sub>12</sub> H <sub>12</sub>	Potassium dodecahydrododecaborate methanolate
KBr	Potassium bromide
Mc	Average molecular mass between crosslinks
MDEB	Methoxydiethylborane
MeCBS	Methyl oxazaborolidine
MeSO <sub>3</sub> H	Methyl sulfonic acid



MEK	Methyl ethyl ketone
MMA	Methyl methacrylate monomers
MPB	Morpholine borane
Mr	Mass (g) of rubber after deswelling
ms	Solvent mass (g) at equilibrium swelling
N <sub>2</sub>	Nitrogen
Ni	Nickel
NMR	Nuclear magnetic resonance spectroscopy
O <sub>2</sub>	Oxygen
[O]	Oxidation
PIB-co-PI	Poly(isobutylene-co-isoprene)
PINB	Pinacolborane
PIN <sub>2</sub> B <sub>2</sub>	Bis(pinacolato)diboron
PS	Polystyrene
PYB	Pyridine borane
RI	Refractive index
SBR	Styrene butadiene rubber
SEC	Size-exclusion chromatography
sia <sub>2</sub> BH	Disiamylborane
SLM	Standard litres per minute
St	Styrene
TBAB	Tert-butylamine borane
t-BMA	t-butyl methacrylate
TEAB	Triethylamine borane
TEB	Triethylborane
TEB-DAP	Triethylborane-1,3-diaminopropane complex
THF	Tetrahydrofuran
TiCl <sub>4</sub>	Titanium tetrachloride
TMAB	Trimethylamine borane
TME	Tetramethylethylene
TNBB	Tri-n-butylborane
UV	Ultraviolet
V <sub>e</sub>	Number of network chains per unit volume
V <sub>m,s</sub>	Molar volume of the solvent
V <sub>r</sub>	Volume fraction of rubber network in the swollen gel
ρ <sub>s</sub>	Density of solvent

# Chapter 1

## Introduction and objectives

### 1.1 Introduction

Polyolefins are important materials because of their excellent combination of cost and performance. They, however, lack polar groups and exhibit poor properties of adhesion, dye-ability, printability and compatibility, which significantly limit their applications. The modified polyolefins are the most studied and used functional polyolefins in industry, for improving the adhesion and compatibility of polyolefins. Properties and applications of polymers can be extended by copolymerization with other polymers to give new materials with tailored properties and performance.

Copolymers have a good combination of cost and performance, good physical and mechanical properties, good chemical stability, high electrical resistance, and excellent processability. In this study the “grafting from” method of copolymerization is used to modify polyolefins by using the hydroboration method.

The first hydroboration reaction was reported by Brown and Subba in 1956 when they used a simple and rapid method for the addition of boranes to alkenes.<sup>1</sup>

Hydroboration has become a highly valuable tool and has extensive applications in organic synthesis. The intermediate borane moiety can be used to introduce free radicals, which can facilitate polymerization (homopolymerization or copolymerization) under favourable conditions. The potential of boron chemistry was reported by emphasizing the extreme importance of boron functional polymers and the versatility with which graft and block copolymers can be synthesized.<sup>2</sup>

The borinate radical generated in situ during oxidation is believed to form a weak and reversible bond with the growing chain-end during the polymerization. Such a process minimizes the undesirable chain transfer and termination reaction, resulting in an observation of an increase in the molecular mass of the produced polymers as a function of monomer conversion. This radical polymerization route has also been

applied to the preparation of graft and block copolymers with the use of borane-containing polymers.

Characterization techniques such as Size-exclusion chromatography (SEC), Fourier-transform infrared spectroscopy (FTIR) and Nuclear magnetic resonance spectroscopy (NMR) have been used to analyze the graft products produced via hydroboration reactions.<sup>3-7</sup>

In this study specialized techniques such as gradient HPLC were developed and extensively used to characterize the graft copolymers. The resulting copolymers can be considered to be potentially interesting materials; they may not only provide materials with a saturated elastic backbone with multiple-phase properties, but also offer low air permeability and broad damping properties in polymer blends and composites.

To optimize the hydroboration reaction conditions the model compound 2-hexenyl-9-BBN was considered and subsequently vinyl-terminated polystyrene prepolymers were blocked with methyl methacrylate. In this study both block and graft formation resulted from an initial hydroboration step of the residual double bonds of the unsaturated polymers such as poly(isobutylene-co-isoprene), polyisoprene, and EPDM, followed by copolymerization of the hydroborated polymers in the presence of oxygen and the monomers methylmethacrylate (MMA) and styrene (St).

## **1.2 Objectives**

This project explores a number of aspects of polymerization via hydroboration, including an investigation of the conditions of the hydroboration reaction, using a model compound, and the effects of the oxygen and monomer concentration. The copolymer products will be analyzed by various chromatographic techniques.

Objectives of the project are summarized below:

- Synthesize a model compound, 2-hexene-9-BBN, to study hydroboration chemistry and translate the knowledge gained to initiate polymerization through hydroboration.

- Use the model compound as a macroinitiator to investigate optimum grafting conditions of MMA.
- Investigate hydroboration of anionically prepared unsaturated polystyrene chain-ends to facilitate chain extension through additional MMA block formation.
- Use the “graft from” approach to prepare graft copolymers with rubbery backbones and different levels of unsaturated segments, including poly(isobutylene-co-isoprene), polyisoprene and EPDM.
- Study the effects of oxygen and monomer concentration on the above mentioned graft reactions.
- Develop chromatographic techniques to monitor the efficiency of the grafting reactions.

### **1.3 Layout of the thesis**

#### **Chapter 1:** Introduction and objectives.

A brief introduction is given to the major areas pertaining to this research, which includes modified polyolefins, the hydroboration method, and the use of the “graft from” approach to synthesise different graft copolymers. This chapter also includes the objectives of this research.

**Chapter 2:** Historical and theoretical background. This is a review of the historical and theoretical background of the hydroboration method used in this research.

**Chapter 3:** Synthesis of graft and block copolymers. This chapter covers the synthesis of copolymers, material and chromatographic techniques that were used in this research.

#### **Chapter 4:** Results and discussion

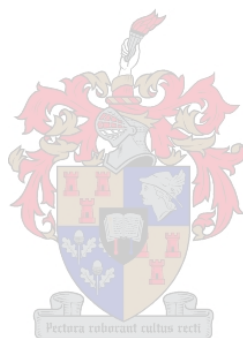
In this chapter the results are discussed, including the analysis of the graft copolymers by different chromatographic techniques.

#### **Chapter 5:** Conclusions and recommendations

General conclusions to the study and recommendations for future work are given.

#### 1.4 References

1. Brown, H. C.; Subba Rao, B. C. *J. Am. Chem. Soc.* **1956**, 78, 2582.
2. Brown, H. C.; Ramachandran, P. V. *Pure Appl. Chem.* **1994**, 66, 201.
3. Chung, T. C.; Jiang, G. J. *Macromolecules* **1992**, 25, 4816.
4. Chung, T. C.; D, R.; Jiang, G. J. *Macromolecules* **1993**, 26, 3467.
5. Chung, T. C.; Lu, H. L.; Janvikul, W. *Polymer* **1997**, 38, 6, 1495.
6. Chung, T. C.; Janvikul, W.; Bernard, R.; Hu, R.; Li, C. L.; Liu, S. L.; Jiang, G. J. *Polymer* **1995**, 36, 3565.
7. Chung, T. C.; Janvikul, W.; Bernard, R.; Jiang, G. J. *Macromolecules* **1994**, 27, 26.



## Chapter 2

### Historical and theoretical background

#### 2.1 Boranes in organic chemistry

##### 2.1.1 Introduction

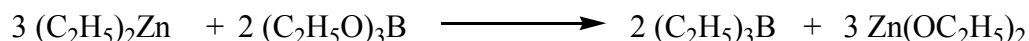
Hydroboration has become a highly valuable tool and has extensive applications in organic synthesis.<sup>1</sup> The intermediate borane moiety can be used to introduce free radicals, which can facilitate polymerization (homopolymerization or copolymerization) under favourable conditions. A brief overview of hydroboration and reactions involving boranes is now presented.

##### 2.1.2 Boranes – a first glance

Boron is unique in its position on the periodic chart as it is a group III metal with a very small atomic radius. As a group III neutral trivalent species, trialkylboranes are electron deficient (Lewis acids) with only a  $2s^2 2p^1$  valence configuration. They are extremely reactive towards Lewis bases, which provide two extra electrons to complete a stable octet. Since boron is small it is easy to sterically protect it with alkyl groups, if necessary. Boron forms covalent bonds with carbon and organoboranes are totally soluble in hydrocarbon solvents.

##### 2.1.3 Historical overview of hydroboration

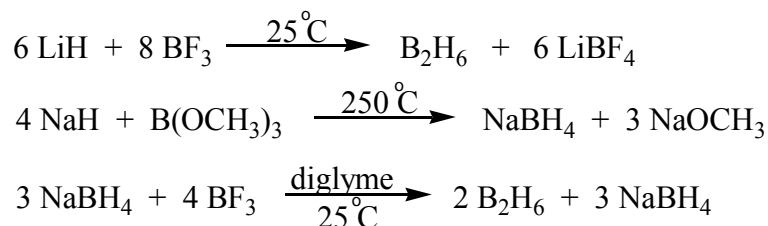
Organoboranes were first produced in 1862 by Frankland using the reactions of dialkylzincs with trialkoxyboranes, as shown in Scheme 2.1<sup>2</sup>.



**Scheme 2.1** Preparation of organoboranes by the reaction of dialkylzincs with trialkoxyboranes.

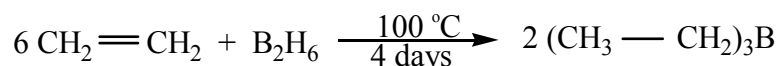
Boron hydrogen compounds such as  $\text{B}_2\text{H}_6$ ,  $\text{B}_4\text{H}_{10}$ ,  $\text{B}_5\text{H}_{11}$  and  $\text{B}_{10}\text{H}_{14}$  were prepared by Alfred Stock between 1910 and 1930.<sup>3</sup> These compounds remained of little interest to organic chemists due to their difficult and inconvenient preparation. In 1938 Brown initiated his research endeavours into the field of boron hydrides, which led to the

introduction of a variety of methods to facilitate the production of both sodium tetrahydroborate and diborane,<sup>4,5</sup> as shown in Scheme 2.2.



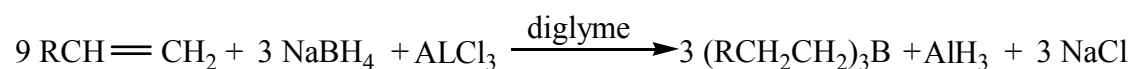
**Scheme 2.2 Formation of sodium tetrahydroborate and diborane.**

Subsequent studies on the reactions of diborane with alkenes and alkynes were carried out by Brown and Subba.<sup>6</sup> It was found that the reactions were slow and required elevated temperatures, e.g., the reaction of ethylene with diborane (Scheme 2.3) was completed only after heating to 100 °C.<sup>6</sup>



**Scheme 2.3 Reaction of ethylene with diborane.**

Hydroboration was not synthetically useful until 1956 when Brown and coworkers discovered a simple and rapid method for the addition of boranes to alkenes.<sup>7</sup> They noted that the unsaturated ester, ethyl oleate, consumed excess hydride while reducing the unsaturated carbonyl compound with NaBH<sub>4</sub>/AlCl<sub>3</sub> in diglyme (Scheme 2.4).<sup>7</sup> Further investigation showed that the double bond participated in the reaction. It was found that alkenes reacted readily with NaBH<sub>4</sub>/AlCl<sub>3</sub> in diglyme at room temperature to produce the corresponding organoboranes in excellent yield.

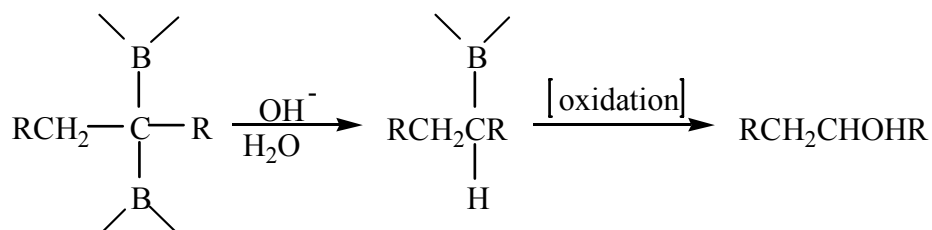


**Scheme 2.4 Addition of boranes to alkenes to yield organoboranes.**

In 1960 Logan and Flautt isolated 2,2,5,5-tetramethyl-3-hexanol and 2,2,5,5-tetramethyl-3,4-hexanediol from the dihydroboration of di-*t*-butylacetylene.<sup>8</sup> They rationalized the formation of the monoalcohol as possibly occurring by reduction of the corresponding carbonyl compound, which formed through hydrolysis and oxidation, by some reducing species (B-H) present in the mixture.

Similar work was done by Brown and Zweifel,<sup>9</sup> in 1961 they studied the isolated hexanal, 1-hexanol and 1,2-hexanediol from the dihydroboration of 1-hexyne, and

3-hexanone, 3-hexanol and 3,4-hexanediol from 3-hexyne. From evidence gathered from the dihydroboration of 1-hexyne, Brown<sup>9</sup> visualized the formation of the monoalcohol as occurring via a base-catalyzed hydrolysis of a geminal diboro derivative to a monoboro derivative, followed by oxidation, as shown below:



In 1971 Pasto and Chung<sup>10</sup> studied the kinetics of the hydroboration of tetramethylethylene (TME) with borane in tetrahydrofuran (THF). They found the rate of formation of 2,3-dimethyl-2-butylborane to be first order in both borane and TME. The reaction is considered to involve the direct reaction between a molecule of the borane-THF complex and the alkene in a very early transition state.

In 1975 Pinazzi et al.<sup>11</sup> first showed that both polyisoprene and polybutadiene could be totally hydroborated under extremely mild conditions.

In 1982 Nelson and Brown<sup>12</sup> studied the kinetics and mechanism of the reaction of borabicyclo [3.3.1] nonane (9-BBN) with representative haloalkenes and also the effect of halogen substitution upon the rate of hydroboration. They investigated the hydroboration of several haloalkenes and found kinetics parallel to those observed for the parent alkenes. The faster reacting haloalkenes showed kinetics that were first order in 9-BBN, while the slower reacting ones displayed kinetics that were three-halves order in haloalkene and one-half order in 9-BBN.

In 1989, block copolymers of 1,2-polybutadiene and 1,4-polybutadiene, polyisoprene, poly(2-methyl-1,3-pentadiene) and styrene were selectively hydroborated at the vinylic C=C using 9-BBN and then oxidized to the block polyalcohol's.<sup>13</sup>

In 1996 Chung et al.<sup>14</sup> Suggested that the polymerizations of methacrylate monomers such as MMA, EMA (ethyl methacrylate), and t-BMA (t-butyl methacrylate) initiated by the oxidation adducts of alkyl-9-BBN may proceed through living polymerization processes. The borinate radical generated in situ during the oxidation was believed to form a weak and reversible bond with the growing chain end during the polymerization. Such a process minimizes the undesirable chain transfer and



termination reaction, resulting in an observation of an increase in the molecular mass of the produced polymers as a function of monomer conversion. This radical polymerization route has also been applied to the preparation of graft and block copolymer with the use of borane-containing polymers.<sup>15-19</sup>

A number of group reported on The hydroboration of an alkene with 9-BBN followed by Suzuki cross-coupling which is a key step in the synthesis of compounds of pharmaceutical interest.<sup>20-22</sup>

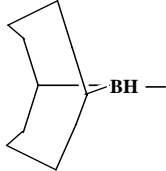
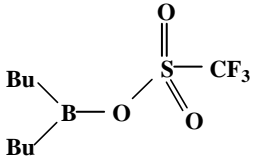
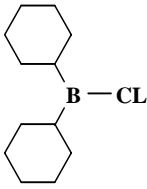
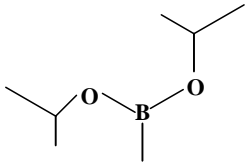
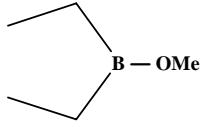
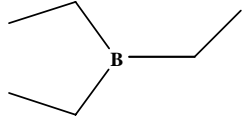
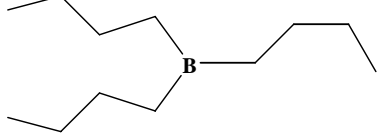
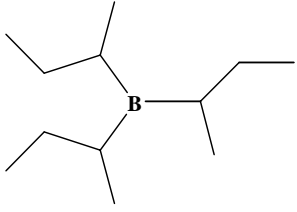
Recently, in 2004, Jeon et al.<sup>23</sup> reported for the first time, the synthesis of novel amorphous boron carbonitride by the hydroboration of borazine derivatives, B-triethynyl, N-trimethyl borazine and borazine, without a catalyst.

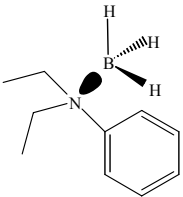
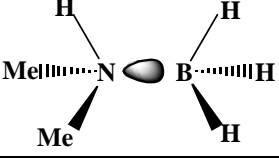
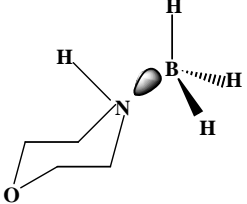
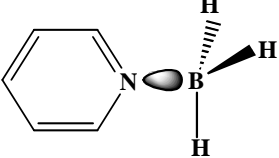
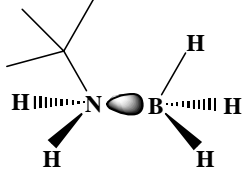
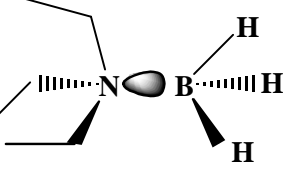
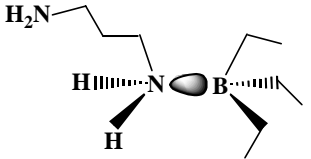
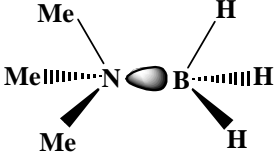
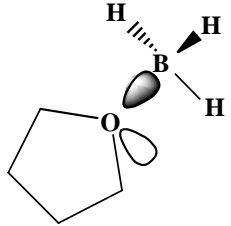
#### **2.1.4 Borane reagents for organic synthesis**

Organoborane reagents are an important part of today's organic syntheses. Commercially available boron compounds have found their way into the synthesis of pharmaceuticals, polymers, electronics, and printed circuit board manufacturing industries.

Borane ( $\text{BH}_3$ ) is a strong Lewis acid (electron-pair acceptor) with an empty p-orbital on the boron atom, which is available for interaction with lone pairs and nucleophiles. Borane exists as either the diborane dimer ( $\text{B}_2\text{H}_6$ ) or as a complex with a Lewis base. Borane complexes are versatile compounds commonly used as regio-, chemo- and stereo-selective reducing agents of a variety of group functionalities such as aldehydes, ketones, carboxylic acids, amides and olefins. A borane-tetrahydrofuran complex is the most reactive while dimethylsulfide borane and diethylaniline borane react more slowly. Most amine boranes react slowly and can be used in aqueous and even acidic media. In this section different organoboranes will be introduced and their particular relevance and importance in organic syntheses explained. To facilitate comparison, the boron reagents are structurally displayed in Table 2.1.

Table 2.1: Examples of boron reagents for organic synthesis

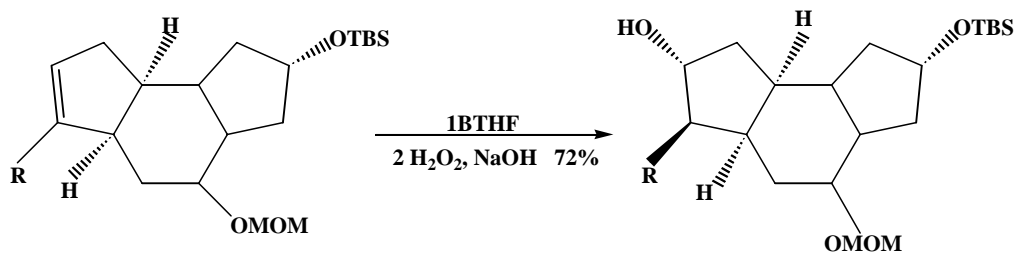
	Compound	Acronym	Structure
Alkyl Boranes	9-Borabicyclo [3.3.1] nonane	9-BBN	
	Dibutylboron triflate	DBBT	
	Dicyclohexylchloroborane	DCBCl	
	Diisopropoxymethylborane	DIMB	
	Methoxydiethylborane	MDEB	
	Triethylborane	TEB	
	Tri-n-butylborane	TNBB	
	Tri-sec-butylborane	TSBB	

Amine Boranes	N,N-Diethylaniline borane	DEANB	
	Dimethylamine borane	DMAB	
	Morpholine borane	MPB	
	Pyridine borane	PYB	
	t-Butylamine borane	TBAB	
	Triethylamine borane	TEAB	
	Triethylborane-1,3-diaminopropane complex (D)	TEB-DAP	
	Trimethylamine borane (D)	TMAB	
Boranes Complexes	Borane-tetrahydrofuran complex	BTHF	

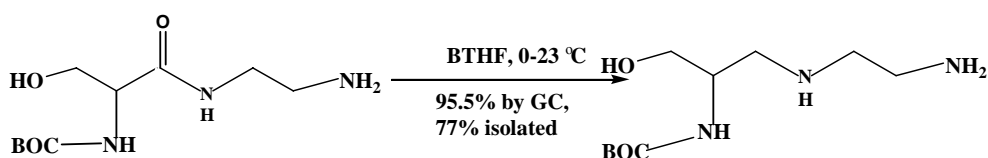
	Dimethylsulfide borane	DMSB	
Boron Hydrides	Cesium dodecahydrododecaborate methanolate	$\text{Cs}_2\text{B}_{12}\text{H}_{12}$	
Boron Hydrides	Potassium dodecahydrododecaborate methanolate	$\text{K}_2\text{B}_{12}\text{H}_{12}$	
Suzuki Reagents	Tetrakis(dimethylamino) diboron (D)	$\text{DMA}_4\text{B}_2$	
	Bis(pinacolato)diboron (D)	$\text{PIN}_2\text{B}_2$	
	Pinacolborane	PINB	

#### 2.1.4.1 Borane-tetrahydrofuran complex (BTHF)

The borane-tetrahydrofuran complex (BTHF) is a valuable reagent for the hydroboration of olefins and for the reduction of organic compounds, although it does have the disadvantage that the solutions are unstable over a period of time. Stabilized borane-tetrahydrofuran solutions can be stored for longer periods of time.<sup>24</sup> An example of the use of BTHF in the hydroboration of an alkene, followed by regioselective oxidation, yields the desired anti-Markovnikov alcohol as shown in Scheme 2.5.<sup>24</sup>

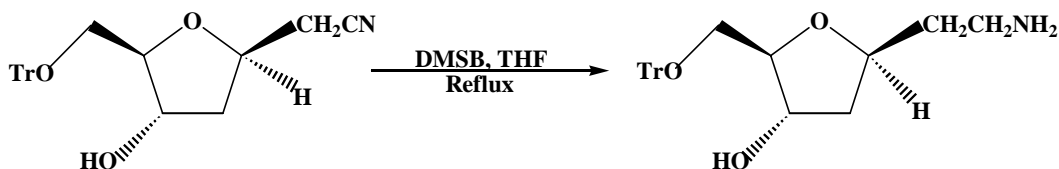
Scheme 2.5 Hydroboration and oxidation of an alkene with BTBF <sup>24</sup>.

EPIX Medical has used BTBF for the reduction of an amide in the synthesis of an injectable vascular contrast agent. Bernard et al.<sup>25</sup> optimized reaction conditions which minimized reduction of the BOC (protecting group). The reduction process is depicted in Scheme 2.6.

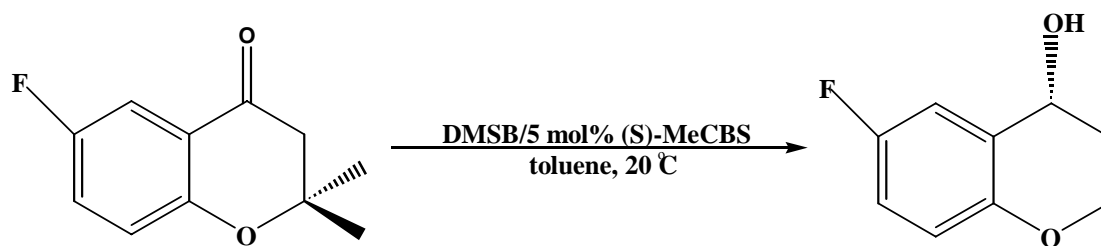
Scheme 2.6 Reduction of an amide using BTBF <sup>25</sup>.

#### 2.1.4.2 Dimethylsulfide borane (DMSB)

Dimethylsulfide borane (DMSB) is a valuable reagent for hydroboration reactions and for the reduction of functional groups. The stability of DMSB allows the preparation of functional groups in high concentration. Oxidation after the hydroboration reaction effectively removes the dimethylsulfide component.<sup>26</sup>

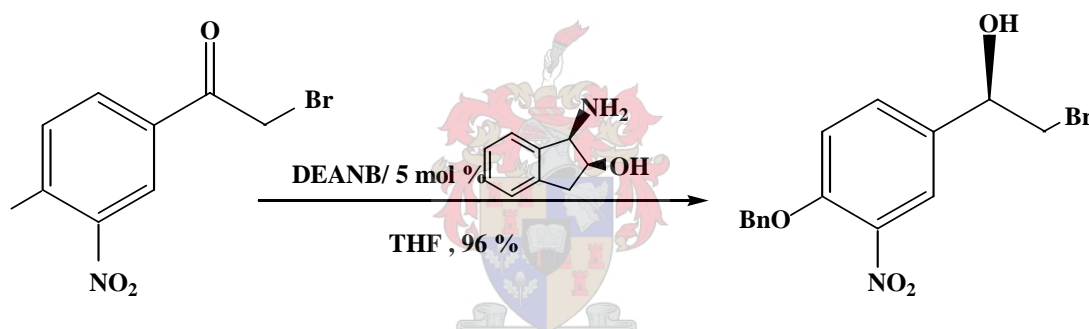
Scheme 2.7 Hydroboration and oxidation by DMSB <sup>26</sup>.

DMSB is an effective borane source for asymmetric ketone reduction using chiral oxazaborolidine catalysts. For example, in the synthesis of potassium channel modulators, the ketone shown in Scheme 2.8 was enantioselectively reduced in high yields.<sup>26</sup>

Scheme 2.8 Ketone reduction using chiral oxazaborolidine catalysts<sup>26</sup>.

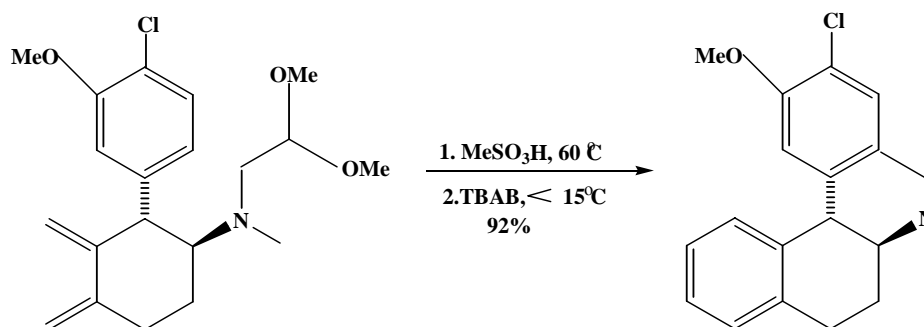
#### 2.1.4.3 Diethylaniline borane (DEANB)

*N,N*-Diethylaniline borane (DEANB) is a moderately reactive amine borane. DEANB is moisture sensitive and must be used in aprotic solvents. When combined with methyl oxazaborolidine (MeCBS) catalyst, DEANB is an excellent borane source for the enantioselective reduction of ketones.<sup>27</sup> As an example, in the scale-up of a key intermediate of formoterol, a bronchodilator, Wilkinson et al.<sup>28</sup> used DEANB as the borane source in the enantioselective ketone reduction.

Scheme 2.9 Ketone reduction with DEANB<sup>28</sup>.

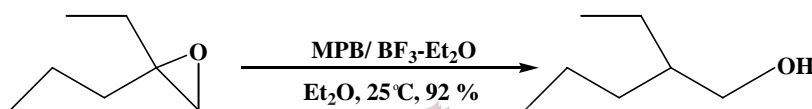
#### 2.1.4.4 *tert*-Butylamine borane (TBAB)

Complexation of the borane moiety  $\text{BH}_3$  with a strong Lewis base, such as an unhindered amine, produces air- and moisture-stable amine borane complexes. The stability, solubility, and ease of handling of amine boranes make them attractive sources of  $\text{BH}_3$  in many organic reductions where aqueous, alcoholic or acidic solvents are desirable. Aldehydes can be selectively reduced in the presence of ketones by using TBAB as the reducing agent. *t*-Butylamine borane is also effective for reductive aminations and for the reduction of enones at room temperature, to give allylic alcohols. The following reaction scheme shows TBAB in a reductive ring closure in the synthesis of a benzazepine drug intermediate.<sup>29</sup>

Scheme 2.10 Formation of a benzazepine <sup>29</sup>.

#### 2.1.4.5 Morpholine borane (MPB)

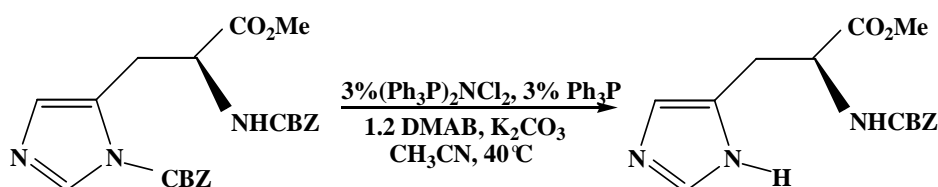
Smith<sup>30</sup> used morpholine borane (MPB) with  $\text{BF}_3$ -etherate to perform an epoxide ring opening. Here the amine borane acts as the reducing agent, while the  $\text{BF}_3$  is required to activate the epoxide oxygen as well as complex the morpholine after reduction.<sup>30</sup>

Scheme 2.11 Epoxide ring-opening using MPB with  $\text{BF}_3$  <sup>30</sup>.

#### 2.1.4.6 Dimethylamine borane (DMAB)

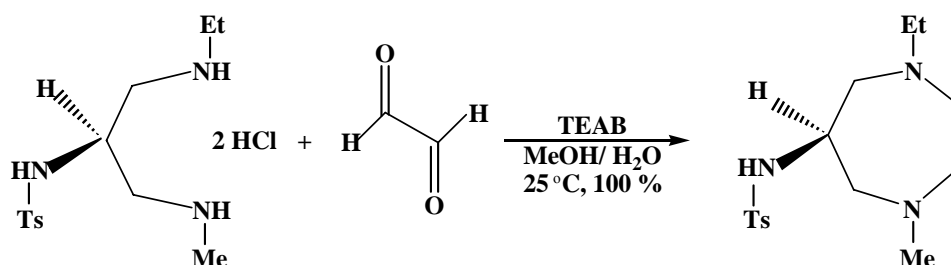
Dimethylamine borane in the presence of acetic acid and a catalytic amount of tetrakis(triphenylphosphine)palladium reductively opens epoxides to homoallylic alcohols. The stereoselectivity is a result of hydride delivery, such that inversion of configuration at the allylic C-O bond occurs.<sup>31</sup>

In solid-phase peptide synthesis, the allyloxycarbonyl (alloc) group (used for the protection of amines) is readily removed through palladium catalyzed cleavage in the presence of amine-borane complexes.<sup>32</sup> Interestingly, the carbobenzoxy group (CBZ)-protected nitrogen of heteroaromatic compounds can be cleaved in the presence of CBZ on a basic amine with DMAB and Ni catalysis.<sup>33</sup>

Scheme 2.12 Reaction of allyloxycarbonyl group for the protection of amines<sup>33</sup>

### 2.1.4.7 Triethylamine borane (TEAB)

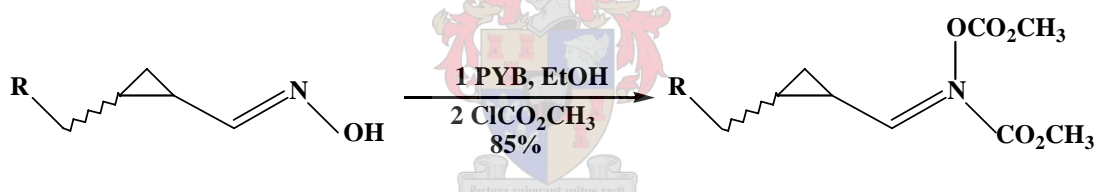
Triethylamine borane (TEAB) can be used in the reduction of carboxylic acid, ketone and aldehyde groups at 80 °C without solvent. In addition, TEAB has been effectively used in reductive amination as shown in Scheme 2.13.<sup>34</sup>



Scheme 2.13 Reductive amination with TEAB<sup>34</sup>

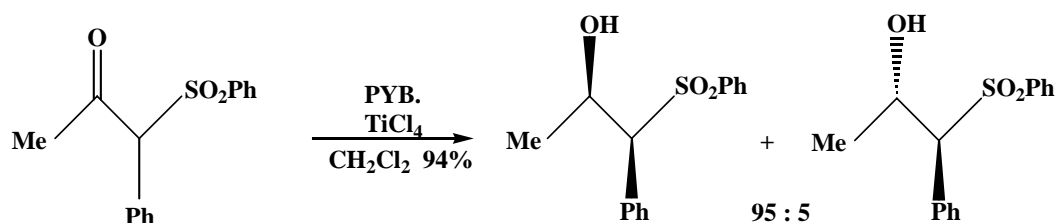
### 2.1.4.8 Pyridine borane (PYB)

Pyridine borane (PYB) can be used to reduce oximes to the corresponding hydroxyl amines. Reductions of oximes take place in the presence of other functional groups such as esters, nitriles, amides, and alkyl halides. Pyridine borane can also be used for reductive aminations.<sup>35</sup>



Scheme 2.14 Reductions of oximes with PYB<sup>35</sup>.

Reduction of  $\beta$ -keto sulfones with PYB in the presence of TiCl<sub>4</sub> results in ketone reduction primarily via a titanium chelated intermediate, yielding erythro- $\beta$ -hydroxy sulfones.<sup>36</sup>



Scheme 2.15 Formation of erythro- $\beta$ -hydroxy sulfones<sup>36</sup>.

### 2.1.4.9 9-Borabicyclo [3.3.1] nonane (9-BBN)

9-BBN is a valuable reagent for hydroboration reactions and is valuable in selected functional group reduction. The hydroboration of alkenes by 9-BBN gives excellent regioselectivity for boron at the least hindered carbon. This is an advantage over other



hydroboration reagents<sup>7</sup>. Hydroboration of an alkene with 9-BBN followed by Suzuki cross-coupling is a key step in the synthesis of a number of compounds of pharmaceutical interest.<sup>21, 37-40</sup>

#### **2.1.4.10 Borane-methyl sulfide (BMS)**

Borane-methyl sulfide (BMS) is much more stable than borane-tetrahydrofuran and is widely used for both hydroboration and reduction. However, it suffers from the serious disadvantage in that it yields a product that contains free dimethyl sulfide. The free dimethyl sulfide is highly volatile (b.p 38 °C) and flammable, and has a very noxious odour. Moreover, it is not soluble in water and can therefore not be disposed of by washing.<sup>41, 42</sup>

#### **2.1.4.11 Borane-1,4-thioxane**

Borane-1,4-thioxane is another valuable hydroboration agent. It has both lower volatility and milder odour than dimethyl sulphide. It has, however, a limited solubility in water and can be easily oxidized to the corresponding sulfoxide, which is miscible in water. This agent is a liquid, 8M in BH<sub>3</sub>, and stable over prolonged periods. Unfortunately, this commercially available reagent is relatively costly compared to borane-tetrahydrofuran and borane-dimethyl sulphide. The growing importance of borane reagents for the synthesis of pharmaceuticals and other compounds and the problems associated with other well-established borane adduct hydroboration agents, e.g., low concentration and stability, high volatility, flammability, unpleasant odour, as discussed above, create a need for easy to handle, stable and environmentally benign hydroborating agents as discussed specifically in Section 2.4.<sup>43</sup>

#### **2.1.4.12 Bis (2-methoxyethyl)sulfide**

Bis (2-methoxyethyl) sulfide was prepared from inexpensive thiodiethanol in an improved yield following the method described by Richter et al.<sup>44</sup> The product is isolated by simple distillation and the unreacted starting material can be recycled. Here, diborane was generated by treating a 2M solution of sodium borohydride with an equivalent amount of boron-trifluoride-triglyme.<sup>44</sup>

## 2.2 The theory of hydroboration

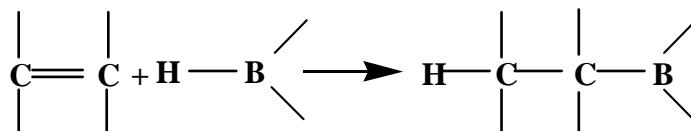
### 2.2.1 Introduction

Hydroboration of alkenes forms an interesting synthetic methodology for the conversion of alkenes to other functionalities since the hydroborated products can conveniently be transformed into alcohols<sup>45</sup>, amines<sup>46</sup> or halides.<sup>47</sup> Furthermore, the intermediate borane moiety can be used to introduce free radical polymerization, which can facilitate polymerization (homopolymerization or copolymerization) under favourable conditions.

The discussion below will focus mainly on the reactions of alkenes, alkynes and carbonyl compounds with the borane moiety 9-BBN, as well as subsequent reactions, due to the respective borane functionalities formed. The particular borane species, 9-BBN forms the basis of the experimental work described in Chapter 3. The mechanisms involved during hydroboration reactions will be considered, as this may help to explain phenomena observed during the course of this study.

### 2.2.2 Hydroboration

Organoboranes are readily available for applications in organic synthesis.<sup>48</sup> Carbon-carbon double bonds react with boron-hydrogen (B-H) bonds, during which boron is added to one end of a double bond and hydrogen to the other (Scheme 2.16). The reaction proceeds via a four-membered ring transition state, which means that the boron and the hydrogen must add to the same face of the double bond. A partial positive charge develops on the carbon that attaches to the hydrogen during the reaction. Boron, on the other hand, becomes attached to the carbon that is less able to stabilize a positive charge.

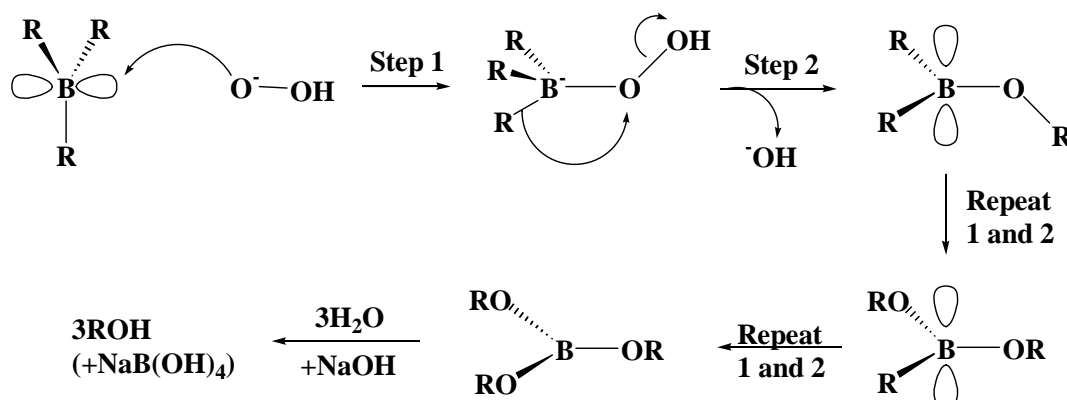


**Scheme 2.16 The hydroboration reaction.**

There are many factors that can affect the hydroboration reaction (see also Section 2.2.7), including temperature and time.

### 2.2.2.1 Oxidation

One of the many interesting reactions that organoboranes undergo is the rapid and essentially quantitative oxidation with alkaline hydrogen peroxide. The mechanism of this reaction procedure is presented in Scheme 2.17.



Scheme 2.17 General hydroxylation reactions of organoboranes<sup>48</sup>

Consequently, hydroboration-oxidation provides a valuable procedure for achieving the hydration of carbon-carbon multiple bonds with high regioselectivity and stereospecificity.<sup>49</sup>

### 2.2.3 Hydroboration of alkenes

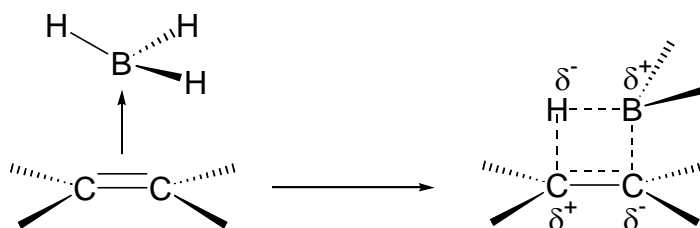
Hydroboration constitutes the most important method for the preparation of organoboranes and has been applied to a wide variety of alkenes. The most common and useful application of the hydroboration reaction of alkenes is to form anti-Markovnikov alcohols by oxidation of the organoborane with hydrogen peroxide or sodium perborate.<sup>48</sup>

Oxidation of the organoborane gives essentially quantitative yields of the alcohol and proceeds with complete retention of configuration. Analysis of the alcohols formed after oxidation serves to locate the precise position of the boron atom in the organoboranes.

### 2.2.4 Mechanism of hydroboration

The mechanism of hydroboration is depicted in Scheme 2.18. It is believed to involve the addition of a monomeric borane to a carbon-carbon double bond via a four-centred transition state, to form an alkylboranes.<sup>50</sup> The hydroboration mechanism proceeds through the establishment of a  $\pi$ -complex, which is formed by donation of the  $\pi$  bond

of the alkene into the vacant  $p$  orbital on the boron atom. The boron atom in borane is  $sp^2$  hybridized and the vacant  $p$  orbital is perpendicular to the plane of the three boron-hydrogen bonds. Boranes are therefore electrophilic and readily combine with electron-rich species. Addition of the borane compound to an alkene takes place through the formation of a four-centre transition state carrying charges on the participating atoms, as shown in Scheme 2.18.



**Scheme 2.18 Mechanism of hydroxylation showing formation of a four-centred transition state.**

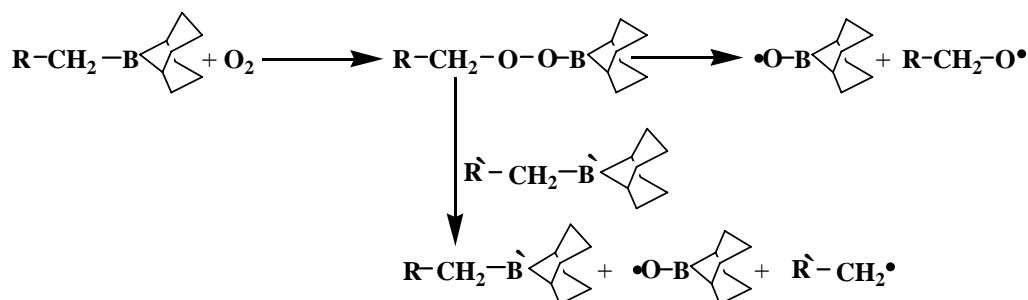
During hydroboration the boron atom follows Markovnikov's rule and adds to the side of the double bond that has the most hydrogen's.

### 2.2.5 Initiation

The borane group positioned along the polymer chains is an asymmetric trialkylborane, with one linear secondary alkyl group attached to the polymer and two secondary alkyl groups that are part of the bicyclononane structure. Upon contact with  $O_2$ , the autoxidation of boranes proceeds via a free-radical homolytic chain mechanism. This mechanism is contradictory to the one proposed by several authors<sup>51-54</sup>, as shown in Scheme 2.19.<sup>55</sup> The driving force is the conversion of B-C bonds (449.4 KJ / mol) to the stronger B-O bonds (806.4 KJ / mol). Oxygen will oxidize boranes, producing boron peroxides, which can react further with an alkylborane.

The reduction of the peroxide by another trialkylborane yields a borinate B-O' radical and an alkyl radical. The boron peroxides will also homolytically cleave to generate an alkoxy radical and a B-O' radical. These radicals can initiate polymerization of monomers such as methyl methacrylate, styrene, 2-ethylhexyl acrylate, vinyl acetate, acrylonitrile at room temperature. To generate the desirable polymeric radicals in "graft-from" polymerization, it is essential to control the oxidation reaction so that it occurs at the linear C-B bond attached to the polymer. The oxidized B-C bonds are readily initiated by oxygen at ambient temperature; the ratio of oxygen to the B-C bond should be less than 10%, added hourly. The best results in the heterogeneous

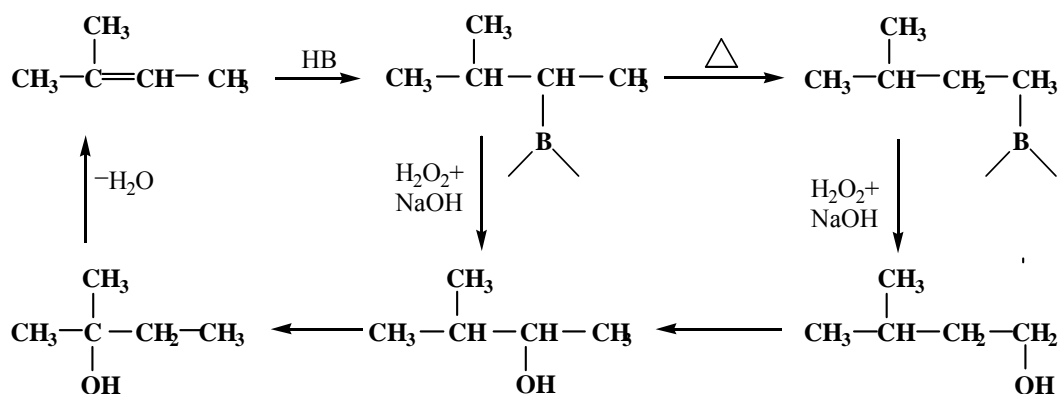
reaction system are realized when the  $O_2$  is introduced slowly, so that at any time  $O \ll B$ , even though the final stoichiometry of oxygen to boron is found to be 0.5:1. Excess  $O_2$  is not only a poison for free-radical polymerizations but also leads to over-oxidation to boronates and borates, which are poor free-radical initiators at room temperature. The polarity of the solution also affects the graft reaction.



Scheme 2.19 Mechanism of autoxidation of boranes <sup>55</sup>.

### 2.2.6 Isomerization of organoboranes

At moderate temperatures organoboranes undergo a facile isomerization that proceeds to place the borane atom predominantly at the least hindered position of the alkyl groups. This facile migration of the boron atom makes possible a number of valuable syntheses that are not otherwise practical. For example, oxidation of the hydroboration product of 3-hexene yields pure 3-hexanol, whereas oxidation of the thermally treated product yields predominantly 1-hexanol. Similarly, the transformations, as shown in Scheme 2.20, are readily achieved in essentially quantitative yields <sup>56</sup>.

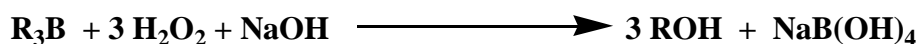


Scheme 2.20 Reaction scheme for the isomerization of organoboranes <sup>56</sup>.

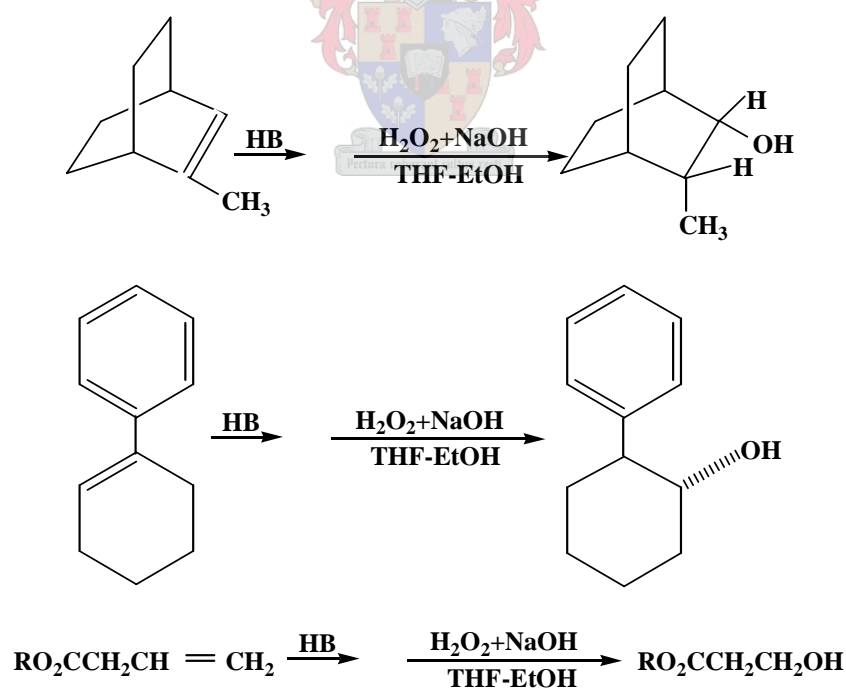
## 2.2.7 Reactions of organoboranes

## 2.2.7.1 Reaction with alkaline hydrogen peroxide

The reaction of alkaline hydrogen peroxide with organoboranes is a remarkably clean and widely used reaction<sup>24</sup> (Scheme 2.21).

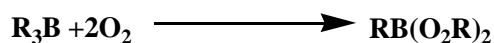
Scheme 2.21 Oxidation via hydroboration<sup>24</sup>.

Oxidation via hydroboration is essentially quantitative and proceeds with clean retention of configuration. The reaction takes place readily in the presence of the usual hydroboration media, such as diglyme, tetrahydrofuran, and ethyl ether. For water insoluble solvents, such as diethyl ether, and for intermediates not easily oxidized, it is desirable to add ethanol as a co-solvent. Oxidation can accommodate all groups that tolerate hydroboration. Consequently, hydroboration followed by in situ oxidation with alkaline hydrogen peroxide provides a simple, broadly applicable procedure to achieve the anti-Markovnikov hydration of double bonds.<sup>57</sup> Examples of hydration through oxidation of hydroborated compounds are shown in Scheme 2.22

Scheme 2.22 Oxidation reactions of hydroborated compounds with  $\text{H}_2\text{O}_2$  and  $\text{NaOH}$ .

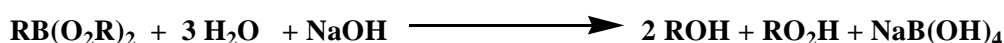
### 2.2.7.2 Reaction with oxygen

The organoboranes react readily with oxygen to produce mixtures of hydroperoxides and alcohols<sup>58</sup>. Careful control of the oxidation conditions leads to the predominant formation of  $\text{RB}(\text{O}_2\text{R})_2$ , as shown in Scheme 2.23.<sup>45</sup>



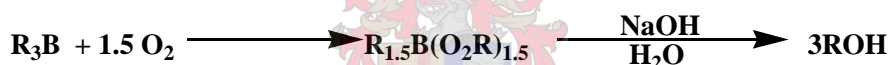
Scheme 2.23 Reaction of organoboranes with oxygen<sup>45</sup>

Treatment of the product with aqueous alkali results in a reaction of the remaining carbon-boron bond with one of the alkyl hydroperoxides formed in the hydrolysis.



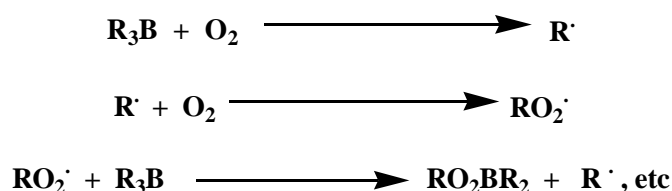
Scheme 2.24 Formation of alkyl hydroperoxides.

By introducing a stoichiometric amount of oxygen, which can be achieved with an automatic gas meter, it is therefore possible to achieve quantitative conversion to alcohols, as depicted in Scheme 2.25.



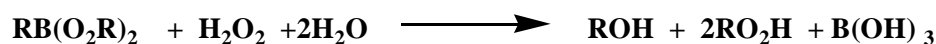
Scheme 2.25 Hydroboration of alkenes to form alcohols.

This procedure provides an alternative route for the conversion of organoboranes to alcohols. The reaction does not possess the stereo-specificity of the alkaline peroxide procedure. For example, whereas the organoborane from norbornene is converted by alkaline hydrogen peroxide to 99.9% exo-norborneol, the oxygen procedure yields 86% exo- and 14% endo-norborneol. The loss of stereo-specificity is probably a result of the free-radical nature of the reaction with oxygen, which is explained in Scheme 2.26.<sup>53</sup>



Scheme 2.26 Reaction scheme for the organoboration with oxygen<sup>53</sup>.

Treatment of the oxidation intermediate with hydrogen peroxide in the absence of base oxidizes the remaining boron-carbon bond.

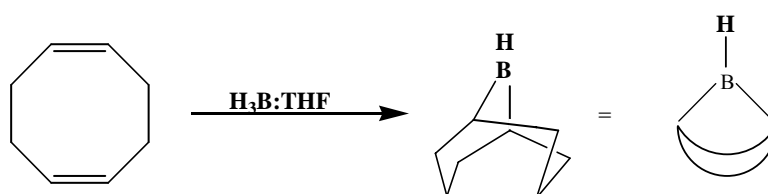


Scheme 2.27 Treatment of oxidation intermediate with hydrogen peroxide.

Extraction with alkali separates the hydroperoxide from the alcohol, providing a convenient route to alkyl hydroperoxides.<sup>59</sup>

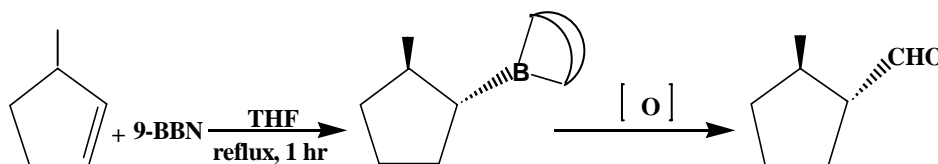
### 2.2.8 9-Borabicyclo [3.3.1] nonane (9-BBN)

The reaction of 1,5-cyclooctadiene with borane in tetrahydrofuran can be controlled to provide the bicyclic borane 9-borabicyclo [3.3.1] nonane (9-BBN), as shown in Scheme 2.28, and briefly mentioned earlier in Section 2.1.4.9.



Scheme 2.28 Formation of 9-BBN.

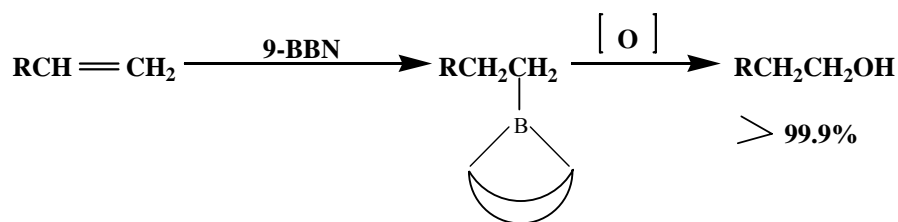
This reagent, termed 9-BBN for convenience, possesses remarkable thermal stability. Moreover, it possesses remarkable air stability for a dialkylborane, permitting it to be weighed out and transferred with approximately the same precautions and relative convenience accompanying the utilization of sodium borohydride and lithium aluminum hydride. Furthermore, its present commercial availability facilitates many synthetic applications of borane chemistry.<sup>48</sup> The rate of reaction of 9-BBN with olefins is considerably lower than that of disiamylborane. However, terminal olefins react readily at 25 °C. Less reactive internal olefins require either an excess of reagent or overnight reaction times, or both, for complete hydroboration.



Scheme 2.29 Hydroboration of cyclic olefins with 9-BBN.

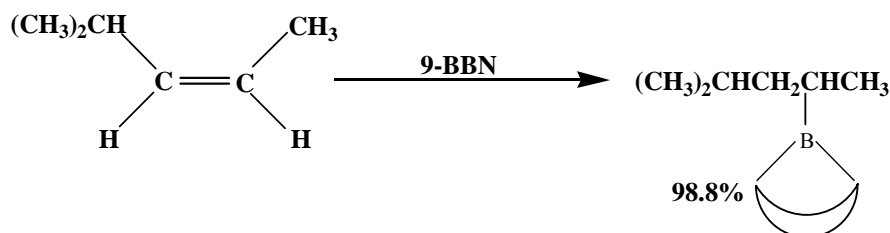
9-BBN exhibits a remarkable regioselectivity in its hydroborations. Terminal olefins place the boron at the terminal position with a selectivity of at least 99.9%.





Scheme 2.30 Hydroboration of terminal olefins with 9-BBN.

Even more surprising is the regioselectivity exhibited on *cis*-4-methyl-2-pentene.<sup>48</sup>

Scheme 2.31 Hydroboration of *cis*-4-methyl-2-pentene.

Hydroboration of the *trans* isomer is much less regioselective. The powerful regioselectivity of the reagent can even overcome the major influence of halogen substituents.

### 2.2.8.1 Stability of 9-BBN

The thermal stability of 9-BBN is quite remarkable. A sample of pure 9-BBN in a sealed, evacuated capillary can be heated repeatedly to 160 °C without noticeable change in the melting point. Samples of 9-BBN have also been heated under N<sub>2</sub> to 200 °C for 24 hr, either as the solid (crystal form) or in the presence of hydrocarbons (e.g. tetradecane), with only minor loss of hydride activity. In sharp contrast, disiamylborane undergoes isomerization at 75 °C<sup>60</sup> and dicyclohexylborane is reported to decompose at 180-200 °C<sup>61</sup>, yielding a polymeric borane and cyclohexene.

The stability of pure 9-BBN towards air oxidation is unique among dialkylboranes. Even so, some loss of purity occurs upon exposure to the atmosphere. Consequently, for quantitative studies it is recommended that reactions of solid 9-BBN be carried out perfectly under a nitrogen atmosphere in order to maintain the maximum hydride activity and purity. Solutions of 9-BBN, on the other hand, are highly reactive towards both oxygen and water and should be carefully protected from these reactants for both preparative and quantitative studies.

From a practical standpoint, 9-BBN is stable at room temperature. The reagent can be stored, either as the solid or in THF solution, for indefinite periods (>2 years) without any noticeable change in activity, provided that an inert atmosphere is maintained. Both 9-BBN and B-R-9-BBN (R=alkyl) exhibit remarkable thermal stabilities for organoboranes. Consequently, the hydroboration can be carried out without difficulty in refluxing tetrahydrofuran, utilizing the theoretical quantity of 9-BBN. Under these conditions almost all olefins are quantitatively converted to B-R-9-BBN. Even the most resistant of olefins, e.g. 2,3-dimethyl-2-butene, which fails to react with disiamylborane, undergoes complete hydroboration in 8 hours.<sup>48</sup>

### **2.2.8.2 Reactions of 9-BBN with hydroxyl compounds**

The reactions of 9-BBN in THF at 25 °C with water and simple alcohols (methanol, tert-butyl alcohol) afford quantitative yields of hydrogen and the corresponding B-hydroxy- and B-alkoxy-9-BBN derivatives. These reactions, however, are by no means instantaneous; they require 10-60 min for complete evolution of hydrogen. This is much slower than the comparable solvolysis of disiamylborane.

The rates of reaction of disiamylborane with various alcohols have been studied by Brown et al.<sup>62</sup> By adding the alcohol to a THF solution containing equivalents of disiamylborane at 0 °C, hydrogen instantaneously evolved with methanol and tert-butyl alcohol. No hydrogen evolution was, however, observed when 3-ethyl-3-pentanol was added. Clearly steric hindrance prevents reaction with the bulky disiamylborane in this case. Yet, when tri-n-butyl carbinol, which is clearly more hindered than 3-ethyl-3-pentanol, was added to a fourfold excess of 9-BBN in THF at 25 °C, the reaction was complete in 60 minutes. Hence, it would appear that 9-BBN is less sterically hindered than disiamylborane. The slower rate of reaction of 9-BBN with simple alcohols therefore appears irregular.

### **2.2.8.3 Effect of structure on olefin hydroboration by 9-BBN**

The function of the 9-BBN group as a blocking group in syntheses via organoboranes<sup>63</sup> and its highly selective hydroboration ability have been previously reported by Brown et al.<sup>63, 64</sup> 9-BBN exhibits remarkable regio- and stereo-selectivity, giving the highest degree of selectivity yet achieved. For example, 1-hexene reacts to give 99.9% of the 1-isomer (regioselectivity) and norbornene reacts to yield 99.5% of the exo isomer (stereo-selectivity). 9-BBN shows a remarkable preference for forming a

carbon-boron bond to the least hindered terminal of a double bond, e.g. 4-methyl-2-pentene.<sup>63, 64</sup> In view of these unique characteristics, Brown and Moerikofer<sup>65</sup> thought it appropriate to explore the effect of olefin structure on the rate of hydroboration with 9-BBN. 9-BBN proved to be a highly selective reagent, very different from the selectivity exhibited by disiamylborane. Diborane, on the other hand, is a relatively insensitive reagent, exhibiting only minor effects of structure upon rate of reaction.<sup>65</sup>

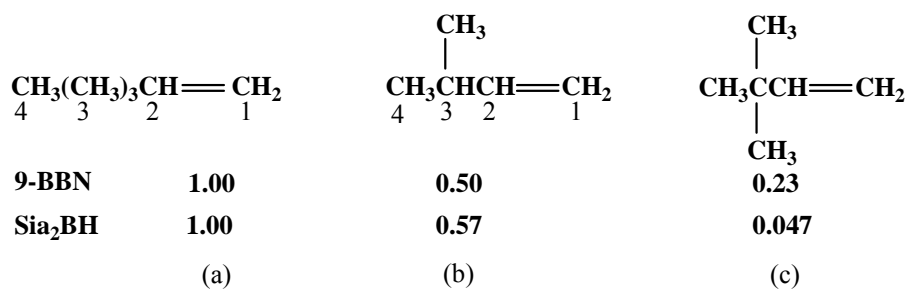
### i) Terminal olefins

The data for straight chain 1-alkenes indicate that the rate of hydroboration is nearly independent of chain length. Thus, 1-hexene, 1-octene, 1-decene, and 1-dodecene all show similar reactivity with either 9-BBN or disiamylborane (sia<sub>2</sub>BH), as indicated by the relative rates (see Scheme 2.32 for the corresponding borane moieties below the relevant chemical structures).



Scheme 2.32 Hydroboration of 1-alkenes with 9-BBN or Sia<sub>2</sub>BH.

In the following Schemes (2.33–2.39) the hydroboration rates for different olefins with 9-BBN or Sia<sub>2</sub>BH will be given. Branching in the R-group (CH<sub>3</sub>) as shown below in Scheme 2.33 decreases the rate of hydroboration significantly. Thus, in going from 1-hexene to 3-methyl-1-butene the rate of reaction with 9-BBN decreases by a factor of two, and 3,3-dimethyl-1-butene reacts four times slower than the straight-chain olefin. A more dramatic decrease in rate is realized with disiamylborane.



Scheme 2.33 Hydroboration of 3,3-dimethyl-1-butene with 9-BBN or Sia<sub>2</sub>BH.

Results, as shown above, suggest that disiamylborane is somewhat more sensitive to the steric requirements of the alkenes than is 9-BBN. Branching at a position more remote from the double bond, such as at position 4, as shown above in Scheme 2.33, has little or no effect upon the rate.

## ii) Internal olefins

The rate of 9-BBN hydroboration of *cis*-2-pentene (Scheme 2.34) is 100 times slower than that of 1-hexene. That is, internal olefins are considerably more sluggish in their reactivity than terminal olefins.



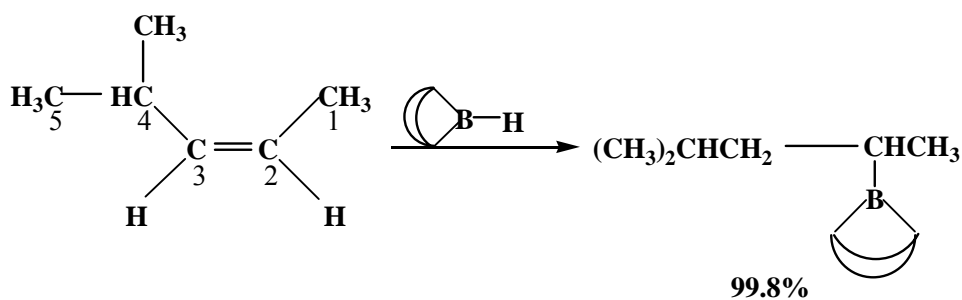
Scheme 2.34 Hydroboration of *cis*-2-pentene.

If only one side of the internal olefin is branched (Scheme 2.35) then the rate of 9-BBN hydroboration is only moderately reduced.



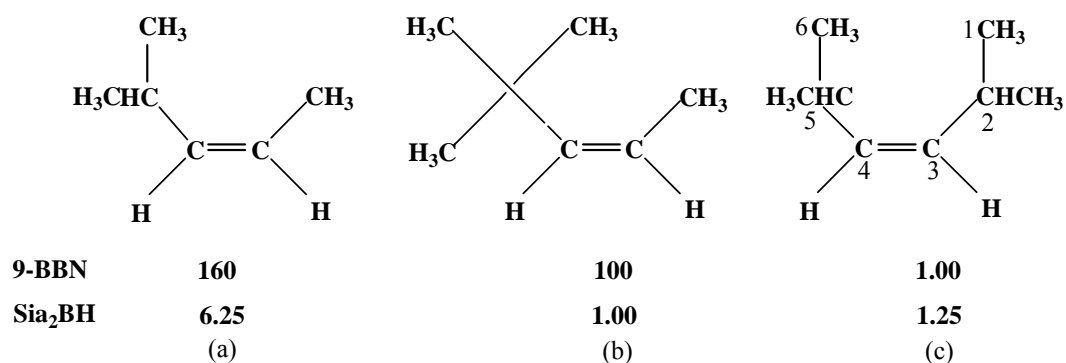
Scheme 2.35 Hydroboration of branched internal olefin.

This behaviour follows from the fact that the 9-BBN reacts almost exclusively at the less-hindered side of the asymmetrically substituted double bond (see Scheme 2.36)



Scheme 2.36 Hydroboration with 9-BBN.

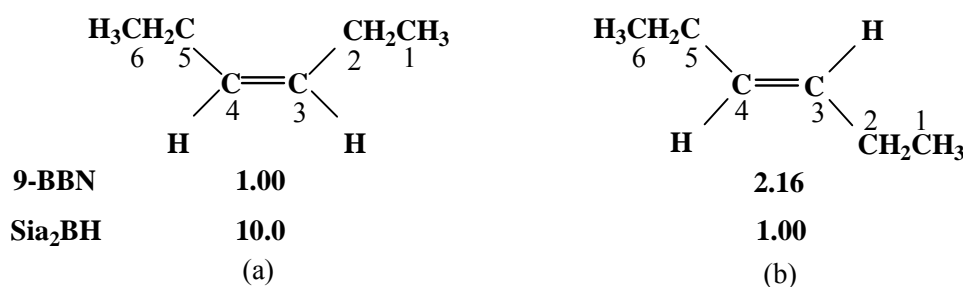
The 9-BBN moieties see the environment at C2 of both olefins in Scheme 2.37 as essentially identical. If the alkyl groups on both sides of the double bond are branched then the rate of 9-BBN hydroboration drops sharply. In a molecule such as 2,5-dimethyl-3-hexene (Scheme 2.37 (c)) there is no means available for the 9-BBN moieties to avoid the strain at the crowded alkyl groups. The rates of reaction of disiamylborane with these hindered internal olefins are all very slow and reveal much smaller effects of structure.



Scheme 2.37 Hydroboration of 2,5-dimethyl-3-hexene.

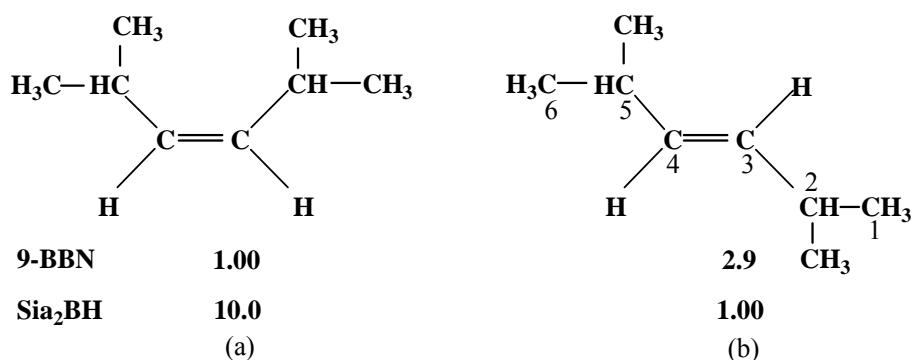
### iii) Cis and trans isomers

It has long been established that cis-alkenes undergo hydroboration with disiamylborane at a rate considerably faster than that of the corresponding trans-alkenes (Scheme 2.38). It is therefore interesting to discover that the reverse is true for 9-BBN.



Scheme 2.38 Reaction rates for cis and trans alkenes for both 9-BBN and Sia<sub>2</sub>BH.

The phenomenon appears to be general and holds even for isomers containing highly branched alkyl groups (Scheme 2.39).

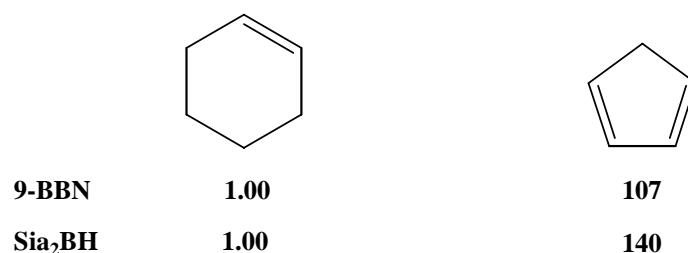


**Scheme 2.39** Reaction rates for cis and trans alkene isomers containing highly branched alkyl groups.

Originally, the greater reactivity of cis alkenes toward disiamylborane was a result of the more strained double bond in the cis isomers.<sup>66</sup> The reason for the reversal in reactivity observed with 9-BBN is not clear. Nevertheless, this reversal in reactivity can be most useful in synthetic applications of hydroboration, and facilitates the preferential hydroboration of either the cis or trans isomer, merely by the suitable selection of the hydroborating agent.

### iii) Cyclic olefins


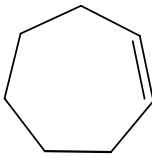
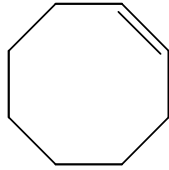
Cyclohexene is remarkably sluggish in the hydroboration reaction involving both disiamylborane and 9-BBN. On the other hand, cyclopentene is quite reactive. Thus, there is major difference in the reactivity of these two structurally quite similar olefins.



**Scheme 2.40** Hydroboration of cyclic olefins with 9-BBN or Sia<sub>2</sub>BH.

The double bond in the cyclopentene molecule is considerably more strained than the double bond in cyclohexene. Presumably this strain is responsible for the higher reactivity of cyclopentene towards both reagents. Both cycloheptene and cyclooctene have highly strained double bonds<sup>66, 65</sup> and both exhibit reactivity considerably higher than that of cyclohexene with both 9-BBN and disiamylborane.

Where as disiamylborane distinguishes considerably between the three strained olefins, 9-BBN does not.

			
<b>9-BBN</b>	<b>1.00</b>	<b>1.10</b>	<b>0.96</b>
<b>Sia<sub>2</sub>BH</b>	<b>1.00</b>	<b>18.6</b>	<b>68.6</b>

**Scheme 2.41 Hydroboration of cyclohexene with 9-BBN or Sia<sub>2</sub>BH.**

Again, the precise basis for this difference in the reactivity pattern for the two-hydroboration agents is not evident<sup>66</sup>.

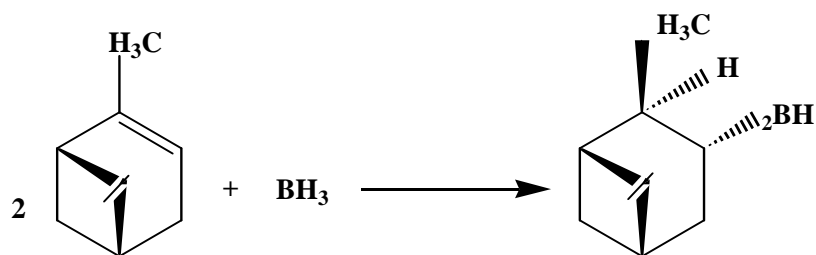
### 2.2.9 Hydroboration of hindered olefins

Reactions of relatively hindered olefins with borane under mild conditions often stop short of the trialkylborane stage. By avoiding the presence of an excess of olefin and by utilizing relatively short reaction times, such reactions can often be controlled to yield the dialkylborane or, in some cases, the monoalkylborane.<sup>67</sup>

Thus the reaction of 2-methyl-2-butene with borane-THF at 0 °C readily produces bis(3-methyl-2-butyl) borane or disiamylborane and the reaction of 2,3-dimethyl-2-butene can be directed quantitatively to the synthesis of the corresponding monoalkylborane, 2,3-dimethyl-2-butylborane or thexylborane. These derivatives actually exist in tetrahydrofuran solution as dimers.<sup>68</sup>

It is, however, convenient to discuss their reactions in terms of the monomeric species in the great majority of cases where the dimeric structure is not an essential part of the reaction. The hydroboration of cyclopentene proceeds rapidly to the tricyclopentyl borane stage, and it is not yet possible to prepare dicyclopentylborane directly. The hydroboration of cyclohexene can, however, be readily controlled to yield dicyclohexylborane. Presumably both the lower reactivity of cyclohexene and the insolubility of the intermediate, dicyclohexylborane, are factors in its synthesis.

The trisubstituted olefin  $\alpha$ -pinene is readily converted into the corresponding dialkylborane as shown in Scheme 2.42.



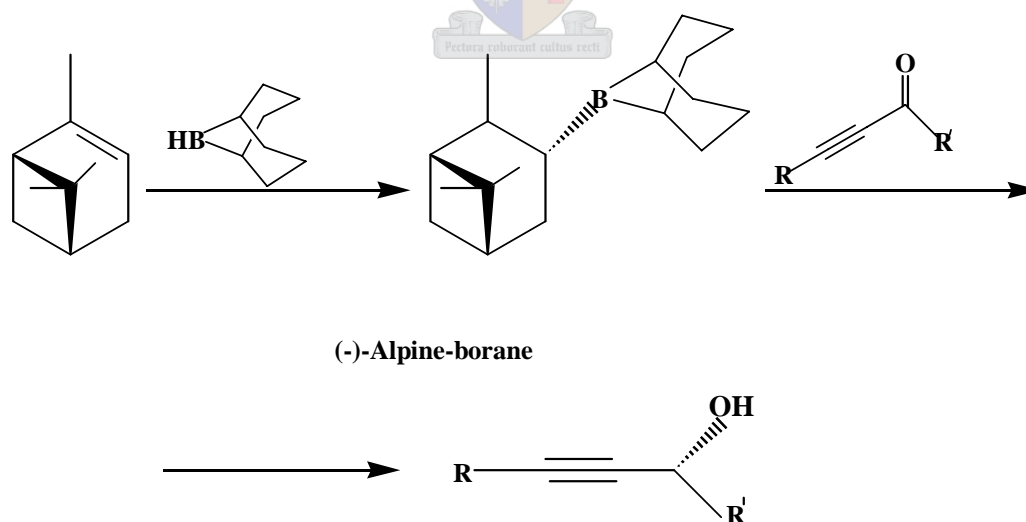
Scheme 2.42 Formation of dicyclohexylborane.

## 2.2.10 Reduction

Boron-containing reducing reagents may be divided into two categories: nucleophilic reducing agents such as sodium borohydride and electrophilic reducing agents such as borane and its derivatives.

### 2.2.10.1 Reduction with alkylboranes

The reaction of trialkylboranes with aldehydes to form alkenes and alcohols was first reported by Mikhailov's group.<sup>69</sup> Later the discovery of pinylborane made the reaction useful for reducing carbonyl compounds. Isopinocampheyl-9-BBN (alpine-borane), which is prepared from the hydroboration of (+)- or (-)- $\alpha$ -pinene with 9-BBN, is most widely used for the asymmetric reduction of propargylic ketones, as shown in Scheme 2.43.



Scheme 2.43 Reduction with alkyboranes.

Propargylic alcohols are obtained in excellent enantiomeric purity by the reduction of propargylic ketones with alpine-borane.<sup>70</sup>



## 2.3 Theory and overview of the polymerization processes and polymer architectures used in this study

### 2.3.1 Graft copolymers

A graft copolymer is a polymer comprising molecules with one or more species of blocks connected to the main chain as side chains, having constitutional or configurational features that differ from those in the main chain, exclusive of branch points (Scheme 2.44 (a)) in a graft copolymer. The distinguishing feature of the side chains is constitutional; the side chains comprise units derived from at least one species of monomer different from those that supply the units of the main chain (Scheme 2.44 (b)). The simplest case of a graft copolymer can be represented by structure (a) (Scheme 2.44), where a sequence of A monomer units is referred to as the main chain or backbone, the sequence of B units is the side chain or graft, and X is the unit in the backbone to which the graft is attached. In graft copolymers the backbone and side chains may both be homopolymeric, the backbone may be homopolymeric and the side chains copolymeric or vice versa, or both backbone and side chains may be copolymeric but of different chemical compositions. Branching in one or more stages and cross-linking may also occur. Cross-linked structures usually cannot be fully characterized because they are insoluble and frequently infusible.<sup>71</sup>



Scheme 2.44 Structure representation of graft copolymers.

### 2.3.2 Block copolymers

Block copolymers are generally defined as macromolecules with linear and/or radial arrangement of two or more different blocks of varying monomer composition.<sup>71</sup>

In the simplest case, a diblock copolymer AB consists of two different homopolymers linked end-to-end. Extension of this concept leads to ABA or BAB triblocks and to (AB) linear multiblocks, whereas ABC copolymers are obtained by the incorporation of a polymer sequence having a third composition. Radial arrangements of block copolymers are in the simplest case star-shaped structures, where a number of block

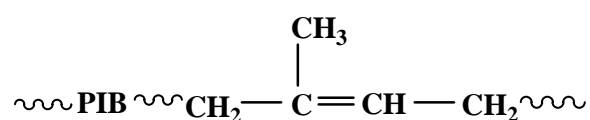
copolymer chains are linked by one of their ends to a multifunctional moiety. Another structural possibility designated by heteroarm block copolymers is to link  $n$  homopolymer sequences to a given junction point.

### 2.3.3 Anionic polymerization

Anionic polymerization was the first and is the most widely used technique for the preparation of well-defined block copolymers. Since its discovery by Szwarc in 1956, a large variety of block copolymers have been prepared from styrene, dienes, methacrylates, oxiranes, thiiranes, lactones and cyclic siloxanes.<sup>71-73</sup> A–B structures are generally obtained by sequential addition of the monomers, either by adding directly the second monomer to the living first block or by end-capping the first block with 1,1-diphenylethylene in order to avoid different side reactions, as reported in the synthesis of PS–PMMA. A–B–A structures can be obtained either with anionic difunctional organometallic initiators or by coupling the living AB copolymer with suitable difunctional reagents, like phosgene, dihalides, esters, etc.<sup>71</sup>

### 2.3.4 Butyl rubber (polyisobutylene-co-isoprene) (PIB-co-PIP)

Butyl rubber is a copolymer of isobutylene and isoprene and was developed in the 1940s. It is a very important commercial elastomer with many desirable physical properties, such as low air permeability and broad damping properties. The principal uses of this material are in the tyre industry using chlorobutyl rubber for the preparation of inner tubes and inner liners for passenger cars. Despite these unique properties, there are some deficiencies associated with this polymer, mainly poor compatibility with other materials, including elastomers, plastics and carbon black. This poor compatibility greatly limits the application of butyl rubber in many application areas.



Scheme 2.45 Structure of polyisobutylene-co-isoprene.

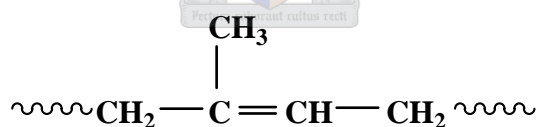
In fact, the improvement of interfacial adhesion among butyl rubber, general-purpose rubbers and carbon black has been an intense research area for some time.<sup>74</sup>

### 2.3.5 Polyisoprene (PIP)

Polyisoprene is made by solution polymerization of isoprene (2-methyl-1,3-butadiene). Polyisoprene compounds, like those of natural rubber, exhibit good tensile strength, good hysteresis, and good hot tensile and hot tear strength. The characteristics, which differentiate polyisoprene from natural rubber, arise from the former's closely controlled synthesis: polyisoprene is chemically purer it does not contain the proteins and fatty acids of its natural counterpart and its molar mass is lower.

Polyisoprene is added to styrene butadiene rubber (SBR) compounds to improve tear strength, tensile strength, and resilience, while decreasing heat build-up. Because of polyisoprene's high purity and high gum (unfilled) tensile strength of its compounds, it is widely used in medical goods and food-contact items. These include baby bottle nipples, milk tubing, and hospital sheeting.

Polyisoprene is typically used in favour of natural rubber in applications requiring consistent cure rates, tight process control, or improved extrusion, moulding, and calendaring. Tyres are the leading consumer. The synthetic elastomer can be produced with a very low level of branching, high molar mass, and relatively narrower molar mass distribution, that contributes to lower heat build up compared to natural rubber.<sup>75</sup>



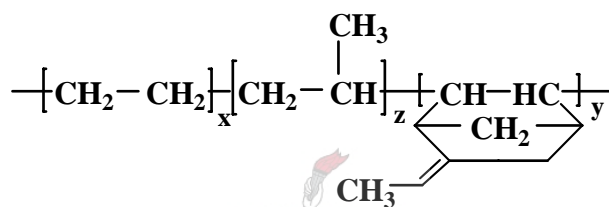
Scheme 2.46 Structure of polyisoprene.

### 2.3.6 Ethylene propylene rubbers (EPDM)

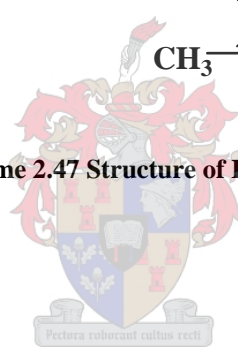
The first commercial ethylene propylene rubbers were made by the random copolymerization of ethylene and propylene in solution using Ziegler-Natta catalysts.<sup>76</sup> The dienes most commonly used today to make the ethylene propylene diene polymers (EPDM) are 1,4 hexadiene, ethylidene, norbornene and dicyclopentadiene, each conferring a different rate and state of cure to the polymer.

In general, the ethylene propylene rubbers are compounded to provide good low-temperature flexibility, high tensile strength, high tear and abrasion resistance, excellent weatherability (ozone, water, and oxidation resistance), good electrical

properties, high compression set resistance, and high heat resistance. Many different types of EPDM are available with different properties. The ethylene amount ranges between 45 (amorphous types) to 55–60 wt% (semi-crystalline types) and 70 wt% (crystalline types). For EPDM with an ethylene-percentage below 50 wt%, the crystalline fraction is zero, but it can increase to 20% for EPDM containing 80 wt% ethylene. The high molecular mass crystalline EPDM can incorporate high levels of fillers. Ethylene propylene rubber (EPMs) and EPDM have low resistance to hydrocarbon oils and their lack of building tack must be compensated for by the use of resin.<sup>74, 75</sup> In this work, the EPDM with 5-ethylidene-2-norbornene content of 9.2 %, as shown in Scheme 2.47 was used.



Scheme 2.47 Structure of EPDM.

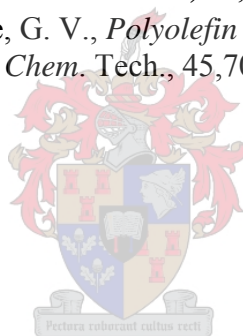


## 2.4 References

1. Brown, H. C.; Ramachandran, P. V. *Pure Appl. Chem.* **1994**, 66, 201.
2. Frankland, E. *J. Chem. Soc.* **1862**, 15, 363.
3. Brock, W. H.; Jensen, K. A.; Jorgensen, C. K.; Kauffman, G. B. *Polyhedron* **1983**, 2, 1.
4. Schlesinger, H. I.; Brown, H. C.; Gilbreath, J. R.; Katz, J. J. *J. Am. Chem. Soc.* **1953**, 75, 195.
5. Brown, H. C.; Schlesinger, H. I.; Sheft, I.; Ritter, D. M. *J. Am. Chem. Soc.* **1953**, 75, 192.
6. Brown, H. C.; Subba Rao, B. C. *J. Am. Chem. Soc.* **1956**, 78, 5694.
7. Brown, H. C.; Subba Rao, B. C. *J. Am. Chem. Soc.* **1956**, 78, 2582.
8. Logan, T. J.; Flautt. *ibid.* **1960**, 82, 3146.
9. Brown, H. C.; Zweifel, G. *ibid.* **1961**, 83, 3634.
10. Pasto, L.; Cheng. *J. Am. Chem. Soc.* **1972**, 94, 6083.
11. Pinazzi, C.; Brosse, J.; Pleureaux, A. *Appl. Polym. Symp.* **1975**, 26, 73.
12. Nelson, D. J.; Brown, H. C. *J. Am. Chem. Soc.* **1982**, 104, 4907.
13. Chung, T. C. *J. Polym. Sci., Part A: Polym. Chem.* **1989**, 27, 3251.
14. Chung, T. C.; Janvikul, W.; Lu, H. L. *J. Am. Chem. Soc.* **1996**, 118, 705.
15. Chung, T. C.; Jiang, G. J. *Macromolecules* **1992**, 25, 4816.
16. Chung, T. C.; D, R.; Jiang, G. J. *Macromolecules* **1993**, 26, 3467.
17. Chung, T. C.; Lu, H. L.; Janvikul, W. *Polymer* **1997**, 38, 6, 1495.
18. Chung, T. C.; Janvikul, W.; Bernard, R.; Hu, R.; Li, C. L.; Liu, S. L.; Jiang, G. J. *Polymer* **1995**, 36, 3565.
19. Chung, T. C.; Janvikul, W.; Bernard, R.; Jiang, G. J. *Macromolecules* **1994**, 27, 26.
20. Chappell, M. D.; Harris, C. R.; Kuduk, S. D.; Balog, A.; Wu, Z.; Zhang, F.; Lee, C. B.; Stachel, S. J.; Danishefsky, S. J.; Chou, T.-C.; Guan, Y. *J. Org. Chem.* **2002**, 67, 7730.
21. Fuwa, H.; Kainuma, N.; Tachibana, K.; Sasaki, M. *J. Am. Chem. Soc.* **2002**, 124, 14983.
22. Collier, P. N.; Campbell, A. D.; Patels, I.; Raynham, T. M.; Taylor, R. J. K. *J. Org. Chem.* **2002**, 67, 1802.
23. Jeon, J.-K.; Uchimaru, Y.; Kim, D.-P. *Inorg. Chem.* **2004**, 43, 4796.
24. Brown, H. C.; Hamaoka, T.; Ravindran, N. *J. Am. Chem. Soc.* **1973**, 95, 6456.
25. Bernard, P. J.; Amedia Jr, J. C.; Fountain, M.; Van Wagenen Jr, G. *Synth. Commun.* **1999**, 14, 2377.
26. Boal, J. H.; Wilk, A.; Scremin, C. L.; Gray, G. N.; Phillips, L. R.; Beaucage, S. L. *J. Org. Chem.* **1996**, 61, 8617.
27. Salunkhe, A. M.; Burkhardt, E. R. *Tetrahedron Lett.* **1997**, 38, 1520.
28. Wilkinson, H. S.; Tanoury, G. J.; Wald, S. A.; Senanayake, C. H. *Org. Process Res. Dev.* **2002**, 6, 146.
29. Hutchins, R. O.; Learn, K.; Nazer, B.; Pytlewski, D.; Pelter, A. *Org. Prep. Proc. Int* **1984**, 16, 335.
30. Smith, W. B. *J. Org. Chem.* **1984**, 49, 3219.

31. David, H.; Dupuis, L.; Guillerez, M. G.; Guibe, F. *Tetrahedron Lett.* **2000**, 41, 3335.
32. Gomez-Martinez, P.; Dessolin, M.; Guibe, F.; Albericio, F.; Trans, P. *J. Chem. Soc. B.* **1999**, 1, 2871.
33. Lipshutz, B. H. *Org. Lett.* **2001**, 3, 4145.
34. Hirokawa, T. *Org. Process Res. Dev.* **2002**, 6, 28.
35. Wu, P. L.; Chen, H. C.; Line, M. L. *J. Org. Chem.* **1997**, 62, 1532.
36. Marcantoni, E. *J. Org. Chem.* **1998**, 63, 3624.
37. Zaidlewicz, M.; Wilkinson, G.; Stone, F. G. A.; Abel, E. W. *Pergamon: Oxford* **1982**, 7, 199.
38. Chappell, M. D.; Harris, C. R.; Kuduk, S. D.; Balog, A.; Wu, Z.; Zhang, F.; Lee, C. B.; Stachel, S. J.; Danishefsky, S. J.; Chou, T. C.; Guan, Y. *J. Org. Chem.* **2002**, 67, 7730.
39. Heald, R. A.; Stevens, M. F. G. *Org. Biomol. Chem.* **2003**, 1, 3377.
40. Collier, P.; Campbell, A. D.; Patel, I.; Raynham, T. M.; Taylor, R. J. K. *J. Org. Chem.* **2002**, 67, 1802.
41. Burg, A. B.; Wagner, R. I. *J. Am. Chem. Soc.* **1954**, 76, 3307.
42. Coyle, T. D.; Kaesz, H. D.; Stone, F. G. A. *J. Am. Chem. Soc.* **1959**, 81, 2989.
43. Brown, H. C. 1981, US Patent 4298750.
44. Richter, F.; Frederick; Augustine; Koft, E.; Emmet Reid, J. E. *J. Am. Chem. Soc.* **1952**, 74, 4076.
45. Brown, H. C.; Midand, M. M.; Kabalka, G. W. *J. Am. Chem. Soc.* **1971**, 93, 1024.
46. Rahtke, M. W.; Inoue, N.; Vaema, K. R.; Brown, H. C. *J. Am. Chem. Soc.* **1966**, 88, 2870.
47. Kabalka, G. W.; Gooch III, E. E. *J. Org. Chem.* **1980**, 45, 3578.
48. Brown, H. C., *Organic syntheses via boranes*. John Wiley and Sons New York, 1975.
49. Zweifel, G.; Brown, H. C. *Org. React.* **1963**, 13, 1.
50. Kalsi, P. S., *Organic Reactions and Their Mechanisms*. 2 ed.; New Age International: New Delhi, 2000.
51. Allies, P. G.; Brindley, P. B. *J. Chem. Soc.* **1969**, (B), 1126.
52. Brown, H. C.; Midland, M. M. *Chem. Commun.* **1971**, 699.
53. Davies, A. G.; Roberts, B., P. *J. Chem. Soc. B.* **1969**, 311.
54. Krusic, P. J.; Kochi, J. K. *J. Am. Chem. Soc.* **1969**, 91, 3942.
55. Mikhailov, B.; Bubnov, Y., *Organoboron Compounds in Organic Synthesis*. Harwood Academic Science: New York, 1984.
56. Zweifel, G.; Brown, H. C. *J. Am. Chem. Soc.* **1964**, 86, 393.
57. Zweifel, G.; Brown, H. C. *Org. React.* **1964**, 13, 1.
58. Brown, H. C.; Rothberg, I.; Vander jagt, D. L. *J. Org. Chem.* **1972**, 37, 4098.
59. Brown, H. C.; Midand, M. M. *J. Am. Chem. Soc.* **1971**, 93, 4078.
60. Brown, H. C.; Zweifel, G. *J. Am. Chem. Soc.* **1966**, 88, 1433.
61. Brown, H. C.; Moerikofer, A. W. *J. Am. Chem. Soc.* **1963**, 85, 2063.
62. Brown, H. C.; Bigley, D. B.; Arora, S. K.; Yoon, N. M. *J. Am. Chem. Soc.* **1970**, 92, 1761.

63. Knights, E. F.; Brown, H. C. *J. Am. Chem. Soc.* **1968**, 90, 5250.
64. Brown, H. C.; Knights, E. F.; Scouten, C. G. *J. Am. Chem. Soc.* **1974**, 96, 7765.
65. Brown, H. C.; Moerikofer, A. W. *J. Am. Chem. Soc.* **1961**, 83, 3417.
66. Turner, R. E.; Meador, W. R. *J. Am. Chem. Soc.* **1957**, 79, 4133.
67. Brown, H. C.; Moerikofer, A. W. *J. Am. Chem. Soc.* **1962**, 84, 1478.
68. Brown, H. C.; Klender, G. J. *Inorg. Chem.* **1962**, 1, 204.
69. Mikhailov, B. M.; Bubnov, Y. N.; Kiselev, V. G. *J. Gen. Chem. USSR.* **1966**, 36, 65.
70. Midland, M. M. *Chem. Rev.* **1989**, 89, 1553.
71. Riess, G.; Hurtrez, G.; Bahadur, P., *Encyclopedia of polymer science and engineering*. New York: Wiley: 1985; Vol. 7, 551.
72. Riess, G.; Dumas, P.; Hurtrez, G., *Block copolymer micelles and assemblies*. MML series 5, London: Citus Books; 2002. 69–110.
73. Quirk, R.; Kinning, D.; Fetters, L., *Comprehensive polymer science*. Oxford, 1989; 1.
74. Ciesielski, A., *An Introduction to Rubber Technology*. 1<sup>st</sup>ed, Rapra Technology Limited: 1999.
75. Sisson, J. *Rubber and Plast. News* **1997**, 26, 21.
76. Baldwin, F. P. and Strate, G. V., *Polyolefin Elastomers Based on Ethylene and Propylene*, in *Rubber Chem. Tech.*, 45,709. 1972.





## Chapter 3

### Synthesis of graft and block copolymers

#### 3.1 Introduction

The potential of boron chemistry was reported by emphasizing the extreme importance of boron functional polymers and the versatility with which graft and block copolymers can be synthesized.<sup>1</sup> In my research endeavour boron chemistry was used to investigate the polymerization of different monomers such as methyl methacrylate (MMA) and styrene (St) and to product graft copolymers using the “grafting from technique”. Characterizations of the products were necessary in order to follow the respective reactions. Extensive use was made of characterizations by specialized techniques such as gradient HPLC.

The research was initiated by first studying the hydroboration of a model compound 2-hexene in order to determine the optimal conditions for the grafting reactions. The model compound was subsequently used as a macroinitiator and facilitated initiation and polymerization of MMA.<sup>2</sup>

The hydroborated product was used to initiate MMA block formation. The “grafting from” polymerization reactions were subsequently carried out with polymers with different levels of unsaturation. Hydroboration of low unsaturated poly(isobutylene-co-isoprene) with 1.6 mol% of double bonds proved to be difficult owing to the relatively small number of double bonds present in the polymer backbone. To increase the number of incorporated monomer molecules into the rubber, highly unsaturated polyisoprene (98% cis 1,4 content) was used. The major difficulty faced here was the possibility of cross-linking due to the abundance of double bonds present.

To overcome this problem standard grade ethylene-propylene-5-ethylidene-2-norbornene rubber (EPDM) with 9.2 mol% of double bonds was used as intermediate unsaturated polymer. To conclude, hydroboration of vinyl-terminated polystyrene was investigated.



## **3.2 Materials**

The following materials were used as received from the suppliers:

2-hexene (99.9%, Sigma-Aldrich), butyl rubber BR365 (1.6 mol% of double bonds, ExxonMobil), polyisoprene (98.2 mol% of cis 1,4 content, Karbochem), ethylene-propylene-diene (2-norbornene) (EPDM) rubber (9.2 mol% of double bonds, ExxonMobil), 9-BBN (Sigma-Aldrich), 2-propanol 99.8% and methanol 99.9%, (Sigma-Aldrich) hydrogen peroxide (30 wt% aqueous solution,) and sodium hydroxide, n-butyllithium (15% in hexane, Aldrich), benzophenone (Sigma), allylchloro-dimethylsilane, (97%, Aldrich,), i-octane (2,2,4-tri-methylpentane) and cyclohexane (Sigma-Aldrich, HPLC grade).

HPLC grade tetrahydrofuran and toluene (99.9%, both Sigma-Aldrich) were dried with molecular sieves for more than 24 hrs and subsequently distilled from sodium and benzophenone under an argon atmosphere. Acetone (99.9%, Aldrich) was used as received, without further purification.

Styrene and methyl methacrylate (both Plascon Research) were purified as explained in Section 3.2.2.

The drying agents calcium hydride, magnesium sulphate and potassium hydroxide solution were purchased from Aldrich and stored in desiccators, under nitrogen, until required. Sodium metal was acquired from the same source and stored under mineral oil.

NMR solvent: deuterated chloroform (Cambridge Isotope Laboratories) was used as received for all NMR experiments, unless otherwise stated.

### **3.2.1 Purifications of solvents**

Tetrahydrofuran was purified by distillation from sodium and benzophenone, under argon. It was boiled under reflux for 10 hrs to allow the sodium metal a chance to dry the solvent. When dry, the solution will have a deep blue to blue-green colour. The purified fraction was immediately used after distillation.

Toluene was purified under similar conditions as used for the purification of the THF.

### **3.2.2 Purification of monomers**

Styrene and methyl methacrylate were washed with a 0.3 M potassium hydroxide solution to remove the hydroquinone inhibitor. The monomers were then distilled under reduced pressure at 55 °C, to avoid polymerization. The distilled monomers were stored on molecular sieve at - 4 °C, until required.

### **3.3 Experimental conditions**

All reactions were performed under a purified argon or nitrogen atmosphere. All glassware, syringes and needles were oven dried at 140 °C for 12 hrs. The glassware was assembled hot and cooled under a stream of dry nitrogen. Syringes were assembled and fitted with needles while hot and then cooled as assembled units.

### **3.4 Experimental reaction procedures**

Reactions were carried out to determine and optimize the reaction conditions, firstly starting with the 2-hexene and secondly with the PS macromonomer (vinyl terminated).

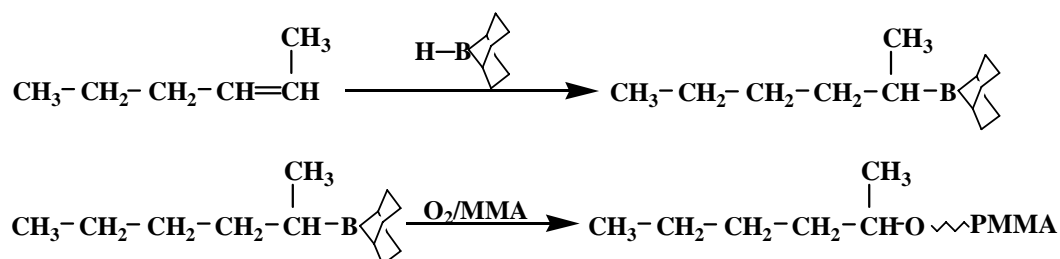
#### **3.4.1 Synthesis of (2-hexenyl-9-BBN)**

Under an argon atmosphere, in a 100-ml flask, 11 ml (0.67 g) of 9-BBN (0.5 M) in THF solution (5.5 mmol of 9-BBN) was allowed to react with 1 ml of 2-hexene (excess) at room temperature for 3 hrs. After the reaction, the excess 2-hexene and THF were removed by vacuum distillation at room temperature. The product (2-hexenyl-9-BBN) was further distilled at 90 °C.

#### **3.4.2 Synthesis of poly(methyl methacrylate-2-hexyl)**

The hydroborated 2-hexene in THF solution was used directly for the graft reaction at room temperature. Purified methyl methacrylate (5.5 ml, 52.0 mmol) was dissolved in 10 ml THF. The initiator, 2-hexenyl-9-BBN (1 g, 5.20 mmol), was transferred into the flask, under argon gas. The polymerization was initiated by allowing air and oxygen to diffuse into the flask through an air-tight septum. The reaction was allowed to progress at room temperature for 48 hrs. Thereafter the reaction mixture was exposed to air for another 2 hrs.

The homopolymer of poly(methyl methacrylate) was subsequently precipitated with isopropanol and vacuum dried overnight. Proton NMR analysis was used to confirm the structure of 2-hexenyl-9-BBN-PMMA. Scheme 3.1 shows the synthesis of 2-hexenyl-PMMA.



Scheme 3.1 Reaction scheme for the synthesis of 2-hexenyl-PMMA.

### 3.4.3 Synthesis of vinyl-terminated polystyrene macromonomers

Polystyrene macromonomers were synthesized by an anionic polymerization technique in order to achieve narrow polydispersity and control in molecular mass, using the relationship:

$$M_n \text{ (g/mol)} = [\text{styrene (g)}] / [\text{BuLi (mol)}] \quad (3.1)$$

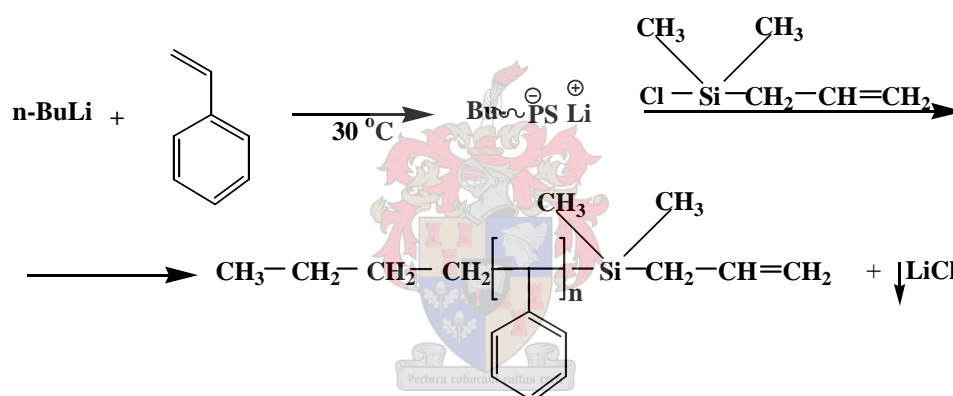
A general procedure for the preparation of the styrene macromonomer vinyl-terminated with allylchloro-dimethylsilane is given by the following example. Under an argon atmosphere, freshly distilled styrene monomer (5 ml) was mixed with 50 ml of toluene solvent which was injected via a syringe into a 100-ml dry round-bottom flask equipped with a magnetic stirrer bar and rubber septum. *n*-Butyllithium (2.5 ml) initiator was added slowly until the characteristic colour (orange) of the styrene anion was achieved, indicating the initiation of the polymerization reaction. The reaction was allowed to proceed for 50 min at 30 °C. Table 3.1 shows the amounts of styrene monomer, butyllithium and termination agent used.

The termination agent used air sensitive hence the reaction was carried out inside a dry box to prevent any contact with air. The reaction was terminated by introduction of an equal amount of terminating agent (0.75 ml) to *n*-BuLi, using a macro syringe, into the reaction mixture. The colour of the reaction mixture immediately became colourless, indicating termination of the polymerization.

**Table 3.1: Anionic polymerization reaction compositions for the synthesis of PS macromonomer using n-butyllithium as initiator and allylchloro-dimethylsilane as termination agent**

Run #	St (mmol)	BuLi (mmol)	Termination agent (mmol)	Mw g/mol From eq (3.1)
1	43.6	0.909	0.909	5000
2	43.6	1.136	1.136	4000
3	43.6	0.757	0.757	6000

The macromonomer was then precipitated in methanol, collected by filtration, and dried overnight under vacuum at room temperature to constant weight. The general preparation reactions of allylchloro-dimethylsilane-polystyrene macromonomers are shown in Scheme 3.2.



**Scheme 3.2 Synthesis of allylchloro-dimethylsilane-polystyrene macromonomers via anionic polymerization.**

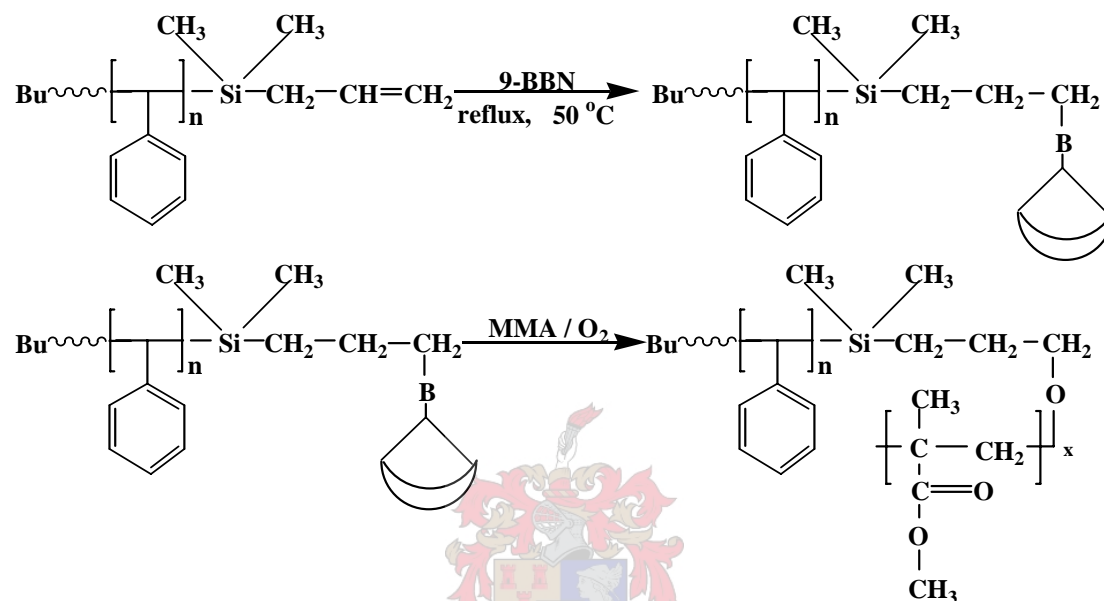
This macromonomer was subsequently used to synthesize block copolymers with methyl methacrylate monomers.

#### 3.4.4 Synthesis of PS-b-PMMA

In a 100-ml round bottom flask, 9-BBN ( $9.4 \times 10^{-3}$  g,  $7.69 \times 10^{-5}$  mmol) was allowed to react with vinyl-terminated polystyrene (0.5 g) at 50 °C for 18 hrs in 15 ml THF. The resulting hydroborated polystyrene in THF solution was used directly for the polymerization reaction. Methyl methacrylate (5.0 g) was mixed with the above-mentioned solution and stirred for 0.5 hrs, after which 0.25 ml of O<sub>2</sub> was injected into the reaction flask. After every hour of stirring another 0.25 ml of O<sub>2</sub> was added, until a

total amount of about  $\pm 2$  ml oxygen was injected. Scheme 3.3 shows synthesis of PS-b-PMMA.

The solution was stirred at room temperature for an additional 24 hrs before termination by precipitation in 50 ml methanol. The crude product was washed twice with extra methanol before drying in a vacuum oven at 45°C for 24 hrs. The product was characterized by  $^1\text{H}$  NMR, SEC and HPLC.



Scheme 3.3 Reaction scheme of the synthesis of PS-b-PMMA.

### 3.4.5 Hydroboration reaction of butyl rubber with 9-BBN.

Commercial butyl rubber, poly(isobutylene-co-isoprene) (1 g), containing 1.6 mol% of isoprene was dissolved in 50 ml THF solvent. A mass of 0.035 g ( $2.86 \times 10^{-4}$  mol%) of 9-BBN crystals was added to the polymer/THF solution and the hydroboration reaction allowed to proceed. Owing to the good solubility of borane reagents and borane-containing polymers, the hydroboration reaction of the polymer is very similar to a reaction of small organic compounds. To ensure complete hydroboration of the internal double bonds, the reaction mixture was boiled under reflux at 70 °C for 18 hrs. In most cases the resulting crude hydroborated butyl rubber in THF solution was used directly for the “graft-from” reaction, to prepare butyl rubber graft copolymers.

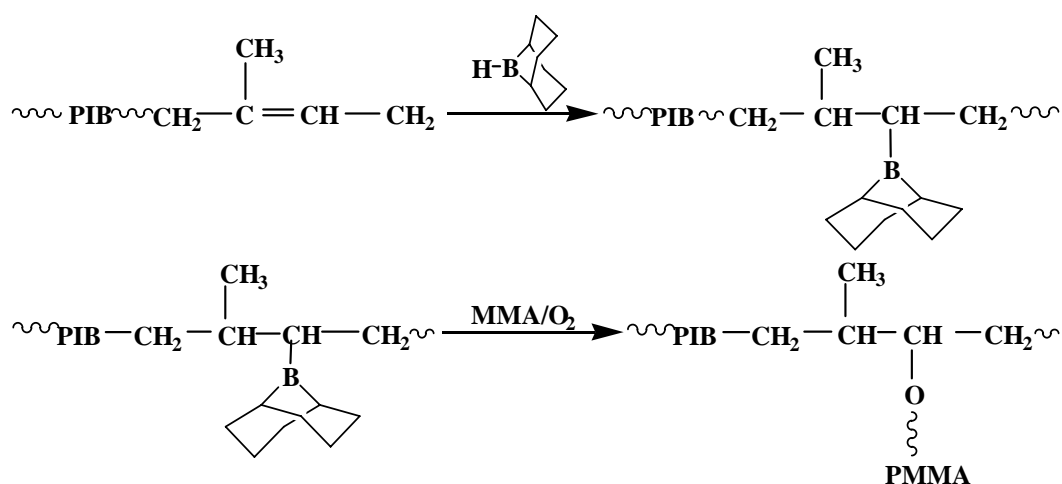
### 3.4.6 Synthesis of methylmethacrylate grafted butyl rubber (PIB-g-MMA)

The resulting crude product of the hydroboration of butyl rubber in THF solution in Section (3.4.5) was used directly for the graft reaction at room temperature. Methyl methacrylate monomer (5.0 g) was mixed with the hydroborated butyl rubber solubilized in THF. The solution was stirred for 0.5 hrs at room temperature. Oxygen was slowly introduced so that at any time  $[O_2] \ll [B]$ . Dry  $O_2$  (0.6 ml) was injected into the reaction flask (20% oxygen is required for  $[O_2]:[B]$  0.5:1). After one hour of stirring, another 0.6 ml of  $O_2$  was added. The same procedure was repeated hourly, for a total of five injections, until a total amount of 3.5 ml of oxygen had been injected.

The solution was stirred at room temperature for an additional 24 hrs before termination by precipitation into 150 ml isopropanol. The isopropanol was decanted and the product washed several times with additional isopropanol, followed by drying in a vacuum oven at 45 °C for 24 hrs.

The extraction processes were carried out by the Soxhlet method. Firstly the homopolymer of butyl rubber was extracted with hexane. Homopolymer PMMA was extracted with acetone and the synthesized graft copolymer, PIB-g-MMA, was extracted with THF.

$^1H$  NMR, FTIR, SEC and HPLC analyses were carried out in order to characterize the resulting graft copolymers. Results are given in Section 4.6. The reaction scheme for PIB-g-MMA is shown in Scheme 3.4.



Scheme 3.4 Reaction scheme for the polymerization of butyl rubber

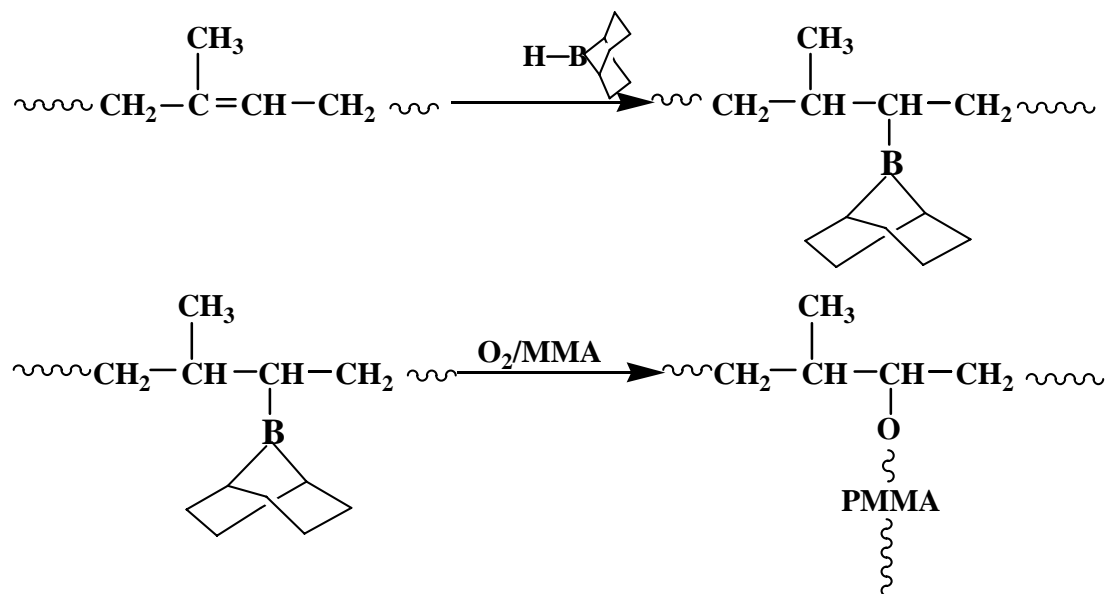
### **3.4.7 Hydroboration reaction of polyisoprene**

Polyisoprene (98% cis-1,4 content, 1.0 g) was dissolved in 50 ml of THF solvent. Hydroboration was carried out under heterogeneous reaction conditions to hydroborate 80% of the double bonds. 9-BBN crystals (1.4 g, 11.45 mmol%) was added to the THF solution. Owing to the good solubility of borane reagents and borane-containing polymers, the hydroboration reaction of the polymer is very similar to reactions of small organic compounds. To ensure complete hydroboration of the internal double bonds, the reaction mixture was boiled under reflux at 65 °C for 18 hrs, under an argon atmosphere. In most cases the resulting hydroborated polyisoprene in THF solution was used directly for the “graft-from” reaction, to prepare polyisoprene graft copolymers.

### **3.4.8 Synthesis of graft copolymer of polyisoprene rubber with methylmethacrylate (PIP-g-PMMA)**

The resulting hydroborated polyisoprene in THF solution was used directly for the graft reaction. Methyl methacrylate (5.0 g) was mixed with the hydroborated polyisoprene solubilized in THF (prepared as described in section 3.4.7) under a nitrogen atmosphere and the solution stirred for 0.5 hrs. The reaction was initiated by injecting dry O<sub>2</sub> (11.5 ml,  $5.87 \times 10^{-6}$  mol% relative to double bonds) into the reaction flask. After every hour of stirring another 11.5 ml of O<sub>2</sub> was added until a total amount approximately 69 ml of oxygen was added.

The solution was stirred at room temperature for an additional 24 hrs before termination by precipitation into methanol. The methanol was decanted and the product washed several times with additional methanol before drying in a vacuum oven at 45 °C for 24 hrs. Scheme 3.5 shows the reaction of the synthesis of polyisoprene-g-PMMA. The resulting graft copolymer was characterised by <sup>1</sup>H NMR, SEC and HPLC analyses (see Chapter 4.5)



Scheme 3.5 Reaction scheme of the synthesis of polyisoprene-g-PMMA.

### 3.4.9 Hydroboration reaction of EPDM rubber with 9-BBN

EPDM (1 g, 9.2 mol% double bond content) was dissolved in THF (50 ml) at 70 °C under an argon atmosphere.

Hydroboration was carried out under heterogeneous reaction conditions by adding 9-borabicyclononane (0.15 g, 1.23 mmol%) into the THF solution of the solution. Owing to the good solubility of borane reagents and borane-containing polymers, the hydroboration reaction of the polymer is very similar to that of small organic compounds. To ensure complete hydroboration of the internal double bonds, the reaction was run for 18 hrs at 70 °C. In most cases the resulting hydroborated EPDM in THF solution was used directly afterwards to prepare EPDM graft copolymers.

### 3.4.10 Synthesis of graft copolymer of ethylene propylene rubber with methylmethacrylate EPDM-g-PMMA

The resulting hydroborated EPDM in THF solution Section (3.4.9) was used directly for graft reactions at room temperature. Methyl methacrylate monomer (0.5 g) was mixed with the above. The solution was stirred for 0.5 hrs, after which 2.5 ml of  $\text{O}_2$  was injected into the reaction flask. After every hour of stirring another 2.5 ml of  $\text{O}_2$  was added, until a total amount of 15 ml oxygen was injected.

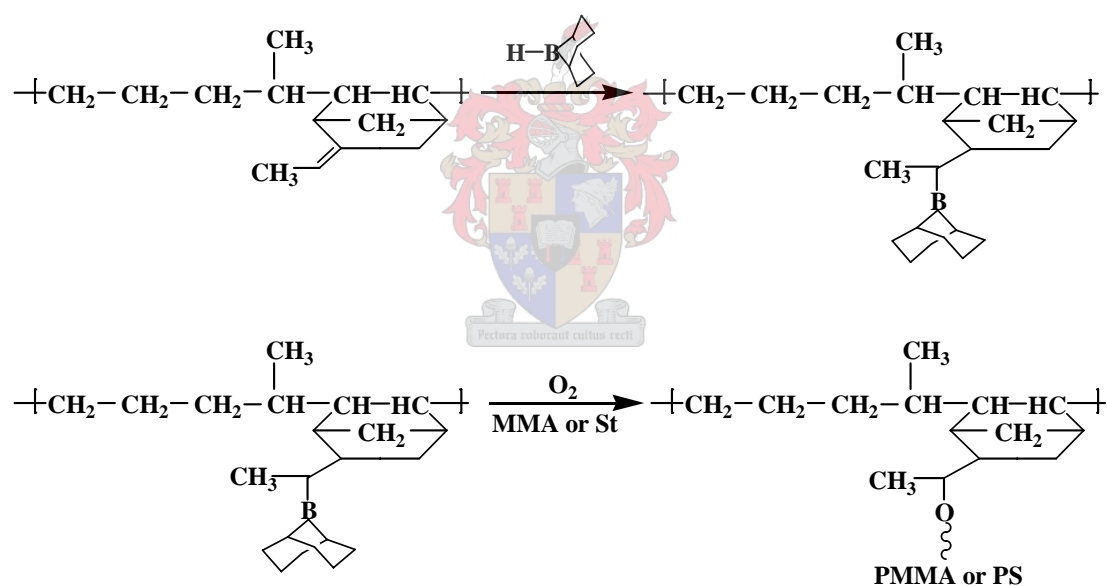


The solution was stirred at room temperature for an additional 24 hrs before termination by precipitation into 150 ml isopropanol. The isopropanol was decanted and the product washed several times with additional isopropanol before drying in a vacuum oven at 45 °C for 24 hrs. The product was characterised by SEC, <sup>1</sup>H-NMR and HPLC analyses

### 3.4.11 Synthesis of graft copolymer of ethylene propylene rubber with polystyrene EPDM-g-PS

EPDM-g-PS was prepared under similar reaction condition as used for EPDM-g-PMMA. The EPDM graft copolymers were separated from the polymerization solution by filtration.

The mixture of polymers was further separated into its components by the Soxhlet extraction method.



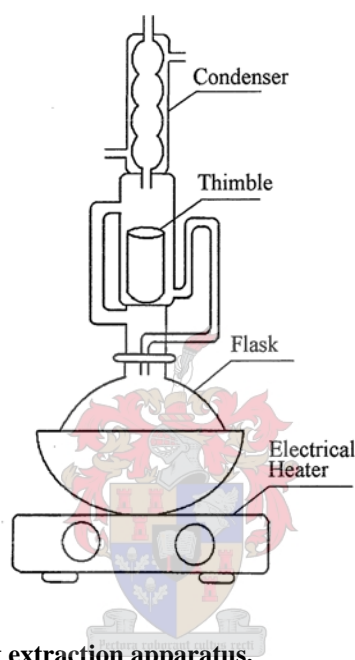
Scheme 3.6 Reaction scheme for the synthesis of EPDM-g-PMMA/PS.

### 3.5 Soxhlet extraction of insoluble polymer fractions

After synthesis of the graft copolymers the mixtures of products were further separated into their respective components by the Soxhlet extraction method. Soxhlet extractions were used to separate polymer fractions differing in solubility. The Soxhlet extractions were used with three different solvents: in this study hexane was used to remove different rubber homopolymers (e.g, poly(isobutylene-co-isoprene), polyisoprene and EPDM), and acetone for PMMA or PS homopolymer removal.

The graft copolymer fraction, soluble in THF solvent, was precipitated in methanol, dried and characterized. The remaining polymers were considered as gels (crosslinked). The mass of insoluble material can be determined by subtracting the mass of the thimble before extraction from the mass of the thimble after extraction.

Figure 3.1 illustrates the Soxhlet apparatus used in this study. In this design the solvent under reflux condenses over a solid sample in the thimble, dissolving the soluble fraction and leaving the insoluble fraction in the thimble.



**Figure 3.1: Conventional Soxhlet extraction apparatus.**

### **3.6 Crosslink density**

In general, the rubber networks contain gel and sol. Gel is insoluble in solvent and sol is soluble and extractable from rubber. The gel fractions of the samples were measured by a Soxhlet extraction method using benzene as a solvent. This technique was used to remove the sol from the rubber network.

Approximately 1g of the crosslink sample (gel fraction) was put into a Whatman cellulose extraction thimble in the extractor. The crosslink density can be determined from the average molecular mass of the network chain, i.e. the average chain length between two crosslink network junctions. This can be expressed either by the average molecular mass between crosslinks ( $M_c$ ) or by the number of the network chains per unit volume ( $V_e$ ).

Crosslink density was measured as a function of solvent evaporation time in air.

$$V_r = \left( \frac{m_r / \rho_r}{\left( \frac{m_r}{\rho_r} + \frac{m_s}{\rho_s} \right)} \right) \quad (3.2)$$

where  $V_r$  is the volume fraction of the rubber network in the swollen gel,  $m_r$  is the mass (g) of rubber after deswelling,  $m_s$  is the solvent mass (g) at equilibrium swelling,  $\rho_r$  is the density of rubber, and  $\rho_s$  is the density of solvent.

The  $V_r$  value can be used to calculate the crosslink density (1/Mc) using the Flory-Rehner equation.

$$\frac{1}{Mc} = \left( \frac{-[\ln(1 - V_r) + \chi \cdot V_r^2 + V_r]}{\rho_r \cdot V_{m,s} \left( V_r^{1/3} - \frac{V_r}{2} \right)} \right) \quad (3.3)$$

where  $Mc$  (g/mol),  $\chi$  is the molar volume of the solvent, and  $V_{m,s}$  is the molar volume of the solvent.

The swelling of solvent is controlled by the entropy of the dilution of the polymer-solvent by the polymer chains assuming elongated configurations, but constrained by the crosslinks of the polymer networks.

### 3.7 Characterization

#### 3.7.1 Nuclear magnetic resonance (NMR) spectroscopy

Proton NMR spectra were used to determine the chemical compositions and the extent of reaction of monomers and copolymers. All samples were recorded in  $CDCl_3$  solvent, using a Varian Unity Inova 400 NMR instrument, or a Varian VXR 300 MHz NMR instrument.

#### 3.7.2 High-performance liquid chromatography (HPLC)

HPLC is used to separate molecules under high pressure in a stainless steel column filled with a suitable matrix. By choosing suitable combinations of solvents and columns we can achieve a successful separation into three different fractions. The solvent/nonsolvent combination is an important parameter in gradient HPLC. The

separation takes place with respect to the polarity of the different components. The nonpolar polymer elutes as the first component from the stationary phase, and it is followed by the graft copolymer and the PMMA homopolymer, which is the most polar component in the product.

The gradient HPLC system comprised a Waters 2690 separation module Alliance equipped with a Nucleosil CN column, pore size 100 Å, particle size 5µm, 12.5×4 (ID) cm. A constant column temperature of 40 °C was maintained through the use of an oven. Two different mobile phase flow rates were used: 0.5 ml/min for polyisobutylene and EPDM, and 1 ml/min for polyisoprene. The detector used was an evaporative light scattering detector (ELSD) PL-ELS 1000 from Polymer Labs, which was operated at 80 °C, with an N<sub>2</sub> carrier gas flow rate of 1 SLM (standard litres per minute). Data collection and processing were performed using PSS Win GPC7 from Polymer Standards Service<sup>3</sup>.

The separation of the complex mixture with respect to the CCDs of the different species can be achieved by gradient HPLC. To determine the CCD of the graft copolymers THF/i-octane or cyclohexane gradient was used, as the mobile phases and a cyano-modified silica gel (Nucleosil CN) as the polar stationary phase<sup>4-6</sup>.

In gradient HPLC, the effects of precipitation and adsorption are combined, and can be used for the separation of different components; at the beginning of the gradient elution starts with a nonsolvent for the polar polymer (PMMA). The samples of the graft product are injected into the nonsolvent and precipitate at the column inlet. During the gradient elution, the solvent composition changes stepwise, in time, from a nonsolvent to a good solvent for the polar polymer (PMMA). According to the chemical compositions and molar mass of the copolymers, the polymers will redissolve at a certain solvent composition. This means that the components with different chemical composition will elute at different retention times, and separation will occur.

### **3.7.2.1 Mobile phase**

Chromatograph: THF/i-octane for polyisoprene and THF/cyclohexane for polyisobutylene and EPDM. The stepwise gradient used for the separation of the polyisoprene graft composition started at 100 vol% i-octane and becoming 100 vol% THF. See Figure 3.2 for a visual representation of the gradient. The gradient was

started at 99:1 (v/v) (i-octane:THF), was held constant there for one min, after which it was linearly changed to 34:66 i-octane:THF within 2 mins. Following this, the gradient was held constant for 10 min and thereafter changed linearly to 0:100 i-octane: THF within 2 mins, held constant for 2 mins, then changed to 99:1 (v/v) (i-octane:THF). The flow rate was 1 ml/min.

In the case of butyl rubber and EPDM graft copolymers i-octane was replaced with cyclohexane, with a flow rate of 0.5 ml/min. The gradient was started at 99:1 (v/v) (cyclohexane:THF), held constant for two mins, after which it was linearly changed to 34:66 cyclohexane:THF within 8 mins. Following this, the gradient was held constant for 10 min and thereafter changed linearly to 0:100 cyclohexane:THF within 3 mins, held constant for 5 mins, then changed in two mins to 99:1 (v/v) (cyclohexane:THF).

The chromatograms of the gradient separation for three different graft products

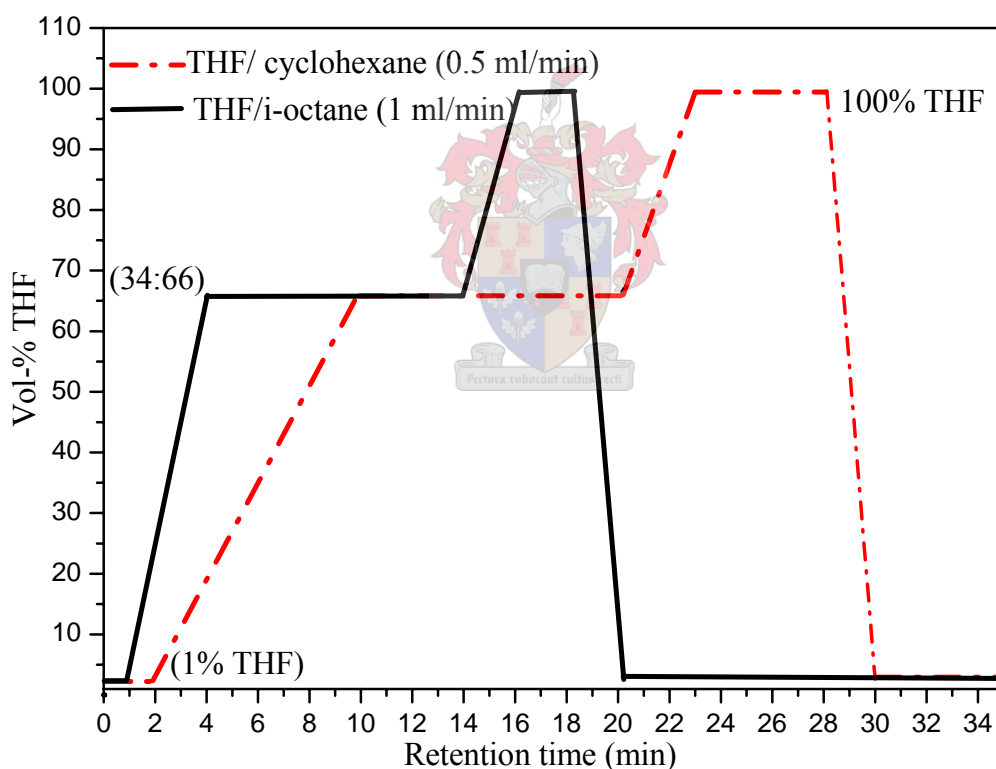


Figure 3.2: Gradient profile for the HPLC separation of the graft products; stationary phase: Nucleosil CN 100 Å, eluent: THF/(i-octane or cyclohexane).

In the case of PS-b-PMMA, different conditions were applied at the critical point of PS.

### **3.7.3 Size-exclusion chromatography (SEC)**

SEC is the most widely used liquid chromatographic technique for the separation of polymers according to their size in solution, or chain length (which can be correlated with molar mass, either from a calibration or using molar mass sensitive detectors).

The SEC system comprises an auto sampler Waters 717 plus, a Waters 600E System Controller, a Waters 610 fluid unit and a Waters 410 differential refractometer as a detector. Two Plgel 5 $\mu$ m Mixed-C columns and a pre-column (Plgel 5 $\mu$ m Guard) were used and the column oven was set at 30 °C. Millennium software was used for data acquisition and data analysis. The volume of the injected samples was 100  $\mu$ L. HPLC-grade THF used as mobile phase at 1 mL/min, polystyrene standards were used for calibration.

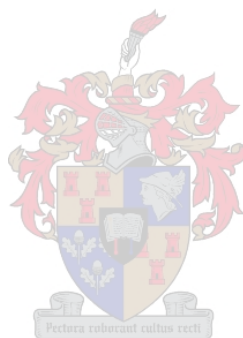
Number average molecular mass ( $M_n$ ) and weight average molecular mass ( $M_w$ ), as well as polydispersity values, were obtained through the use of SEC, using two concentration dependent detectors, UV and RI. The UV detector was adjusted to 254 nm, corresponding to the absorption of the aromatic ring of polystyrene, and 235 nm, for PMMA. This detector therefore only shows a response when there is a styrene or methylmethacrylate unit present in the polymer.

### **3.7.4 Fourier-transform infrared (FTIR) spectroscopy**

FTIR was used to characterize the chemical composition of graft copolymers. IR spectra were obtained using KBr disks. FTIR spectra were recorded on a Perkin-Elmer Spectrum One, in the range 3500-500  $\text{cm}^{-1}$ , with a resolution of 4  $\text{cm}^{-1}$ . Samples were prepared by grinding about 2-5 mg of the graft copolymer (after extraction) with 120 mg KBr, after which it was pressed to form transparent disks. Samples of the homopolymer starting material were also characterized using films.

### 3.8 References

1. Brown, H. C., *Organic syntheses via boranes*. John Wiley and Sons, New York, 1975.
2. Chung, T. C.; Janvikul, W.; Bernard, R.; Hu, R.; Li, C. L.; Liu, S. L.; Jiang, G. J. *Polymer* **1995**, 36, 3565.
3. Christensen, S. F.; Everland, H.; Hassager, O.; Almdal, K. *Int. J. Adhes.* **1998**, 18, 131.
4. Mori, S.; Taziri, H. *J. Liq. Chromatogr.* **1994**, 17, 305.
5. Cools, P. J. C. H.; van Herk, A. M.; Staal, W.; German, A. L. *J. Liq. Chromatogr.* **1994**, 17, 3133.
6. Philipsen, H. J. A.; Klumpermann, B.; German, A. L. *J. Chromatogr., A* **1996**, 13, 727.



## Chapter 4

### Results and discussion

#### 4.1 Introduction

Graft reactions were used to prepare graft copolymers with a rubbery backbone, such as poly(isobutylene-co-isoprene), polyisoprene and EPDM, with several free radical polymerized polymers, such as PMMA and PS, in the side chains. The resulting copolymers can be considered to be potentially interesting materials; they may not only provide materials with a saturated elastic backbone with multiple-phase properties, but also offer low air permeability and broad damping properties in polymer blends and composites. To optimize the hydroboration reaction conditions the model compound 2-hexenyl-9-BBN and the chain extension via novel block formation were considered and subsequently vinyl-terminated polystyrene prepolymers were blocked with methyl methacrylate.

In this study both block and graft formation resulted from an initial hydroboration step of the residual double bonds of the unsaturated polymers followed by copolymerization of the hydroborated polymers in the presence of oxygen and monomers (MMA and styrene). The different graft copolymers that were prepared are now discussed.

#### 4.2 Copolymerization of methyl methacrylate with 2-hexenyl-9-BBN in a continuous reaction

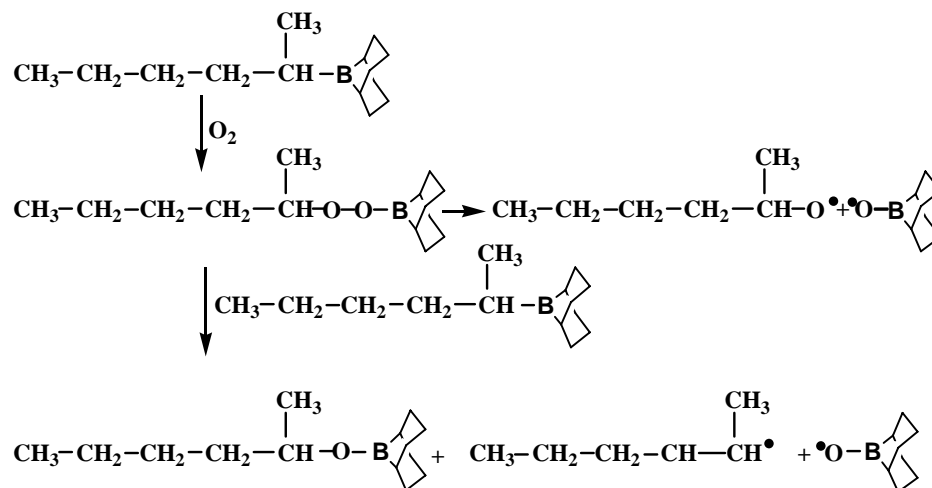
##### 4.2.1 2-Hexenyl-9-BBN

The model compound 2-hexenyl-9-BBN was used to study the hydroboration reaction. Suitable reaction conditions for the selective autoxidation reaction of 2-hexenyl-PMMA had to be determined. 2-hexenyl-9-BBN was prepared from 2-hexene (see Section 3.4.1). The model compound was subsequently used as a macroinitiator and facilitated initiation and polymerization of MMA<sup>1</sup>. Scheme 4.1 illustrates the reaction mechanism of 2-hexenyl-9-BBN preparation, as also described



in Section 2.2.4.1. It was reasonable to predict that during the graft reaction oxygen insertion

into 2-hexenyl-9-BBN starts at the linear alkyl group, instead of the bicyclic ring.



Scheme 4.1: Reaction mechanism of 2-hexenyl-9-BBN preparation

#### 4.2.2 Characterization of polymethylmethacrylate made via 2-hexenyl-9-BBN macroinitiator

<sup>1</sup>H-NMR analysis was used to confirm the structure of PMMA-2-hexenyl prepared as described in Section 3.4.2. Figure 4.1 shows the <sup>1</sup>H-NMR spectra of the following compounds (in CDCl<sub>3</sub> solvent): (a) 2-hexene before hydroboration, (b) 2-hexene after hydroboration (2-hexenyl-9-BBN), and (c) after polymerization in the presence of MMA to form PMMA-2-hexenyl. In Figure 4.1 (a) the chemical shift at 5.45 ppm corresponds to the double bond protons (=CH) in the starting material 2-hexene. In Figure 4.1 (b) the chemical shifts at 0.91 and 1.61 ppm correspond to the methyl groups of the hydrocarbon chain of hexane. The hydroboration of 2-hexene is indicated by the disappearance of the double bond signal at 5.45 ppm, upon hydroboration. The appearance of new chemical shifts between 1.0 and 2.5 ppm corresponds to the methylene units in the basic structure of 9-BBN. Figure 4.1 (c), the <sup>1</sup>H-NMR spectrum of PMMA-2-hexenyl, shows a new peak at 3.62 ppm corresponding to the methoxy groups (CH<sub>3</sub>O) in PMMA. The peaks at 2.1-0.7 ppm are due to the CH<sub>3</sub> and CH<sub>2</sub> protons of PMMA. SEC analysis of PMMA-2-hexenyl yielded a weight-average molecular mass of about 32 400 g mol<sup>-1</sup> for the polymer.

This study confirmed the suitable reaction conditions needed in order to initiate the hydroboration reaction and the polymerization reaction. The results show that, under the conditions used as described, the polymerization reaction could be initiated with 2-hexenyl-9-BBN as macroinitiator.

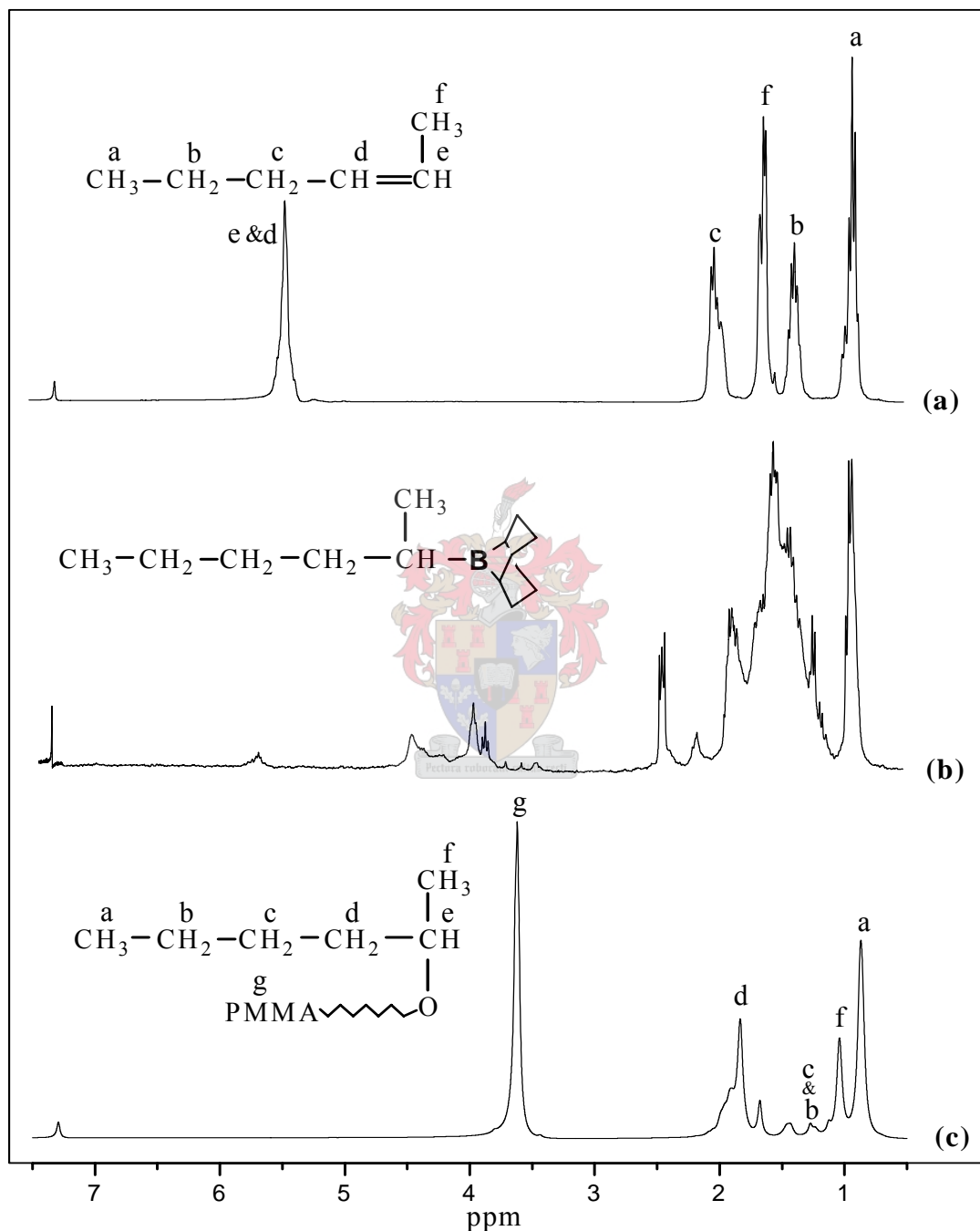


Figure 4.1:  $^1\text{H-NMR}$  spectra of 2-hexene (a) before hydroboration, (b) after hydroboration, and (c) PMMA-2-hexenyl, in  $\text{CDCl}_3$  solvent.

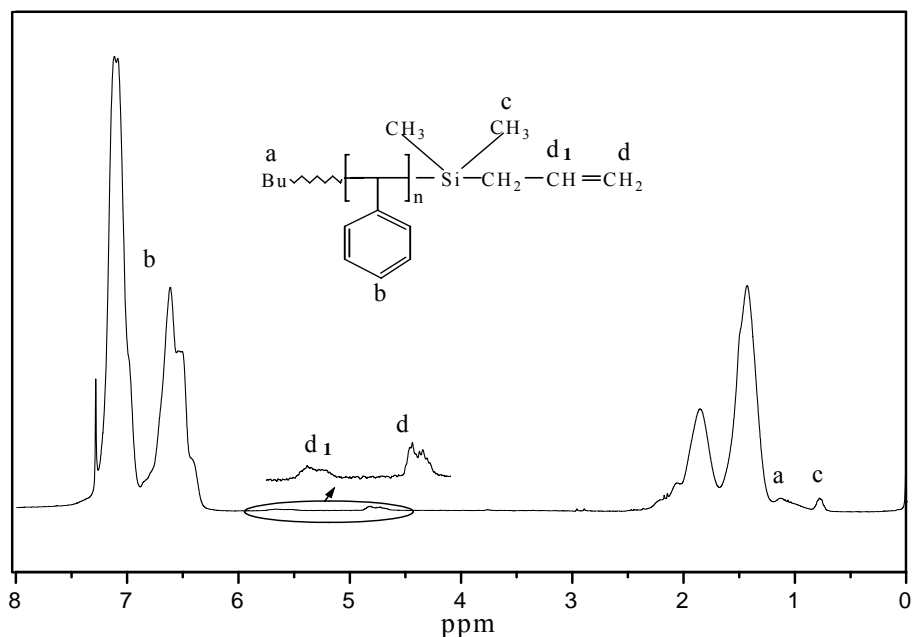
### 4.3 Block copolymer of polystyrene with methyl methacrylate (PS-b-PMMA)

Block copolymerization of vinyl-terminated polystyrene with methyl methacrylate was used to optimize the hydroboration reaction by sequential addition of the MMA monomer onto the hydroborated polystyrene macromonomer at room temperature using  $O_2$  as an initiator. The polystyrene macroinitiators were synthesized by procedures described in Sections 3.4.3 and 3.4.4. These macroinitiator polymers were hydroborated and used for the synthesis of block copolymers by the addition of MMA monomer. The PS-b-PMMA block copolymers were fully characterized by means of liquid chromatography (SEC),  $^1H$ -NMR and FTIR. Complete separation of all components was achieved by HPLC at the critical point of polystyrene as well as the critical point of the PMMA. Use of HPLC at the critical point of PMMA was used in order to distinguish between the block copolymer and PMMA homopolymer.

#### 4.3.1 Synthesis and characterization of polystyrene macromonomer

Styrene macromonomers with different molecular masses terminated by allylchloro-dimethylsilane were synthesized by anionic polymerization as described in Section 3.4.4. Structures and molecular mass of PS macromonomers were confirmed by SEC and  $^1H$ -NMR.

SEC was used to confirm the molecular mass of the PS macromonomer and  $^1H$ -NMR was used to confirm the structure of PS macromonomer. A typical  $^1H$ -NMR spectrum of the polystyrene vinyl-terminated macromonomer is shown in Figure 4.2. It confirms the presence of the terminating agent in the PS chains. The signals at 5.6 and 4.8 ppm, designated as d in the spectrum, correspond to the protons of the double bond of the terminating agent.



**Figure 4.2:** <sup>1</sup>H-NMR spectrum of styrene macromonomer terminated by allylchloro-dimethylsilane, in CDCl<sub>3</sub> solvent.

### 4.3.2 Characterization of PS-b-PMMA by proton nuclear magnetic resonance spectroscopy (<sup>1</sup>H-NMR)

Proton NMR analysis was used to confirm the structure of PS-b-PMMA. Figure 4.3 shows typical <sup>1</sup>H-NMR spectra of the PS macromonomer (a) before hydroboration, (b) after hydroboration and (c) after block formation with PMMA. Figure 4.3 (a) shows the PS vinyl-terminated starting material. The chemical shifts at 5.6 and 4.8 ppm correspond to the olefinic (CH=CH<sub>2</sub>) units of the PS macromonomer, and the chemical shifts around 6.3-7.3 ppm correspond to the aromatic protons.

Figure 4.3 (b) indicates that hydroboration of the PS macromonomer had taken place: the signals at 5.6 and 4.8 ppm disappeared upon hydroboration. Unfortunately the boronated compound is very sensitive to out-oxidation in the presence of air. This means that spectrum 4.3 b had to be taken from a sample removed directly from the reaction mixture and transferred under an inert atmosphere to the NMR tube which is then sealed. This means that there are large THF solvent peaks present in the spectrum. These solvent peaks obscure the 9-BBN peaks between 1.8 and 2.0 ppm. Nevertheless, the decrease in the olefinic peaks can still be seen.

The crude products were always impure, all contained unreacted PS and PMMA homopolymers, which were removed before characterization. The PS-b-PMMA

copolymer was isolated from the crude product by sequential extraction with selective solvents, as described in Section 3.5 (cyclohexane was used for PS removal). The insoluble fraction of crude product (block copolymer mixed with some PMMA homopolymer) was soluble in THF. In order to achieve a good extraction, the soluble fraction in THF was reprecipitated in cyclohexane at 45 °C and the product was washed in methanol, and then dried.

Figure 4.3 (c) shows a typical  $^1\text{H-NMR}$  spectrum of a PS-*b*-PMMA block copolymer (run #2 in Table 4.1) after extraction. The spectrum shows characteristic peaks of the methyl methacrylate methoxy group, appearing at 3.62 ppm. The signals at 2.2-0.7 ppm are due to  $\text{CH}_3$  and  $\text{CH}_2$  protons of PMMA. Characteristic peaks of the styrene ring protons appear at 6.3-7.3 ppm. The block copolymer composition after extraction was quantitatively determined from the ratios of the two integrated intensities at 3.62 ppm ( $\text{CH}_3\text{O}$ ) and 6.3-7.3 ppm (aromatic protons), by using eq. 4.1. The results are summarized in Table 4.1

$$\%PMMA = \left[ \frac{AX/3}{AX/3 + AY/5} \right] \times 100 \quad (4.1)$$

where %PMMA is the percentage of PMMA incorporated into the block copolymer, AX is the integration intensity of the methoxy group in PMMA, AY is the integration intensity of the styrene ring protons, and 5 is the numbers of protons in the PS ring.

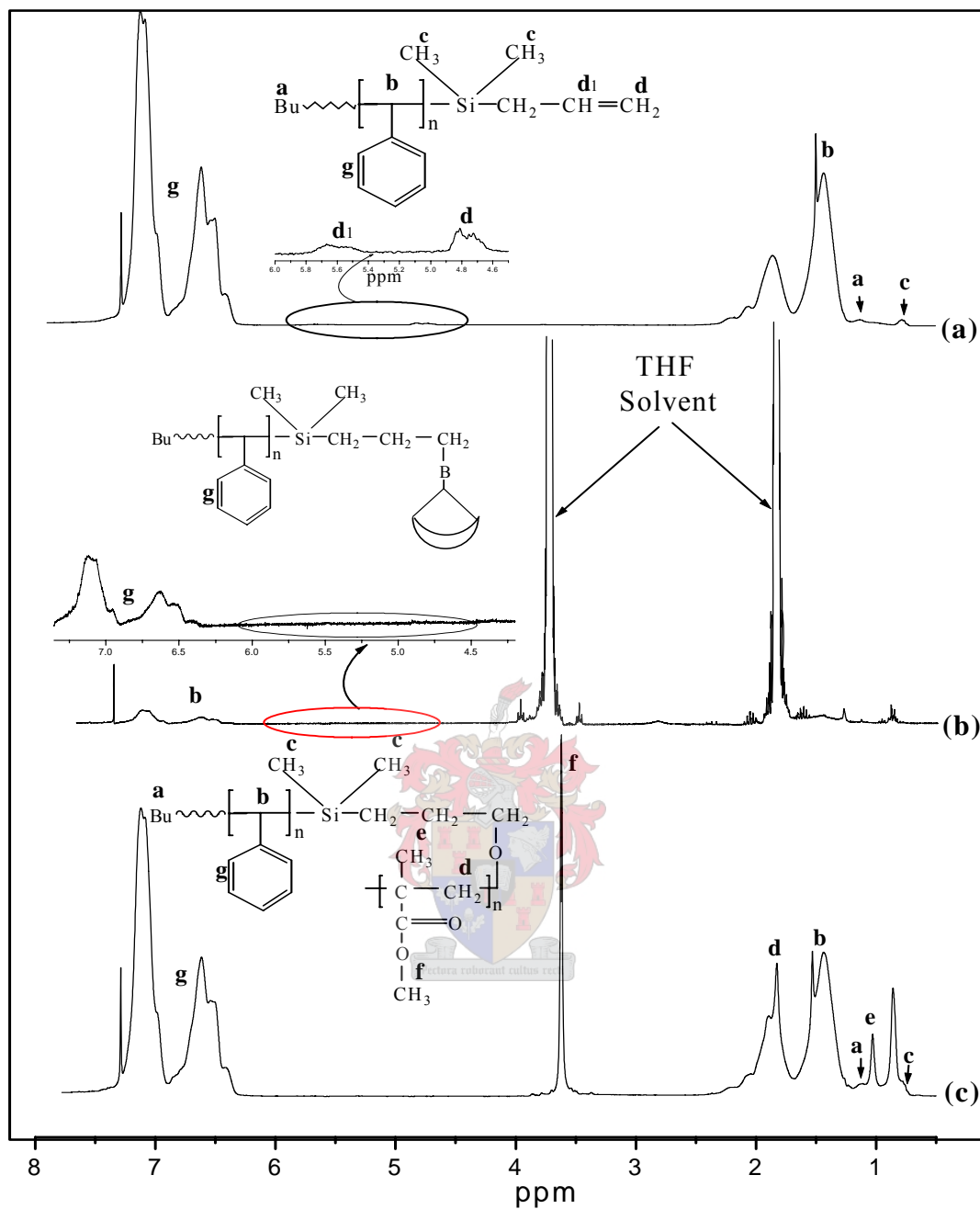


Figure 4.3:  $^1\text{H-NMR}$  spectra of PS macromonomer (a) before hydroboration, (b) after hydroboration, and (c) PS-b-PMMA, in  $\text{CDCl}_3$  solvent.

By varying the monomer concentration, the boron content (9-BBN) in the polymer and the amount of oxygen, the composition and microstructure of the block copolymers could be varied, as indicated in Table 4.1. Table 4.1 also shows the difference of the block compositions when different reaction conditions were employed.

**Table 4.1: Reaction conditions used in the synthesis of the PS-b-PMMA block copolymer, using hydroborated polystyrene macromonomer**

run	reaction conditions*			product fractions (g)		%PMMA in insoluble fraction (calculated from NMR results, using eq. 4.1)
#	9-BBN/Olefin	MMA (g)	O <sub>2</sub> / 9BBN	Cyclohexane-soluble	Insoluble fraction**	
1	2/1	7	1/2	0.50	2.85	72.8
2	1/1	5	1/2	0.56	2.00	58.2

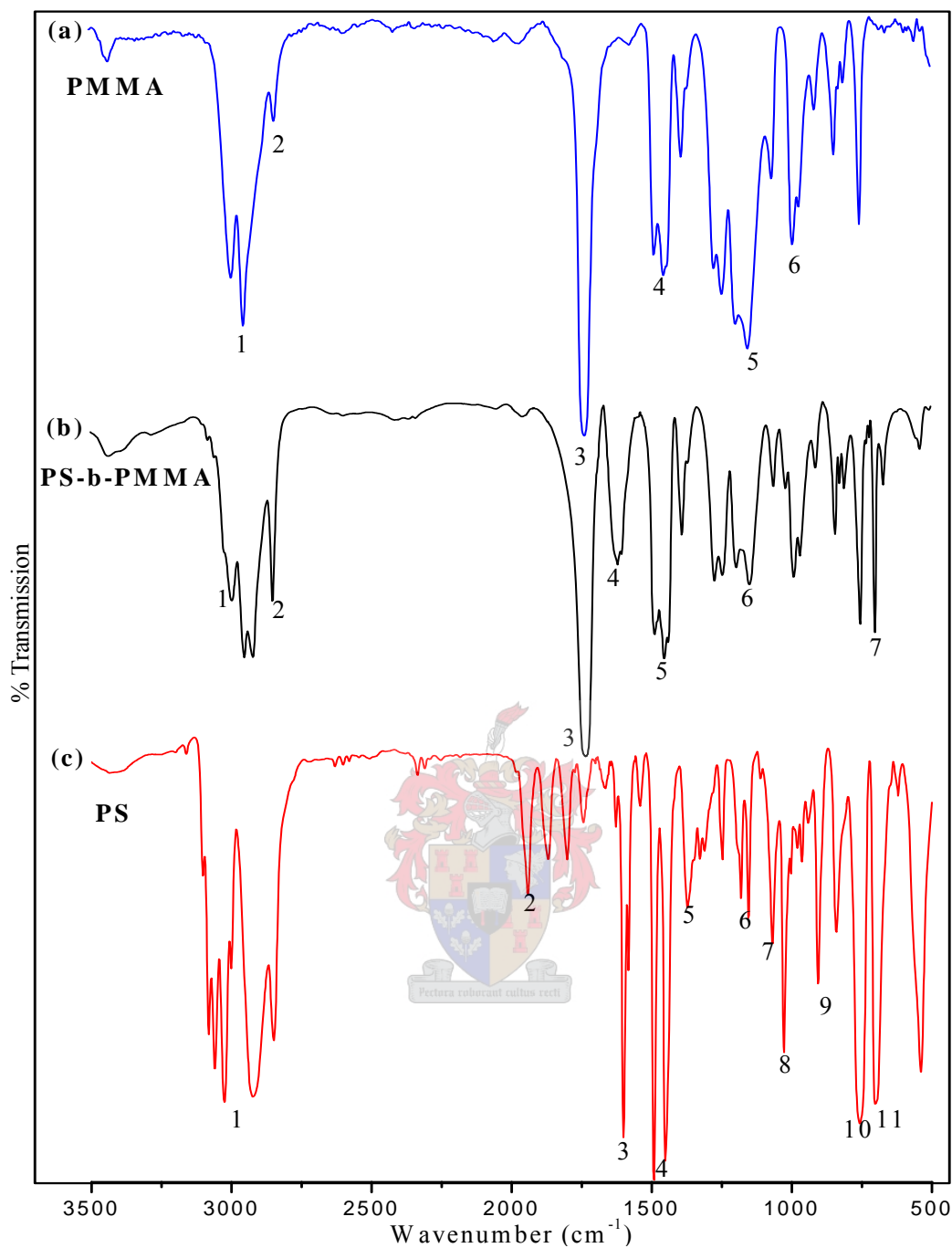
\* All the “block copolymer” reactions were performed by using 1 g of the PS macromonomer in 20 ml of THF. The oxygen was slowly introduced into the reaction solution (10 mole% oxygen ~ 0.50 ml per hour) at ambient temperature.

\*\* Block copolymer and some homopolymer PMMA.

Table 4.1 shows differences in composition of the block copolymer, as the concentrations of 9-BBN and MMA monomer were changed (runs #1, and #2) (under similar reaction conditions). For runs #1 and #2 the cyclohexane-soluble fraction decreased with an increase in the quantity of 9-BBN used. Furthermore, the concentration of the MMA monomer will influence the block composition of the product, as can be seen by comparing results of runs #1 and #2. A higher initial monomer concentration resulted in a higher PMMA content in the block copolymers.

### 4.3.3 Characterization of block copolymer PS-b-PMMA by Fourier-transform infrared spectroscopy (FTIR)

FTIR was also used to investigate the composition of the block copolymers. Samples were analyzed as KBr pellets. FTIR spectra of (a) PMMA, (b) extracted PS-b-PMMA copolymer (run #2) and (c) vinyl-terminated PS spectra are shown in Figure 4.4. Peak assignments are given in Table 4.2.



**Figure 4.4:** FTIR spectra of (a) PMMA, (b) extracted PS-b-PMMA copolymer (run #2) and (c) vinyl-terminated PS (peak assignments given in Table 4.2).

Overall, the results obtained from FTIR analyses are in agreement with those obtained from  $^1\text{H-NMR}$ , confirming block copolymer formation.



**Table 4.2: Characteristic infrared peaks in spectra of PS, extracted PS-b-PMMA, and PMMA homopolymer.**

peak number (Fig. 4.4)	peak intensity	wave number cm <sup>-1</sup>	absorption group	assignment
PMMA				
1 and 2	strong	2925, 2850	CH	stretching vibration
3	strong	1734	C=O	stretching
4	strong	1460	CH <sub>2</sub>	angular deformation
5	medium	1377	CH <sub>3</sub>	angular deformation
6	medium	727	CH <sub>2</sub>	angular deformation
PS-b-PMMA				
1 and 2	strong	2950, 2850	CH	stretching vibration
3	strong	1734	C=O	stretching
4	medium	1610	ring	stretching vibration
5	strong	1460	CH	stretching vibration
6	strong	1100-1260	C-O (ester bond)	stretching vibration
7	strong	710	ring	stretching vibration
PS				
1	strong	3025-2923	CH	stretching
2	medium	1700-1900	CH-CH <sub>2</sub>	stretching
3	strong	1600	ring	stretching vibration
4	strong	1492	ring	stretching vibration
5	weak	1244	CH	stretching
6	weak	1180	CH	stretching vibration
7	weak	1072	CH	stretching vibration
8	medium	1030-1024	CH	stretching vibration
9	medium	800-900	CH	deformation
10	strong	770-730	CH (5 adjacent)	deformation
11	strong	710-690	ring	stretching vibration

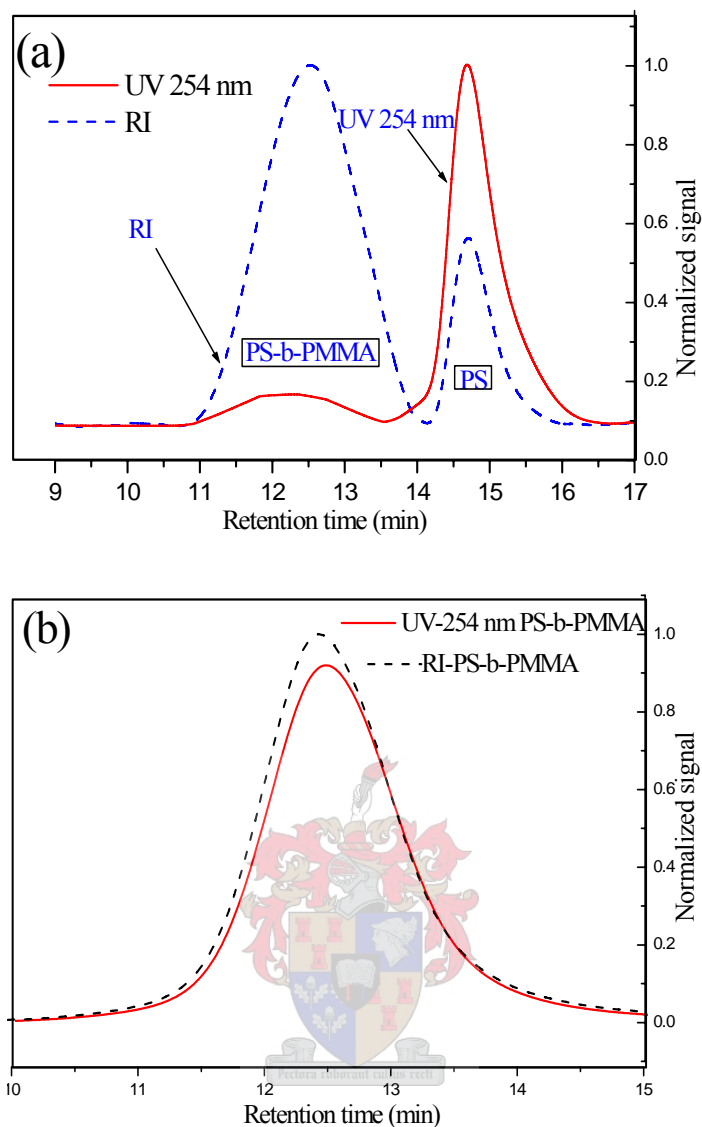
#### 4.3.4 Characterization of PS-b-PMMA block copolymers by size-exclusion chromatography (SEC)

The block copolymers were characterized by SEC using a dual detector (UV and RI) configuration. The UV detector was used for the analysis of the block copolymers at a wavelength of 254 nm. The values of the number average molecular mass ( $M_n$ ), the weight average molecular mass ( $M_w$ ) and the polydispersities of the block copolymers were obtained by SEC measurements. Generally speaking, the molecular mass of the block copolymers increased from 6,000 to 95,500 g/mole, which is consistent with the  $^1\text{H-NMR}$  results (Section 4.3.2). The distribution of the PS units across the elution peaks can be obtained by a comparison of the signals of the RI and UV (254 nm) detectors; only PS absorbs UV light at this wavelength.

Figure 4.5 compares the normalized RI & UV signals of (a) PS-b-PMMA before extraction and (b) after extraction. Figure 4.5 (a) shows an example of the SEC results of the block copolymers before extraction. The high molecular mass peak with a low UV intensity matches well with the corresponding high molar mass RI peak, which indicates a homogeneous distribution of PS in the high molecular mass fraction of the block copolymer. The low molecular mass peak with associated UV response indicates the high amount of unreacted PS macromonomers present in the sample.

Figure 4.5 (b) shows an example of the SEC results of the block copolymers after extraction. The UV curve shows a homogeneous distribution of PS in the high molar mass fraction of the block copolymer.

Molar mass and polydispersity results of the components of PS-b-PMMA block copolymers, as determined by SEC chromatography, after extraction of the unreacted PS macromonomer and PS-b-PMMA, are shown in Table 4.3.



**Figure 4.5:** (a) Comparison of the normalized RI & UV signals of the product before extraction and (b) comparison of the normalized RI & UV signals of product after extraction.

**Table 4.3:** Molar mass and polydispersity of the components of PS-b-PMMA block copolymers, as determined by SEC chromatography

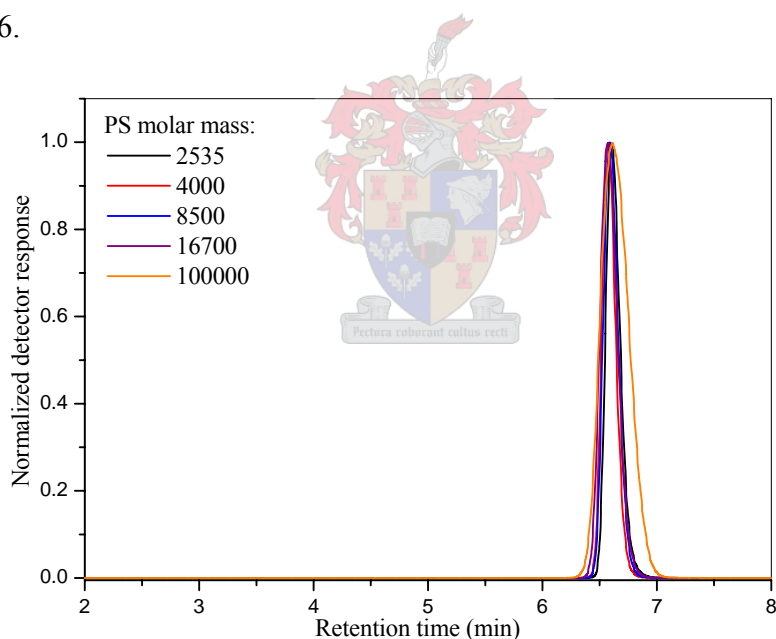
PS-b-PMMA sample	component	Mw (g/mol)	polydispersity (Mn/Mw)
1	PS	6000	1.30
	PS-b-PMMA	101000	1.66
2	PS	5800	1.23
	PS-b-PMMA	90000	1.81

SEC results cannot give accurate information about the block copolymer. In order to confirm SEC results and to obtain additional information about the block formation, HPLC at the critical points of polystyrene and polymethyl methacrylate was used.

#### 4.3.5 Characterization of block copolymers with high-performance liquid chromatography (HPLC) at the critical point of both polystyrene and methyl methacrylate

Block copolymers of polystyrene and methyl methacrylate were analyzed by liquid chromatography at the critical points of adsorption of polystyrene and polymethylmethacrylate. Critical point chromatography is a technique used to assess very small chemical changes in polymer molecules.<sup>2</sup>

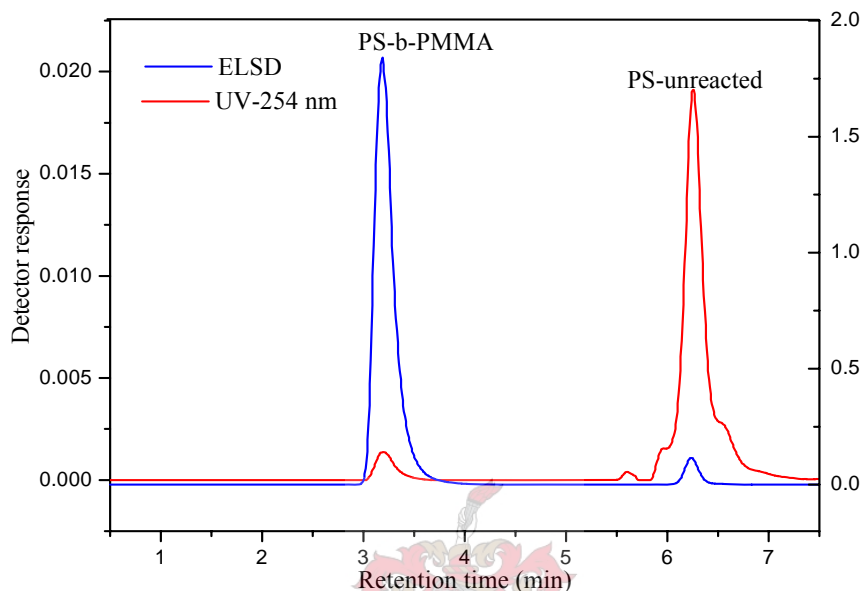
The critical condition of polystyrene was measured by injecting a series of polystyrene standards. The mobile phase composition consisted of ACN and THF, and two C18 columns (Nucleosil and Symmetry 300, both 5  $\mu\text{m}$ ) were used in series. The critical point of polystyrene was determined at the composition of a 50.2-49.8 ACN-THF mobile phase mixture. At this point, the polystyrene molecules will elute at the same time regardless of the molar mass or hydrodynamic volume, as shown in Figure 4.6.



**Figure 4.6: Chromatogram showing the critical point of adsorption of polystyrene standards. Mobile phase composition: ACN-THF (50.2-49.8), flow rate 0.5 ml/min, and the highest molar mass polystyrene 100000 g/mol.**

Under the critical condition of polystyrene the block copolymer and methyl methacrylate homopolymer will elute in SEC mode; where the high PMMA molecular mass molecules will elute first irrespective of the PS block size. The unreacted polystyrene macromonomer will elute at the critical point of polystyrene.

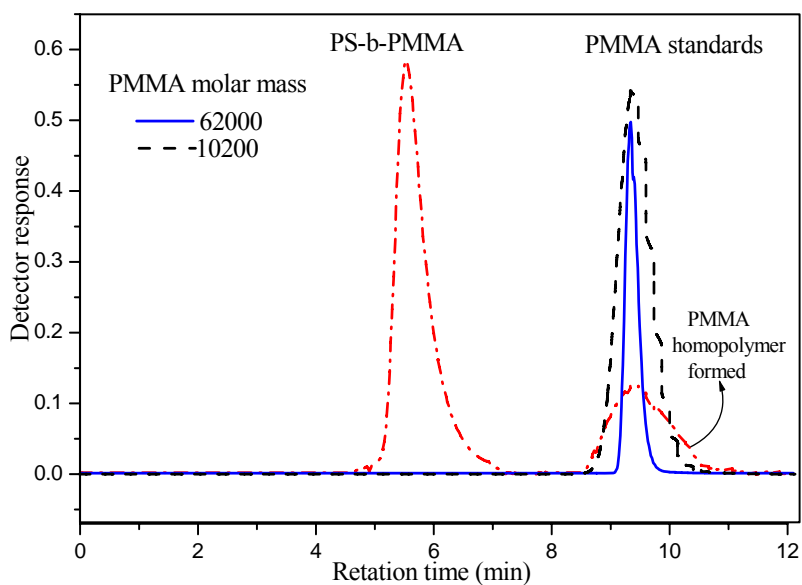
A UV detector was used to analyze the block copolymers at a wavelength of 254 nm (only PS absorbs UV light at 254 nm). The UV response of the detector at 254 nm also appeared in the elution range of methyl methacrylate, which indicates that the PS was blocked to PMMA through the double bond during free-radical polymerization. See Figure 4.7.



**Figure 4.7:** Typical example of a chromatogram of PS-b-PMMA at the critical point of polystyrene (Stationary phase Nucleosil C18 and symmetry C18, mobile phase 49.8:50.2% by volume CAN:THF, flow 0.5 ml/min, samples dissolved in 50:50% by volume CAN:THF).

Under the critical conditions of polystyrene it was not clear if any PMMA homopolymer was present during the polymerization reaction, therefore the critical point of PMMA was also used. The critical condition of methyl methacrylate was measured by injecting a series of polymethyl methacrylate standards and varying the mobile phase composition, using a mixed MEK-Cyclohexane solvent. Two silica gel HPLC columns (Si-300 and Si-100, both 5 $\mu$ m) were used. The critical point was determined at a composition of 70:30 MEK-Cyclohexane mobile phase mixture. At this point of adsorption the polymethyl methacrylate molecules will elute at the same time regardless of the molar mass or hydrodynamic volume, as shown in Figure 4.8.

The block copolymer will elute in SEC mode where the high molecular masses elute first followed by polymethylmethacrylate, which will elute at the critical point.



**Figure 4.8:** Elution curves of PS-b-PMMA and a PMMA standard at the critical point of polymethylmethacrylate. (Stationary phase column system of silica gel Si-300 and Si-100, mobile phase 70:30% by volume MEK-Cyclohexane, flow 0.5 ml/min, samples were dissolved in 70:30% by volume MEK-Cyclohexane).

The results in Figure 4.8 show that in addition to the PS-b-PMMA peak a small peak eluted at the same retention time as the PMMA standards indicative of an amount of PMMA homopolymer formed during the polymerization reaction. This may occur when the boron radical initiates MMA homopolymerization in addition to the alkyl radical which leads to block formation. This is an unavoidable side reaction. It is also observed in the graft reaction and will be discussed later.

The above study confirmed the suitable reaction conditions needed in order to initiate the hydroboration reaction and the polymerization reaction. Critically important is the delivery of the  $O_2$  to initiate the polymerization. This study was important because an excess of  $O_2$  is not only a poison for free-radical polymerizations but also leads to overoxidation of boranes to boronates and borates, both of which are poor free-radical initiators for polymerization at room temperature.<sup>3</sup> The polarity of the solution also affects the graft reaction.

The best results in the heterogeneous reaction system used in this study are realized when the  $O_2$  is introduced slowly, the ratio of oxygen should be less than 10%, added hourly so that at any time  $O \ll B$ , even though the final stoichiometry of oxygen to boron is found to be 0.5:1.

## 4.4 Methylmethacrylate grafted poly(isobutylene-co-isoprene) (PIB-co-PIP)-g-PMMA

### 4.4.1 Preparation

Methylmethacrylate grafted poly(isobutylene-co-isoprene) (PIB-co-PIP) rubber was synthesized by the procedure described in Section 3.4.6, using the “graft-from” approach. The products were fully characterized by  $^1\text{H-NMR}$ , FTIR and SEC. Complete separation of all components was achieved by gradient HPLC (PIB-co-PIP)-g-PMMA

### 4.4.2 Characterization of (PIB-co-PIP)-g-PMMA graft copolymers by proton nuclear magnetic resonance spectroscopy ( $^1\text{H-NMR}$ )

Figure 4.9 shows an example of the  $^1\text{H-NMR}$  spectra of (PIB-co-PIP) (a) before hydroboration, (b) after hydroboration, and (c) after polymerization in the presence of MMA to form (PIB-co-PIP)-g-PMMA. In Figure 4.9 (a) the chemical shift at 5.15 ppm corresponds to the olefinic (=CH) units in the PIB starting material. The chemical shifts at 1.1 and 1.42 ppm are due to the  $\text{CH}_3$  and  $\text{CH}_2$  protons in PIB respectively. Figure 4.9 (b) indicates the hydroboration spectrum of PIB-co-PIP rubber; the signal at 5.15 ppm has disappeared upon the hydroboration reaction.

The crude products of (PIB-co-PIP)-g-PMMA were always impure; they contained ungrafted butyl rubber and homopolymer PMMA, which is generated by chain transfer to monomer. These contaminants were removed before characterization. The (PIB-co-PIP)-g-PMMA graft copolymer was isolated from the crude reaction product by sequential extraction with selective solvents, as described in Section 3.5 (hexane was used for PIB-co-PIP removal and acetone for PMMA removal). The insoluble fraction of crude product (graft copolymer) was soluble in THF and was precipitated in 2-propanol, dried and characterized. Figure 4.9 (c) illustrates an example of the  $^1\text{H-NMR}$  spectrum of the third THF soluble (PIB-co-PIP)-g-PMMA copolymer fraction of the product. The spectrum shows a new peak appearing at 3.62 ppm, corresponding to the methoxyl group ( $\text{CH}_3\text{O}$ ) in PMMA. The peaks at 1.1 and 1.42 ppm are due to  $\text{CH}_3$  and  $\text{CH}_2$  protons in PIB respectively and the peaks between 0.7 and 2 ppm are due to the protons of the methyl and methylene groups in PMMA.

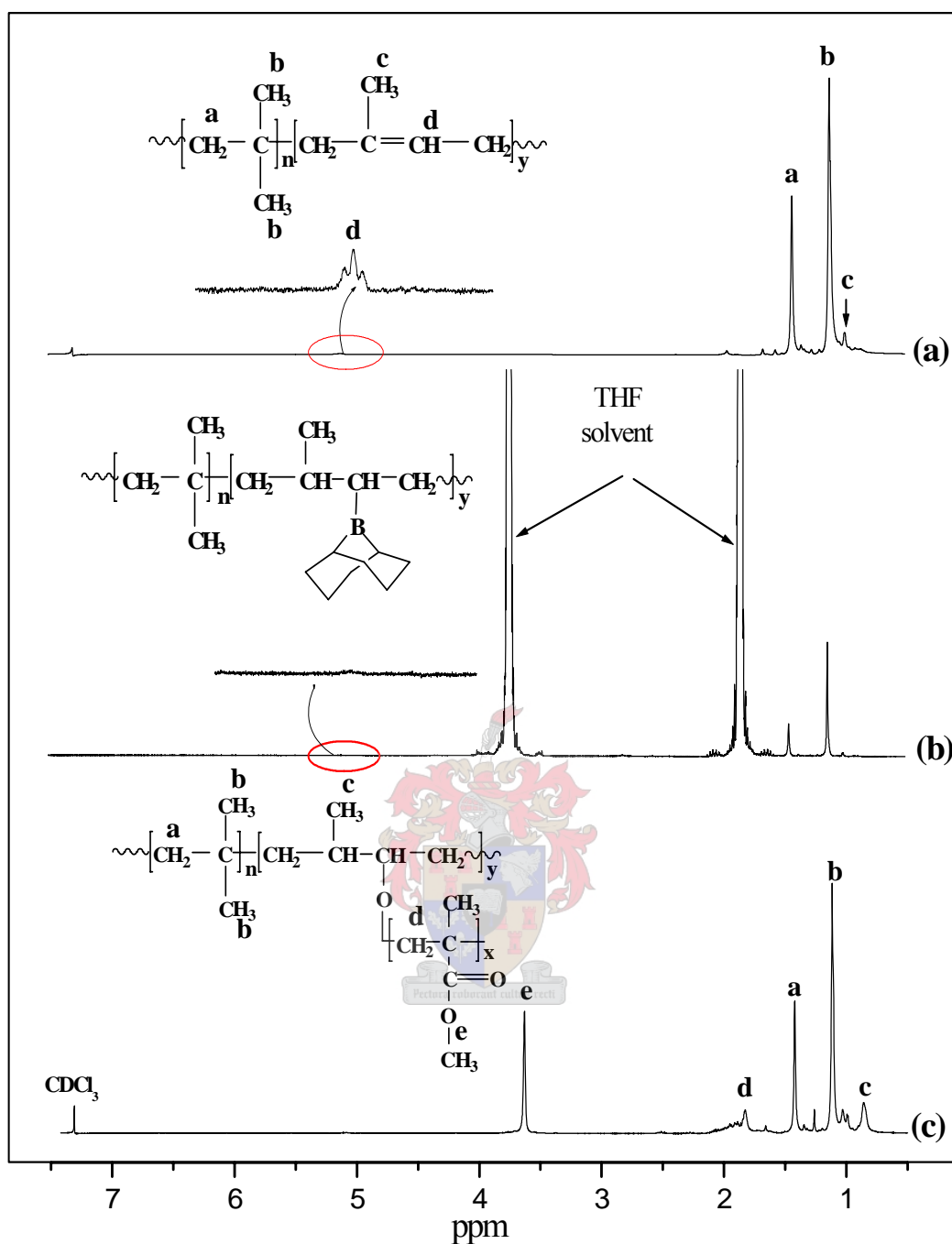


Figure 4.9:  $^1\text{H-NMR}$  spectra of PIB-co-PIP, #2 in Table 4.4, (a) before hydroboration, (b) after hydroboration, and (c) (PIB-co-PIP)-g-PMMA copolymer, in  $\text{CDCl}_3$  solvent.

The copolymer composition after extraction was quantitatively determined from the ratios of the integrated intensities of the two peaks at 3.62 ppm for the PMMA and 1.42 ppm for the PIB, and the number of protons represented by both chemical shifts. These calculations were performed for all graft copolymers by using equations 4.2. The results will be shown individually, in the respective discussions for the graft copolymers.



$$X\% = \left[ \frac{AX/3}{AX/3 + AY/3} \right] \times 100 \quad (4.2)$$

$X\%$  is the percentage of PMMA incorporated into the graft copolymer,  $AX$  is the integration area of the methoxy group in PMMA,  $AY$  is the integration area of  $\text{CH}_3$  in the polymer.<sup>1</sup> In the case of the EPDM polymer where the number of  $\text{CH}_3$  units in the polymer is unknown the integration was done in the 0.7-2.1 ppm region and includes all the protons in the EPDM and the five protons in the methyl groups of PMMA.<sup>4</sup>

By varying the boron content in the hydroborated PIB-co-PIP, the monomer concentration and the amount of oxygen, the composition and microstructure of the graft copolymers could also correspondingly be varied, as indicated in Table 4.4.

**Table 4.4: Different reaction conditions used during the ‘graft-from’ approach to prepare (PIB-co-PIP)-g-PMMA, using hydroborated poly(isobutylene-co-isoprene)**

run	reaction conditions*			fraction products (g)			% grafted PMMA in the insoluble fraction calculated by NMR, using eq 4.2
	9-BBN /Olefin	MMA (g)	O <sub>2</sub> / 9-BBN	Hexane soluble	Acetone soluble	Insoluble** fraction	
1	2/1	10	1/2	0.49	2.67	0.86	38
2	1/1	7	1/2	0.56	1.27	0.62	30

\*All “graft-from” reactions were performed using 1 g of PIB in 60 ml of THF. The oxygen was slowly introduced into the reaction solution (10 mole% oxygen, ~ 0.6 ml per hour) at ambient temperature.

\*\* Insoluble fraction ((PIB-co-PIP)-g-PMMA)

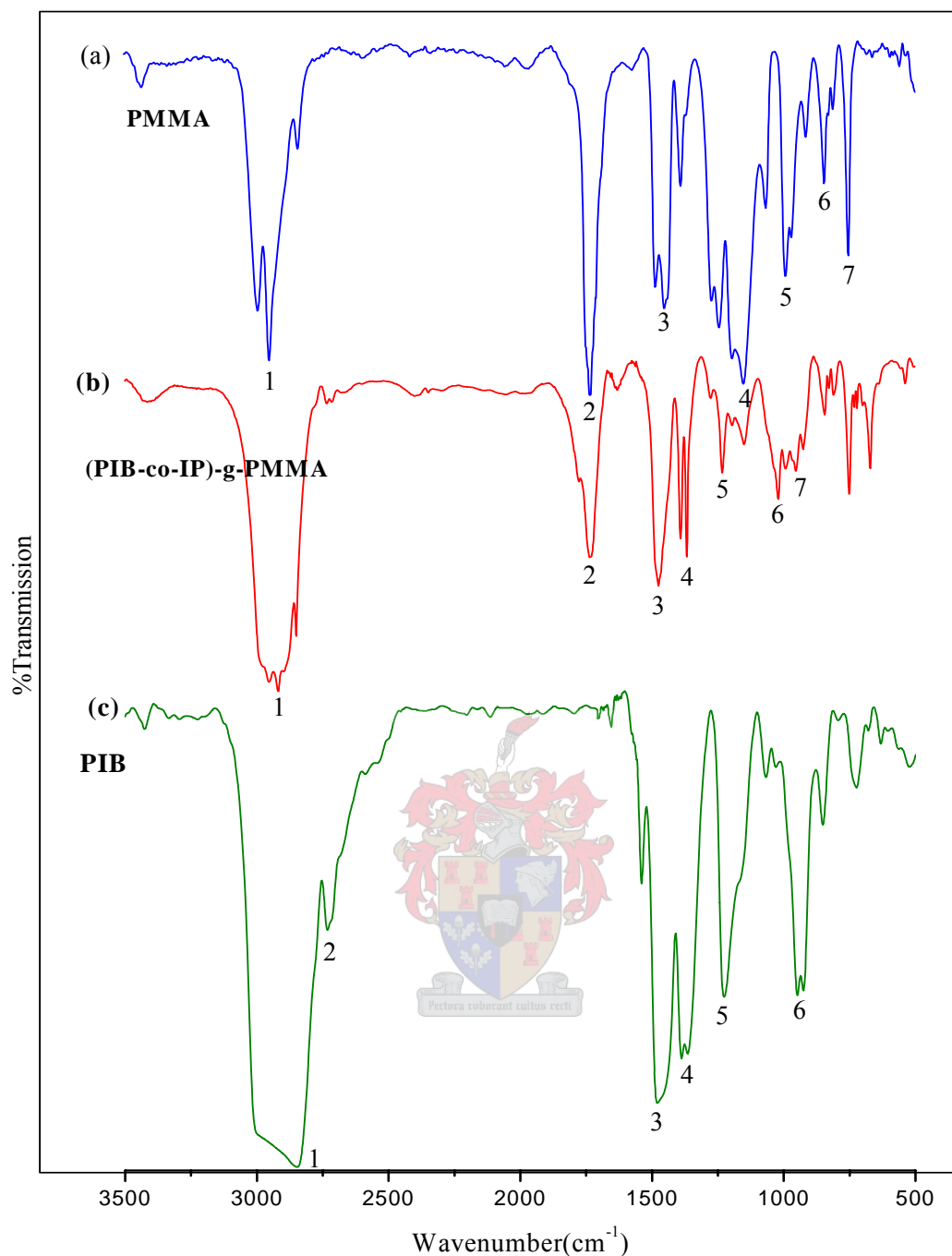
Table 4.4 shows differences in the graft compositions, where the concentration of 9-BBN and MMA monomer were changed (runs #1 and #2) under similar reaction conditions. Usually the ungrafted butyl rubber (hexane soluble fraction) is only a small portion. During the hydroboration reaction of runs #1 and #2 the hexane-soluble fraction decreased with an increase in 9-BBN used. Also, the concentration of the MMA monomer will influence the graft composition in the product, which can be seen by comparing runs #1 and #2. A higher initial monomer concentration resulted in a higher PMMA graft content in the graft copolymers. This might be due to the increase of PMMA molecular mass in the side chains.

#### 4.4.3 Characterization of (PIB-co-PIP)-g-PMMA graft copolymers by Fourier-transform infrared spectroscopy (FTIR)

Infrared spectroscopy was used to investigate the chemical compositions of the graft copolymers. Samples were analyzed in the form of KBr pellets prepared from the grafted PIB (after extraction) and also films of the PIB starting material. Figure 4.10 shows the FTIR spectra of PMMA, PIB-co-PIP and (PIB-co-PIP)-g-PMMA. A complete list of FTIR assignments for PIB-co-PIP, PMMA and (PIB-co-PIP)-g-PMMA is given in Table 4.5.

**Table 4.5: Characteristic infrared peaks of PIB-co-PIP, (PIB-co-PIP)-g-PMMA and PMMA**

peak number (see Fig 4.10)	peak intensity	wave number ( $\text{cm}^{-1}$ )	absorption group	assignment
PIB-co-PIP				
1 and 2	strong	2954 -2897	$\text{CH}_2\text{-CH}_3$	methyl stretching
3	strong	1473	CH	methyl deformation
4	medium	1390-1367	$\text{CH}_2$	stretching
5	medium	1230	$\text{CH}_3$	methyl rock vibration
6	weak	924 -951	$\text{CH}_2$	methyl rock vibration
PIB-g-PMMA (run # 2)				
1	strong	2950, 2850	CH	stretching vibration
2	medium	1734	C=O	stretching
3	strong	1470	$\text{CH}_2$	deformation
4	medium	1384	$\text{CH}_2$	stretching vibration
5	medium	1226	$\text{CH}_2$	stretching
6	medium	1018	O-CH-C	stretching
7	medium	945	$-\text{CH}_2$	methyl vibration
PMMA				
1	strong	2958-2893	$\text{CH}_3$ and $\text{CH}_2$	methyl stretching
2	strong	1730	C=O	stretching
3	medium	1466	-CH	methyl deformation
4	medium	1244	C-O	stretching
5	strong	1152	C-(C=O)-O	symmetric
6	medium	1066	O-CH-C	stretching



**Figure 4.10:** FTIR spectra of (a) PMMA, (b) (PIB-co-PIP)-g-PMMA run #2 in Table 4.4, and (c) PIB-co-PIP starting material (peak assignments are given in Table 4.5).

Figure 4.10 (b) shows an example of the (PIB-co-PIP)-g-PMMA after extraction: The strong peak at  $1734\text{ cm}^{-1}$  is ascribed to the ester group in PMMA and the peak at  $2934\text{ cm}^{-1}$  arises from the  $-\text{CH}_2$  stretch vibration. The peak at  $1384\text{ cm}^{-1}$  is from the methyl gem dimethyl in PIB. Furthermore, the positions of all other groups have shifted to slightly higher wavelengths. The FTIR spectrum of (PIB-co-PIP)-g-PMMA confirms that the PMMA was “grafted from” the PIB-co-PIP through the double bond during

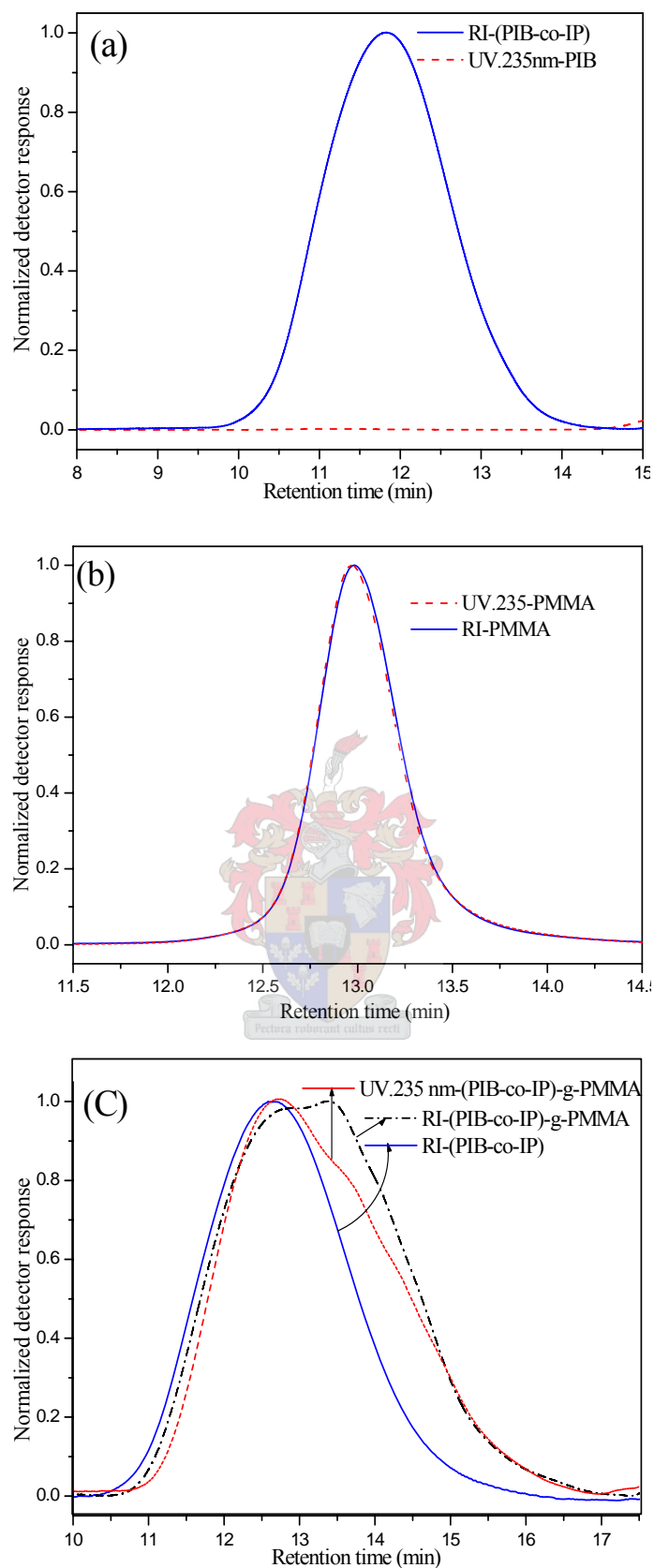
free-radical copolymerization. Overall, the results obtained from FTIR analyses are in agreement with those obtained from  $^1\text{H-NMR}$ .

#### **4.4.4 Characterization of (PIB-co-PIP)-g-PMMA graft copolymers by size-exclusion chromatography (SEC)**

The graft copolymers were characterized by SEC, using a dual detector (UV and IR) setup. The UV detector was used for the analysis of the graft copolymers at  $\lambda=235$  nm for PIB-g-PMMA. The values of the number average molecular mass ( $M_n$ ), the weight average molecular mass ( $M_w$ ) and polydispersities of the graft copolymers were obtained by SEC measurements. Generally the results showed that the molecular masses of the graft copolymers were lower than expected because of the much larger hydrodynamic volume of the linear polymers (starting materials) compared to the corresponding graft copolymers of the same molar masses.<sup>1,5</sup> SEC measurements obtained by simply comparing elution volumes (or times) between branched and linear structures alone cannot offer an accurate molar mass result for the graft polymer.

There are three main reasons for the decrease of the molecular masses. The first reason is cyclization during the preparation of graft copolymers, which decreases the molecular masses<sup>5</sup>. The second reason is that the hydrodynamic volume of the branch polymer does not increase linearly with increasing molecular masses.<sup>1,5</sup> The third reason is that the graft reaction occurred only in the short chains of the polymers. This result implies that some of the graft copolymers have smaller hydrodynamic volumes than the starting PIB-co-PIP. In addition the polarity of the MMA units is very different than the rubber back bond which will also affect salvation and folding of the polymer molecules.

The distribution of MMA units across the elution peaks can be obtained by a comparison of the signals of the RI and UV (235 nm) detectors, as shown in Figure 4.11 (b). Only PMMA absorbs UV light at a wave length of 235 nm, with no response from PIB-co-PIP (Figure 4.11 (a)).



**Figure 4.11: Comparison of the normalized RI & UV signals of (a) PIB-co-PIP homopolymer and (b) PMMA with the normalized RI and UV signals of (c) (PIB-co-PIP)-g-PMMA copolymer.**

Figure 4.11 (c) shows an example of the SEC results of the graft copolymer; the high molar mass peak in the UV curve matches well with the corresponding RI peak, which indicates a homogeneous distribution of PMMA in the high molar mass fraction of the graft copolymer. The low molar mass peak with only low UV response indicates a quite a low concentration of PMMA in the low molar mass fraction.

Molar mass and polydispersities of the graft products after extraction of PIB-co-PIP and PMMA homopolymer are summarized in Table 4.6.

**Table 4.6: Molar mass and polydispersities of the components of (PIB-co-PIP)-g-PMMA graft copolymers, as determined by SEC chromatography**

sample	component	$M_w$ (g/mol)	polydispersity ( $M_w/M_n$ )
1	PIB-co-PIP	266 400	2.04
	(PIB-co-PIP)-g-PMMA	230 900	2.96
	PMMA	107 700	3.53
2	PIB-co-PIP	266 400	2.04
	(PIB-co-PIP)-g-PMMA	211 300	2.90
	PMMA	105 400	3.50

As already mentioned, SEC results cannot give accurate information about the graft copolymer molecular mass. HPLC was therefore used for further investigation.

#### 4.4.5 Characterization of (PIB-co-PIP)-g-PMMA graft copolymers by high-performance liquid chromatography (HPLC)

The graft reaction of PIB-co-PIP with methyl methacrylate was investigated by different chromatographic techniques, including HPLC. When PIB-co-PIP is grafted with methyl methacrylate the soluble fraction of the reaction product contains: residual ungrafted PIB-co-PIP, the graft copolymer PIB-co-PIP-g-PMMA and PMMA homopolymer. In order to carry out a detailed analysis the components must be separated from each other by suitable chromatographic techniques.

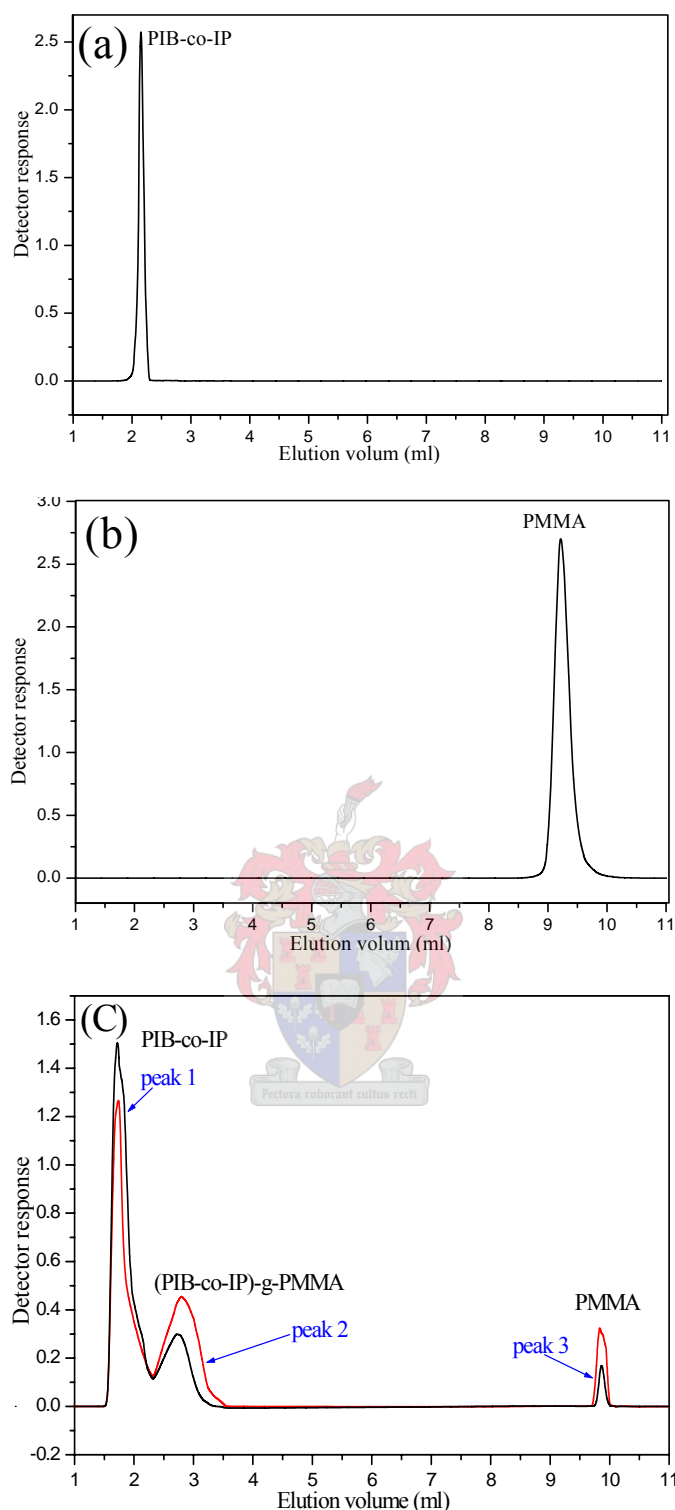
Gradient HPLC is the most useful technique for the separation of copolymers according to chemical composition. The gradient HPLC separation mechanism is based on the differences in solubility between copolymer fractions with different

chemical compositions.<sup>2,7</sup> Hence a method was developed for complete separation of all components by gradient HPLC.

The chromatogram recorded for an example of the graft copolymer (PIB-co-PIP)-g-PMMA after gradient profile separation is presented in Figure 4.12 (a, b). The assignment of the peaks was carried out by comparison with the chromatographic behaviour when using a reversed phase column (Nucleosil CN 100Å) of PIB-co-PIP and PMMA; PIB-co-PIP is the least polar component and therefore elutes first, followed by the graft copolymer (PIB-co-PIP)-g-PMMA and the more polar PMMA homopolymer.

In Figure 4.12 (c), in both runs 1 and 2, the first peak is that of PIB-co-PIP, and the shoulder following the first peak is an indication of the presence of PIB-co-PIP and PMMA graft copolymer. Based on a comparison with a standard PMMA sample, injected under the same conditions, the third peak is assigned to PMMA homopolymer. As expected, it is retained most strongly on the stationary phase.

The difference between run #1 and #2 are shown in Figure 4.12. In #1 both the PMMA and graft peaks increased with a decrease in the PIB-co-PIP peak, which indicated that the amount of PMMA homopolymer and graft copolymer increased with decreases in amount of PIB-co-PIP. Overall, the results obtained from HPLC analyses are in agreement with those presented in table 4.4.



**Figure 4.12: Gradient HPLC chromatograms of (a) PIB-co-PIP starting material, (b) PMMA standard and (c) graft product (PIB-co-PIP)-g-PMMA. (Stationary phase: Nucleosil CN 100Å; eluent: THF/Cyclohexane; detectors: ELSD and UV at 235 nm). The gradient was started at 1:99 (v/v) (THF:Cyclohexane), held constant for 2 mins, changed linearly to 34:66 (THF:Cyclohexane) within 8 mins, held constant for 10 min, and changed linearly to 100:0 (THF:Cyclohexane) within 3 min, held constant for 5 min. The flow rate was 0.5 ml/min.**



## 4.5 Graft copolymer of polyisoprene rubber with methylmethacrylate (PIP-g-PMMA)

### 4.5.1 Preparation

Pinazzi et al.<sup>8</sup> reported that low molecular mass. Polyisoprene can be totally hydroborated under extremely mild conditions Polyisoprene rubber graft methyl methacrylate (PIP-g-PMMA) was synthesized by the procedure described in Section 3.4.8 by using the “graft-from” approach. The reaction was initiated by the slow introduction of anhydrous oxygen to the reaction mixture (10% oxygen hourly at ambient temperature). Products were characterized by <sup>1</sup>H-NMR, FTIR and SEC. Separations of all components were achieved by gradient HPLC.

### 4.5.2 Characterization of PIP-g-PMMA graft copolymers by proton nuclear magnetic resonance spectroscopy (<sup>1</sup>H-NMR)

Figure 4.13 shows an example of the <sup>1</sup>H-NMR spectra of PIP (a) before hydroboration, (b) after hydroboration, and (c) after polymerization in the presence of MMA to form PIP-g-PMMA. In Figure 4.13 (a) the chemical shift at 5.15 ppm corresponds to the olefinic (=CH) units in the starting material PIP. The chemical shifts at 1.687 and 2.05 ppm correspond to CH<sub>3</sub> and CH<sub>2</sub> in polyisoprene respectively. The disappearance of the intense signal at 5.15 ppm in Figure 4.13 (b) indicates the hydroboration of 80% of the PIP rubber.

During the grafting reaction the homopolymerization of PMMA also took place. The PMMA homopolymer was generated by a chain transfer reaction, either to a monomer or a solvent (THF in this case). A very complex reaction product is obtained. This consisted of the desired graft copolymer, PIP-g-PMMA, as well as non-grafted PIP and PMMA. These were separated prior to characterization and quantitative determination of the components in the graft product. The PIP-g-PMMA copolymer was isolated from the crude product by sequential extraction with selected solvents, as described in Section 3.5. The insoluble fraction of crude product (graft copolymer soluble in THF) was precipitated in methanol, dried and characterized. The remaining polymer was considered as gels (cross-linked) and the cross-link density was measured by the Flory-Rehner equation.<sup>9</sup> These gels form during the polymerization reaction due to the high number of double bonds present in PIP.

The liquid chromatography analysis in this section is only for the soluble (none crosslinked) polymer.

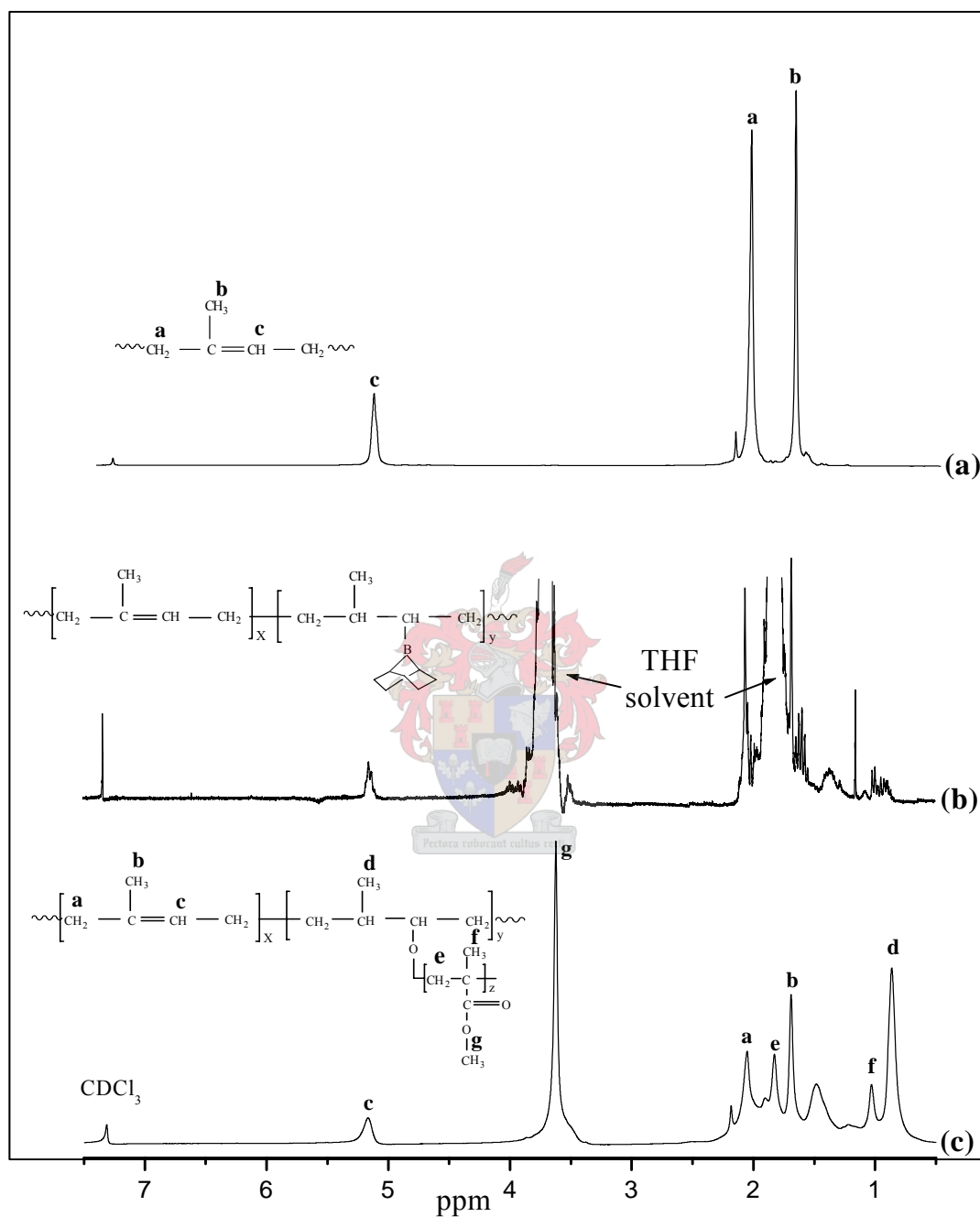


Figure 4.13:  $^1\text{H-NMR}$  spectra of PIP (a) before hydroboration, (b) after hydroboration, and (c) PIP-g-PMMA copolymer, in  $\text{CDCl}_3$  solvent.

Figure 4.13 (c) illustrates an example of the  $^1\text{H-NMR}$  spectrum of the third fraction extracted from the product (PIP-g-PMMA copolymer). The spectrum shows a new peak appearing at 3.62 ppm, corresponding to the methoxyl groups ( $\text{CH}_3\text{O}$ ) in

PMMA. The peaks between 0.7 - 2.1 ppm are due to the protons of the methyl and methylene groups in PIP and PMMA.

The copolymer composition after extraction was quantitatively determined from the ratios of the two integrated intensities at 3.62 ppm, for the CH<sub>3</sub>-O proton and 1.69 ppm for the CH<sub>3</sub> proton by using equation 4.2. The detailed experimental conditions and results are tabulated in Table 4.3.

By varying the boron content in the polymer, the monomer concentration, and the amount of oxygen, the composition and microstructure of the copolymers could be correspondingly varied, as indicated in Table 4.7. Table 4.7 also shows differences in the graft compositions when different reaction conditions were employed.

**Table 4.7: Different reaction conditions used during the ‘graft-from’ approach to prepare PIP-g-PMMA, using hydroborated polyisoprene**

Run #	Reaction conditions*			Fraction products (g)					PMMA % grafted in the insoluble fraction calculated by NMR, using eq 4.2
	9-BBN/Olefin	MMA (g)	O <sub>2</sub> /9-BBN	Hexane soluble	Acetone soluble	Insoluble fraction**	Remaining gel***		
							Weight (g)	Cross-link density	
1	2/1	10	1/2	0.10	3.0	0.59	1.9	4.8x10 <sup>-5</sup>	73
2	1/1	7.0	1/2	0.15	2.0	0.55	1.7	5.5x10 <sup>-6</sup>	27

\*All “graft-from” reactions were performed using 1 g of PIP in 60 ml of THF. The oxygen was slowly introduced into the reaction solution (10 mole% oxygen, ~11.5 ml per hour) at ambient temperature.

\*\* Insoluble fraction (PIP-g-PMMA)

\*\*\* Remaining gel, insoluble fraction in THF (cross-linked)

Table 4.7 shows differences in the graft compositions, where the concentrations of 9-BBN and MMA monomer were changed (runs #1 and #2), under similar reaction conditions. Usually the ungrafted butyl rubber (hexane soluble fraction) is only a small portion. For the amount of 9-BBN used during the hydroboration reaction, the hexane-soluble fraction decreased with an increase in 9-BBN. The concentration of the MMA monomer also influences the graft composition in the product as can be seen by comparing runs #1 and #2. A higher initial monomer concentration resulted in a higher PMMA graft content in graft copolymers and PMMA homopolymers.

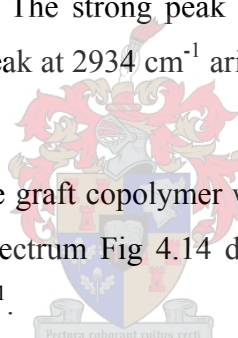
Table 4.7 shows the remaining gel (cross-linked) was increased with increases in the MMA monomer. The cross-link densities were determined by swelling the polymer solvent interaction parameters used in the Flory-Rehner equation<sup>9</sup> were 0.435 for IR-benzene.<sup>10</sup> The cross link densities are tabled in Table 4.7.

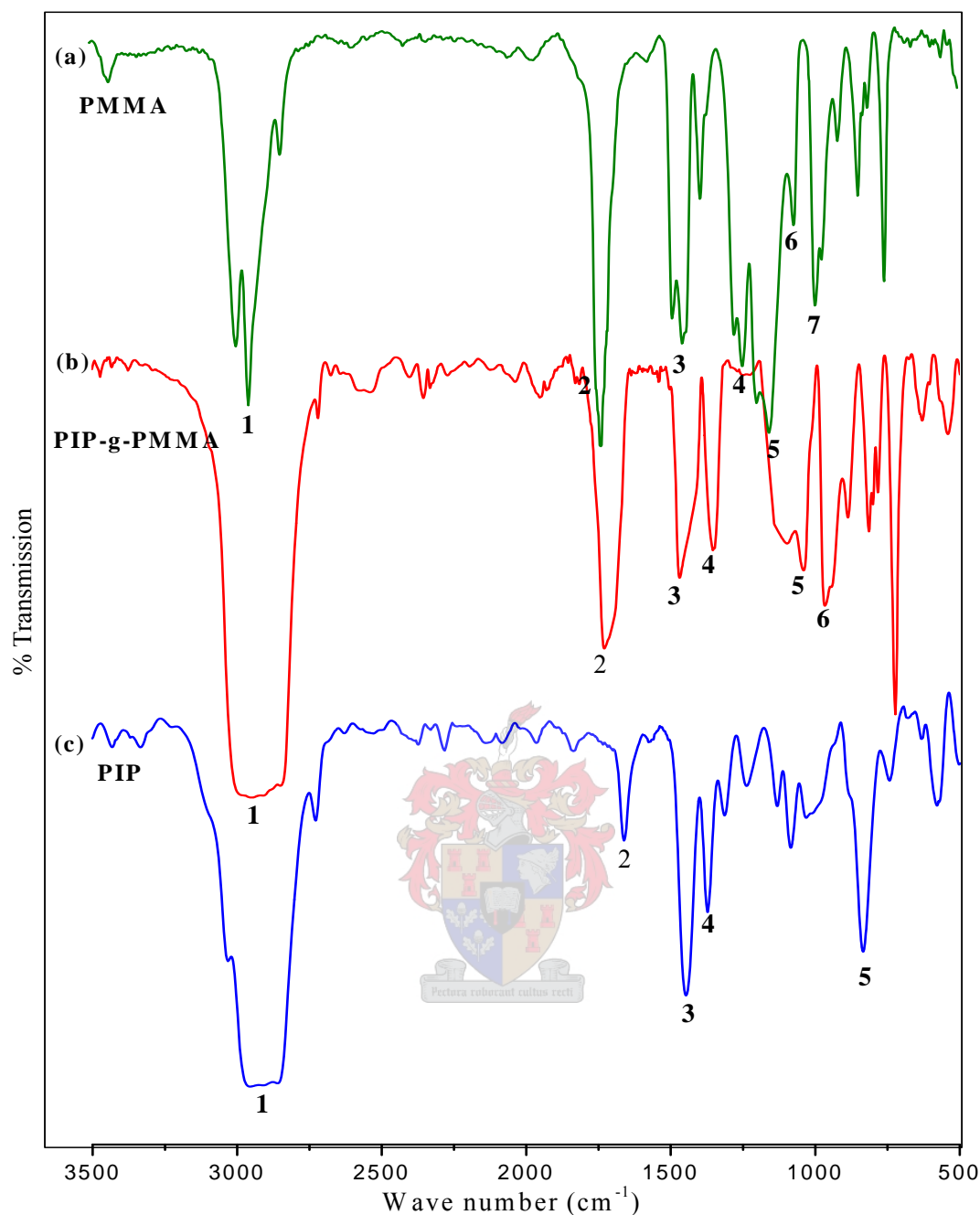
#### 4.5.3 Characterization of PIP-g-PMMA graft copolymers by Fourier-transform infrared spectroscopy (FTIR)

FTIR spectroscopy was used to investigate the chemical composition of the PIP graft copolymers. Samples were analyzed in the form of KBr pellets prepared from the grafted PIP (after extraction) and films of the PIP starting material. Figure 4.14 compares the FTIR spectra of PMMA, PIP and PIP-g-PMMA. A complete list of FTIR spectra assignments of PIP, PMMA and PIP-g-PMMA is given in Table 4.8.

Figure 4.14 (b) illustrates the FTIR spectrum of the third fraction of the product (THF soluble fraction PIB-g-PMMA). The strong peak at  $1734\text{ cm}^{-1}$  was ascribed to the carbonyl group in PMMA, the peak at  $2934\text{ cm}^{-1}$  arises from the  $-\text{CH}_3$  and the peak at  $1465\text{ cm}^{-1}$  from the  $\text{CH}_2$  in PIP.

The remaining double bonds in the graft copolymer which have been not hydroborated can not be seen in the FTIR spectrum Fig 4.14 due to the overlapping effect with carbonyl group band at  $1737\text{ cm}^{-1}$ .





**Figure 4.14:** FTIR spectra of (a) PMMA, (b) PIP-g-PMMA and (c) PIP. (Peak assignments given in Table 4.8)

FTIR analysis of the polymerized PIP therefore indicates that a change in chemical structure of the PIP occurred during the grafting reaction. The FTIR spectrum of PIP-g-PMMA provides strong proof that the PMMA was grafted to the residual PIP through the double bond during free-radical polymerization. Overall, results obtained from FTIR analyses are in agreement with those obtained from <sup>1</sup>H-NMR.

**Table 4.8: Characteristic infrared peaks of PIP, PIP-g-PMMA and PMMA**

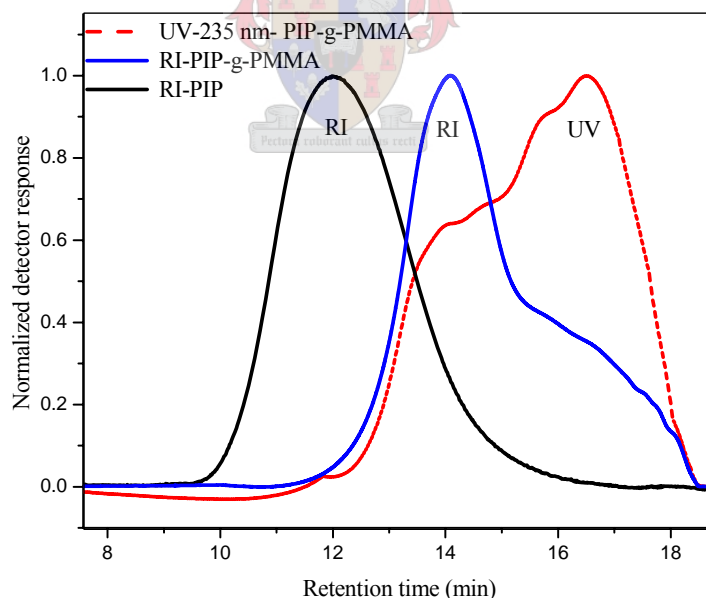
peak number (see fig Fig 4.14)	peak intensity	wave number (cm-1)	absorption group	assignment
PIP				
1	strong	2925, 2850	CH <sub>3</sub>	asymmetric stretching
2	medium	1665	C=C	stretching
3	strong	1465	CH <sub>2</sub>	deformation
4	strong	1377	CH <sub>3</sub>	asymmetric deformation
5	weak	840	=C-H	wagging
PIP-g-PMMA				
1	strong	2950- 2850	CH <sub>3</sub> and CH <sub>2</sub>	stretching vibration
2	strong	1734	C=O	stretching
3	medium	1460	CH <sub>2</sub>	deformation
4	strong	1380	CH <sub>3</sub>	stretching vibration
5	strong	1000-1100	O-CH-C	stretching
6	medium	930	CH <sub>2</sub>	angular deformation
PMMA				
1	strong	2958-2893	-CH <sub>3</sub> and CH <sub>2</sub>	stretching symmetric
2	strong	1730	C=O	stretching
3	medium	1466	-CH	deformation
4	medium	1244	C-O	stretching
5	strong	1152	C-(C=O)-O	symmetric
6	medium	1066	O-CH-C	stretching
7	medium	942	-CH <sub>2</sub>	angular deformation

#### 4.5.4 Characterization of PIP-g-PMMA graft copolymers by size-exclusion chromatography (SEC)

The graft copolymers were also characterized by SEC using dual detectors (UV and IR). The UV detector was used for the analysis of the graft copolymers at  $\lambda=235$  nm for PIP-g-PMMA. The values of the number average molecular mass (Mn), the weight average molecular mass (Mw) and polydispersities of the graft copolymers were obtained by SEC measurements. Generally speaking the results showed the

molecular masses of the graft copolymers were lower than expected because of the much larger hydrodynamic volume of the linear polymers (starting materials) compared to the corresponding graft copolymers of the same molar masses.<sup>1,5</sup> (see Figure 4.15). This result implies that some of the extracted graft copolymers have smaller hydrodynamic volumes than the starting PIP. Obviously, the SEC measurements obtained by simply comparing elution volumes (or times) between branched and linear structures alone cannot offer an accurate molar mass.

Figure 4.15 show that the maximum extracted graft copolymer peak was shifted toward a high retention time compared to the maximum peak of PIP. Figure 4.15 compares RI and UV ( $\lambda = 235$  nm) detector curves at 235 nm where only PMMA absorbs UV light, thus no response from PIP. The high molar mass peak in the UV curve matches well with the corresponding RI peak, which indicates a homogeneous distribution of PMMA in the high molar mass fraction of the graft copolymer. However, the low-molar mass peak with high UV response indicates quite a high concentration of PMMA in the low molar mass fraction.



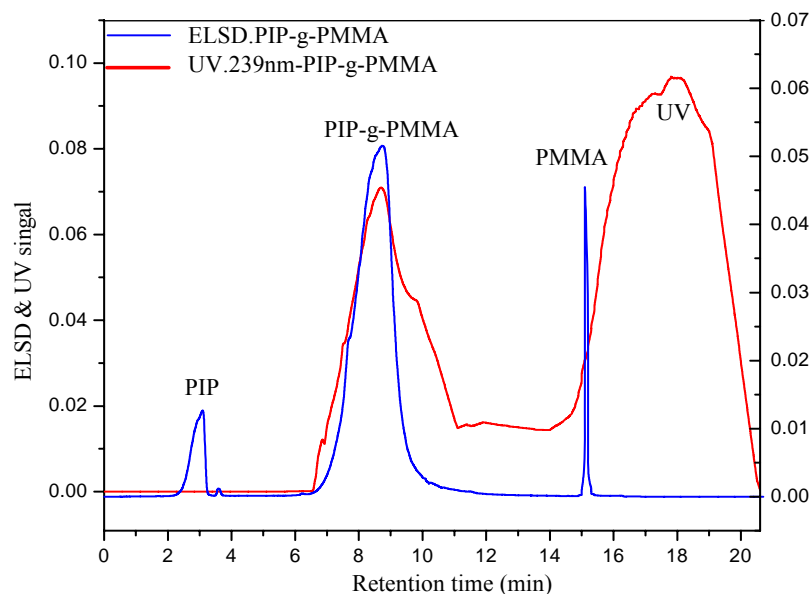
**Figure 4.15: Comparison of the normalized RI signal of PIP with the normalized RI and UV signals of the PIP-g-PMMA copolymer.**

#### 4.5.5 Characterization of PIP-g-PMMA graft copolymers with high-performance liquid chromatography (HPLC)

The “grafting from” reaction of methyl methacrylate to PIP was investigated by different chromatographic techniques, including HPLC. When PIP is grafted with methyl methacrylate, the soluble fraction of the reaction product contain residual ungrafted PIP, the graft copolymer PIP-g-PMMA and homopolymer PMMA. Prior to a detailed analysis the components must be separated from each other by suitable chromatographic techniques.

The resulting chromatogram of the graft copolymer is presented in Figure. 4.16. A very good separation into three fractions was obtained for all product samples. The assignment of the peaks was carried out by comparison of PIP and PMMA with the chromatographic behaviour when using a reversed phase column (Nucleosil CN-100Å) PIP is the least polar component and therefore elutes first, followed by the graft copolymer PIP-g-PMMA and subsequently followed by the more polar compound (PMMA homopolymer). The three elution peaks can therefore be assigned to the sample constituents PIP, PMMA and PIP-g-PMMA. The second peak is significantly retained, indicating that it contains polar MMA units (graft copolymer PIP-g-PMMA). Based on comparison with a reference sample of PMMA, the third peak could be assigned to PMMA homopolymer. As was expected, it is retained most strongly on the stationary phase. As shown in Figure 4.16, the UV detector can be used to detect different MMA-containing species; it gives some UV signal response for the second peak and the third peak. It does not give a direct concentration profile for all species of the samples. Unfortunately the UV response is not clear for the later part of the elution profile as the change in mobile phase results in a stronger absorbance by the mobile phase.





**Figure 4.16:** Gradient HPLC chromatogram of the PIP-g-PMMA graft product. (Stationary phase: Nucleosil CN 100Å, eluent: THF/i-octane; detectors: ELSD and UV at 239 nm. The gradient was started at 99:1 (v/v) (THF:i-octane), held constant for 1 min, changed linearly to 34:66 (THF:i-octane), within 2 mins, held constant for 10 mins, and changed linearly to 100:0 (THF:i-octane), within 2 mins. ELSD and UV detectors were used).

#### 4.6 EPDM rubber grafted with methylmethacrylate (EPDM-g-PMMA) and styrene (EPDM-g-PS)

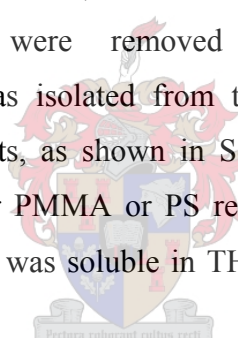
Ethylene-propylene diene norbornene (EPDM) is an important commercial rubber. Currently EPDM is third or fourth in terms of the synthetic elastomers in total tonnage produced, substantially behind only the general-purpose tyre elastomers, styrene-butadiene copolymers and butadiene (PB).<sup>11</sup>

However EPDM, like other polyolefins has low surface energy, resulting in a limitation of its end uses, especially where adhesion and compatibility with other functional materials are important. The extension of graft copolymer compositions to polyolefins is both technically difficult and commercially important. It is very desirable to synthesize polyolefin graft copolymers with the second polymer functioning as functional groups, such as poly(methyl methacrylate) and polystyrene. This will improve the interaction between polyolefins and a wide range of materials. Characterization of products resulting from the grafting of methyl methacrylate onto EPDM has been carried out by Augenstein and Stickler<sup>12</sup>.

Ethylene-propylene rubber graft methyl methacrylate and styrene monomers were synthesized by the procedures described in Sections 3.4.10 and 3.4.11, respectively. All “graft-from” reactions were performed by using 1 g of EPDM in 60 ml of THF solvent. The oxygen was slowly introduced to the reaction solution: 10% of oxygen hourly, at ambient temperature. Reaction products were characterized by  $^1\text{H-NMR}$ , FTIR and SEC. Complete separation of all components was achieved by gradient HPLC.

#### 4.6.1 Characterization of EPDM-g-PMMA and EPDM-g-PS graft copolymers by proton nuclear magnetic resonance spectroscopy ( $^1\text{H-NMR}$ )

$^1\text{H-NMR}$  analysis was used to identify the structure of the respective EPDM graft polymers. The crude products were always impure; they contained ungrafted rubber and homopolymer PMMA and PS respectively. PMMA and PS homopolymers could be generated by chain transfer reactions, either to a monomer or a solvent (THF in this case). These contaminants were removed before characterization. The EPDM-g-PMMA copolymer was isolated from the crude products by sequential extraction with selective solvents, as shown in Section 3.5, (hexane was used for EPDM removal and acetone for PMMA or PS removal). The insoluble fraction of crude product (graft copolymer) was soluble in THF and precipitated in 2-propanol, dried and characterized.



##### 4.6.1.1 EPDM-g-PMMA

Figure 4.17 illustrates examples of  $^1\text{H-NMR}$  spectra of EPDM (a) before hydroboration (b) after hydroboration, and (c) after polymerization in the presence of MMA to form EPDM-g-PMMA. Figure 4.17 (a) shows the chemical shift at 5.2 ppm corresponding to the olefinic ( $=\text{CH}$ ) units in the EPDM rubber starting material. All EPDM protons appear at chemical shifts ranging from 0.7 to 2.1 ppm, in addition to the chemical shift at 0.8 ppm, corresponding to  $\text{CH}_3$  in the propylene units.

Figure 4.17 (b) indicates the hydroboration of EPDM rubber and shows that, upon hydroboration the intensity disappears at 5.2 ppm.

Figure 4.17 (c) shows an example of the  $^1\text{H-NMR}$  spectrum of EPDM-g-PMMA after extraction; the typical spectrum shows a new peak appearing at 3.62 ppm corresponding to the methoxyl groups ( $\text{CH}_3\text{O}$ ) in PMMA. The peaks at 2.1-0.7 ppm

are due to the methyl and methylene protons in EPDM and PMMA respectively. In addition to the chemical shift of the CH<sub>3</sub> in propylene units at 0.8 ppm, the copolymer composition after extraction could quantitatively be determined from the ratios of the two integrated intensities at 3.62 ppm for the -CH<sub>3</sub>O- proton and 2.1-0.7 ppm for the methyl and methylene protons, by using equation 4.2. The <sup>1</sup>H-NMR spectra of the 35% grafted PMMA in EPDM-g-PMMA copolymers are shown in Figure 4.17 (c). The detailed experimental conditions and results are summarized in Table 4.9.

By varying the boron content in the hydroborated polymer, the monomer concentration and the amount of oxygen, the compositions and microstructures of the copolymers could be varied, as indicated in Table 4.9. Table 4.9 also shows the differences in the graft compositions when different reaction conditions were employed.

**Table 4.9: Different reaction conditions used during the ‘graft-from’ approach to prepare EPDM-g-PMMA**

#	Reaction conditions*			Fractionated products (g)			% grafted PMMA in the insoluble fraction calculated by <sup>1</sup> H-NMR
	9-BBN/Olefin	MMA (g)	O <sub>2</sub> / 9-BBN	Hexane soluble	Acetone soluble	Insoluble** fraction	
1	2/1	10	1/2	0.50	2.62	0.92	45
2	1/1	7.0	1/2	0.56	1.26	0.80	35

\*All “graft-from” reactions were performed using 1 g EPDM in 60 ml THF. The oxygen was slowly introduced into the reaction solution (10 mole% of oxygen ~ 2.5 ml per hour) at ambient temperature.

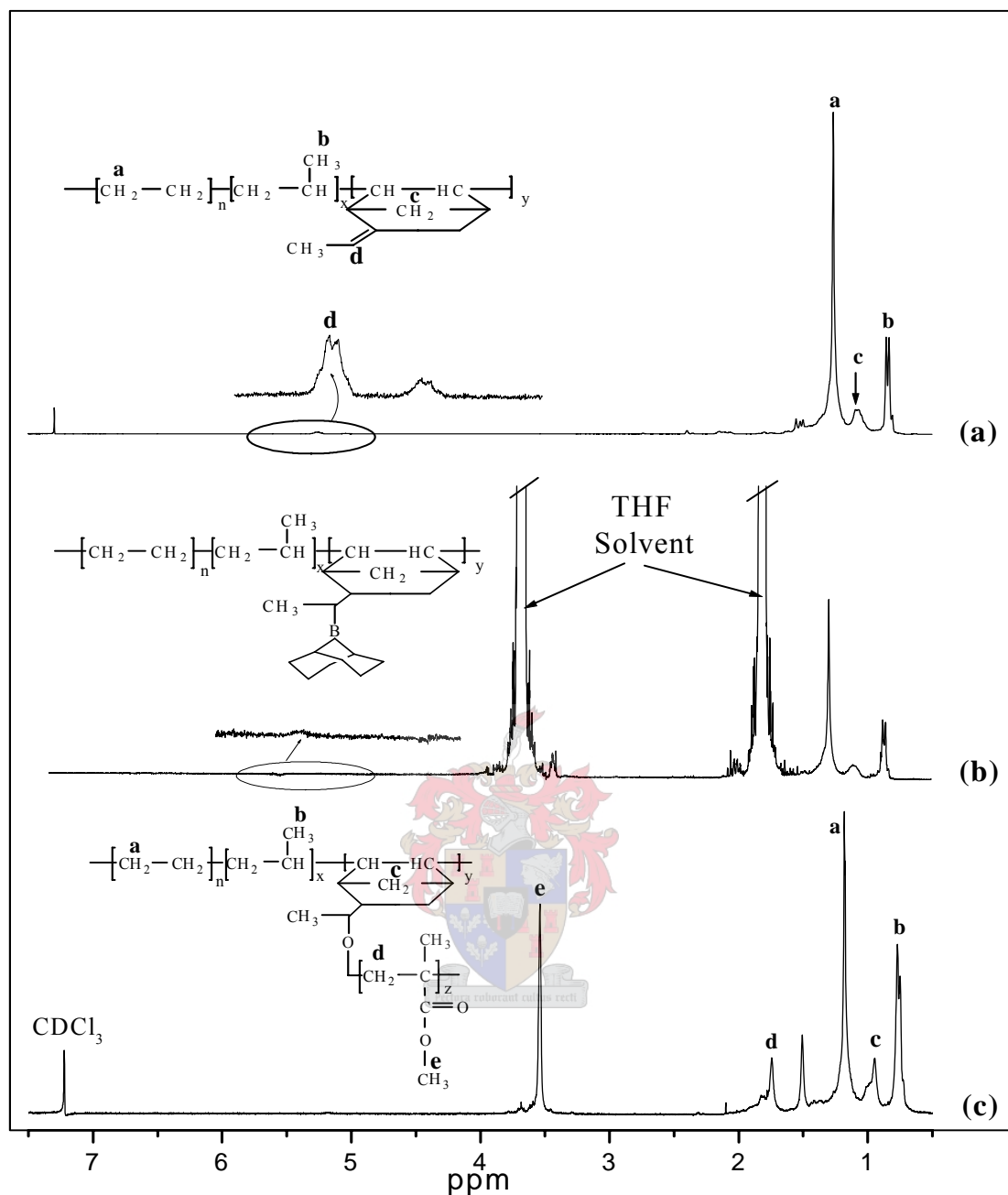
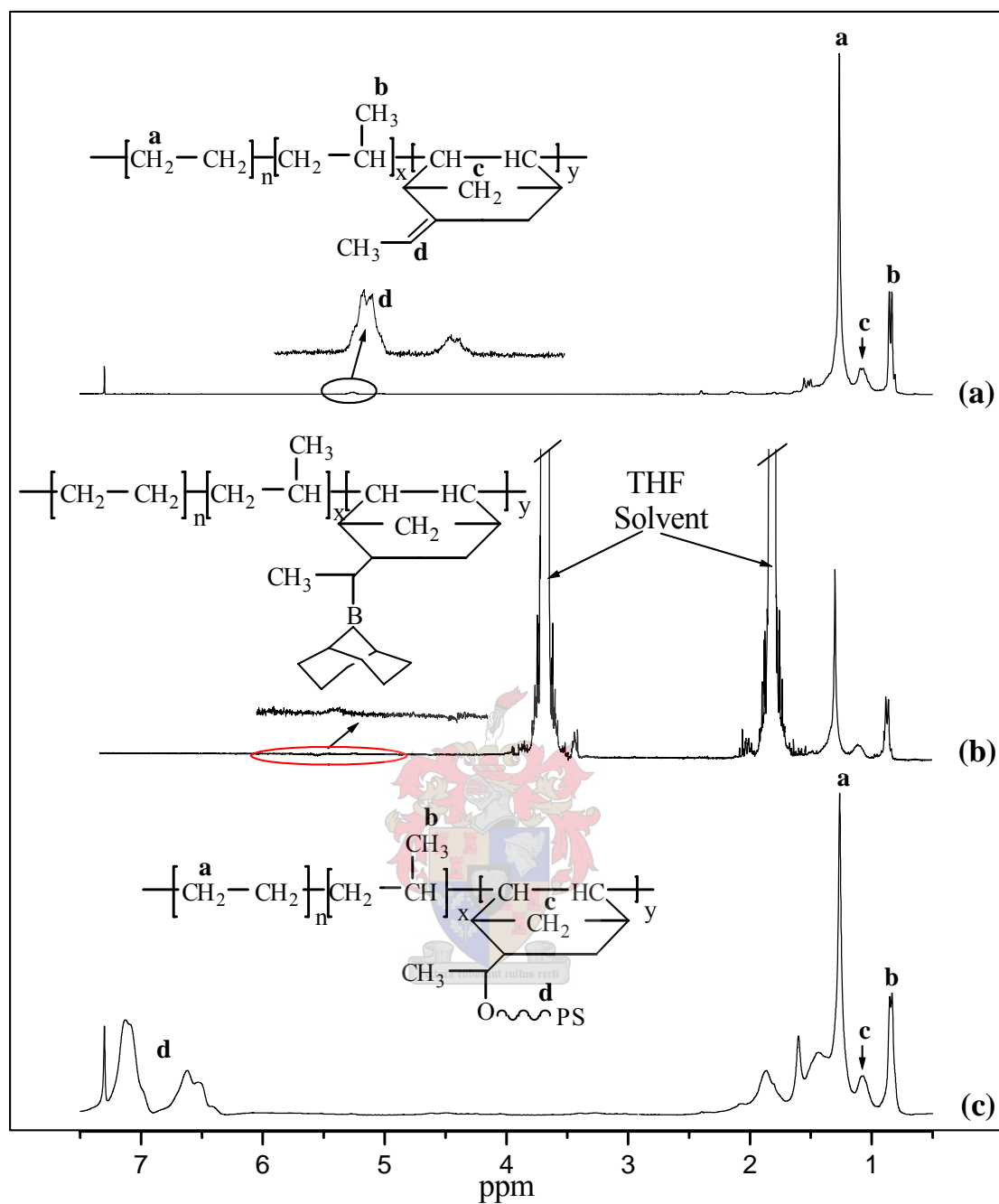


Figure 4.17:  $^1\text{H-NMR}$  spectra of EPDM (a) before hydroboration, (b) after hydroboration, and (c) EPDM-g-PMMA copolymer, in  $\text{CDCl}_3$  solvent.

#### 4.6.1.2 EPDM-g-PS

Figure 4.18 shows the  $^1\text{H-NMR}$  spectra of EPDM (a) before hydroboration, (b) after hydroboration, and (c) after polymerization in the presence of St to form EPDM-g-PS.



**Figure 4.18:**  $^1\text{H-NMR}$  spectra of EPDM (a) before hydroboration, (b) after hydroboration, and (c) EPDM-g-PS copolymer, in  $\text{CDCl}_3$  solvent.

Figure 4.18 (c) shows an example of the  $^1\text{H-NMR}$  spectrum of the EPDM-g-PS (run #2 in table 4.10) after extraction. The typical spectrum shows new peaks appearing at 6.5-7.2 ppm which can be ascribed to the aromatic structure of the polystyrene; the signals at 2.1-0.7 ppm are due to  $\text{CH}_3$  and  $\text{CH}_2$  protons in EPDM, in addition to the chemical shift at 0.8 ppm that corresponds to  $\text{CH}_3$  in the propylene units.

The copolymer composition after extraction was quantitatively determined from the ratios of the two integrated intensities, namely at 6.5-7.2 ppm 5 protons (peak d) and at 0.85 ppm 3 protons (peak b) in Figure 4.18 (c), by using equation 4.1. The results are illustrated in Table 4.10.

By varying the boron content in the polymer, the monomer concentration and the amount of oxygen, the compositions and microstructures of the copolymers could also be varied correspondingly. The results are summarized in Table 4.10. Table 4.10 also shows the difference of the graft compositions when different reaction conditions were used.

**Table 4.10: Different reaction conditions used during the ‘graft-from’ approach to prepare EPDM-g-PS, using hydroborated EPDM**

Run #	Reaction conditions*			Fraction products (g)			% grafted of PS in the insoluble fraction calculated by <sup>1</sup> H-NMR
	9-BBN/Olefin	MMA (g)	O <sub>2</sub> /9-BBN	Hexane soluble	Acetone soluble	Insoluble**	
1	2/1	10	1/2	0.51	2.60	0.69	36
2	1/1	7.0	1/2	0.58	1.28	0.63	33

\*All “graft-from” reactions were performed using 1 g EPDM in 60 ml THF. The oxygen was slowly introduced into the reaction solution (10 mole% of oxygen, ~ 2.5 ml per hour) at ambient temperature.

\*\*EPDM-g-PS

#### 4.6.2 Characterization of EPDM-g-PMMA and EPDM-g-PS graft copolymers by Fourier-transform infrared spectroscopy (FTIR)

Infrared spectroscopy was used to investigate the chemical compositions of the respective EPDM graft copolymers as well as extracted homopolymers EPDM, PMMA and PS.

Samples were analyzed in the form of KBr pellets of the grafted EPDM (after extraction) and films of the EPDM starting material. The FTIR spectrum of EPDM (Figure 4.19 (c)) was used as reference for the graft copolymerization.<sup>13</sup>

##### 4.6.2.1 EPDM-g-PMMA

Figure 4.19 compares the FTIR spectra of EPDM, PMMA, and EPDM-g-PMMA. A complete list of FTIR structure assignments is given in Table 4.11. In addition, the positions of all other groups have shifted to slightly higher wavelengths. The FTIR spectrum of EPDM-g-PMMA confirms that the PMMA was “grafted from” the

EPDM through the double bond during free-radical copolymerization. Overall, results obtained from FTIR analysis are in agreement with those obtained from  $^1\text{H-NMR}$ .

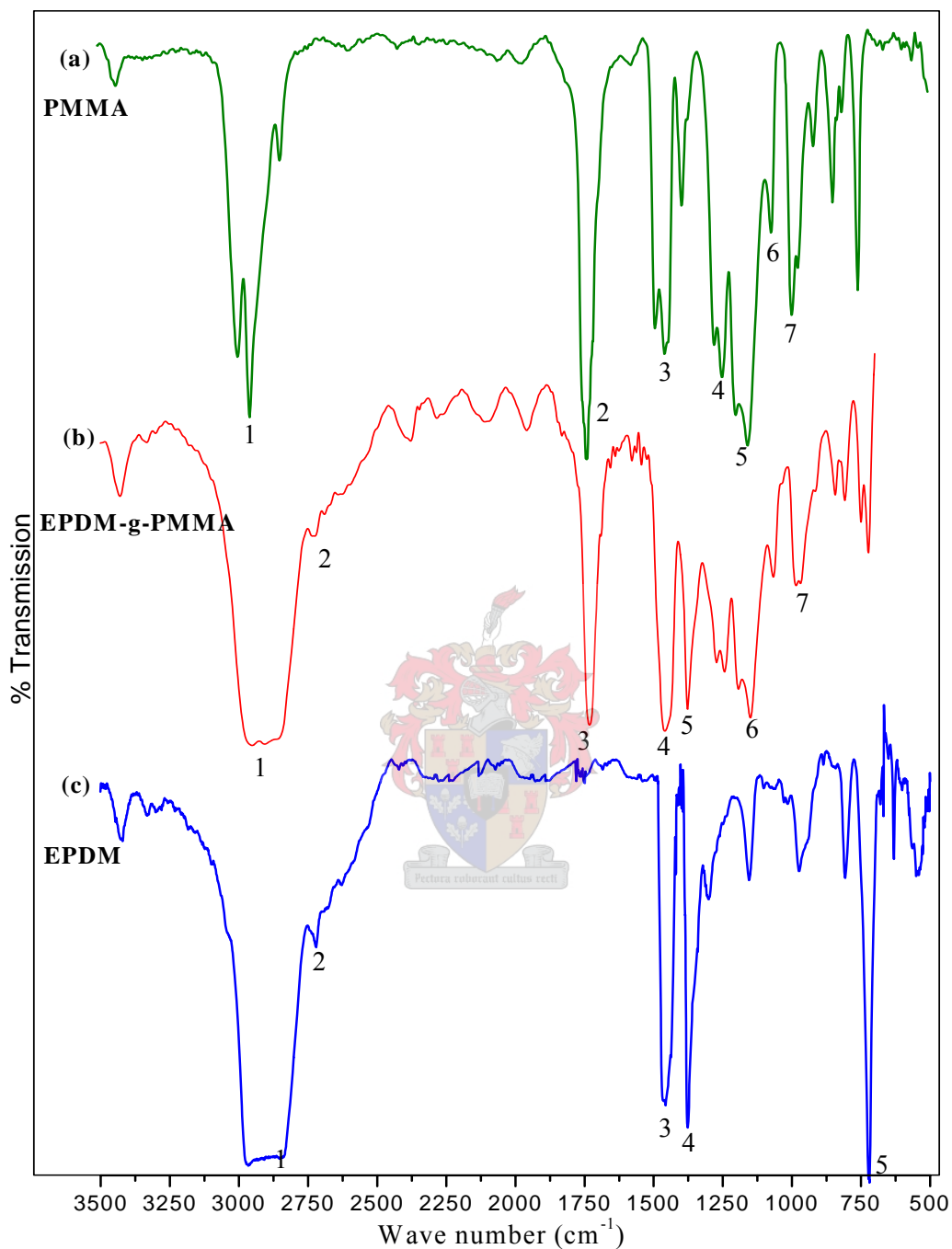


Figure 4.19: FTIR spectra of (a) PMMA, (b) EPDM-g-PMMA and (c) EPDM (peaks explained in Table 4.11).

**Table 4.11: Characteristic infrared peaks of EPDM, EPDM-g-PMMA and PMMA homopolymer**

peak number (see Fig. 4.19)	peak intensity	wave number ( $\text{cm}^{-1}$ )	absorption group	assignment
EPDM				
1 and 2	strong	2925, 2850	CH	stretching vibration
3	strong	1460	$\text{CH}_2$	angular deformation
4	medium	1377	$\text{CH}_3$	angular deformation
5	medium	727	$\text{CH}_2$	angular deformation
EPDM-g-PMMA				
1 and 2	strong	2950, 2850	CH	stretching vibration
3	strong	1734	C=O	stretching
4	medium	1460	$\text{CH}_2$	angular deformation
5	strong	1260	C-O (ester bond)	stretching vibration
6	strong	1000-1100	O-CH-C	stretching
7	strong	720	$\text{CH}_2$	angular deformation
PMMA				
1	strong	2958-2893	$\text{CH}_3$ and $\text{CH}_2$	symmetric stretching
2	strong	1730	C=O	stretching
3	medium	1466	CH	deformation
4	medium	1244	C-O	stretching
5	strong	1152	C-(C=O)-O	symmetric
6	medium	1066	O-CH-C	stretching
7	medium	942	$\text{CH}_2$	angular deformation

#### 4.6.2.2 EPDM-g-PS

The reference FTIR spectrum of PS, in Figure 4.20 (a), indicates the details of functional groups present in the synthesized PS. A sharp, intense peak at  $700 \text{ cm}^{-1}$  is assigned to the aromatic ring, the peaks at  $1492$  and  $1600 \text{ cm}^{-1}$  are assigned to the aromatic rings, the broad peak ranging from  $2925$ - $2850 \text{ cm}^{-1}$  is due to the presence of the stretching vibration of C-H in PS. Figure 4.20 (c) shows the FTIR spectrum of EPDM. A complete list of FTIR structure assignments is given in Table 4.10.

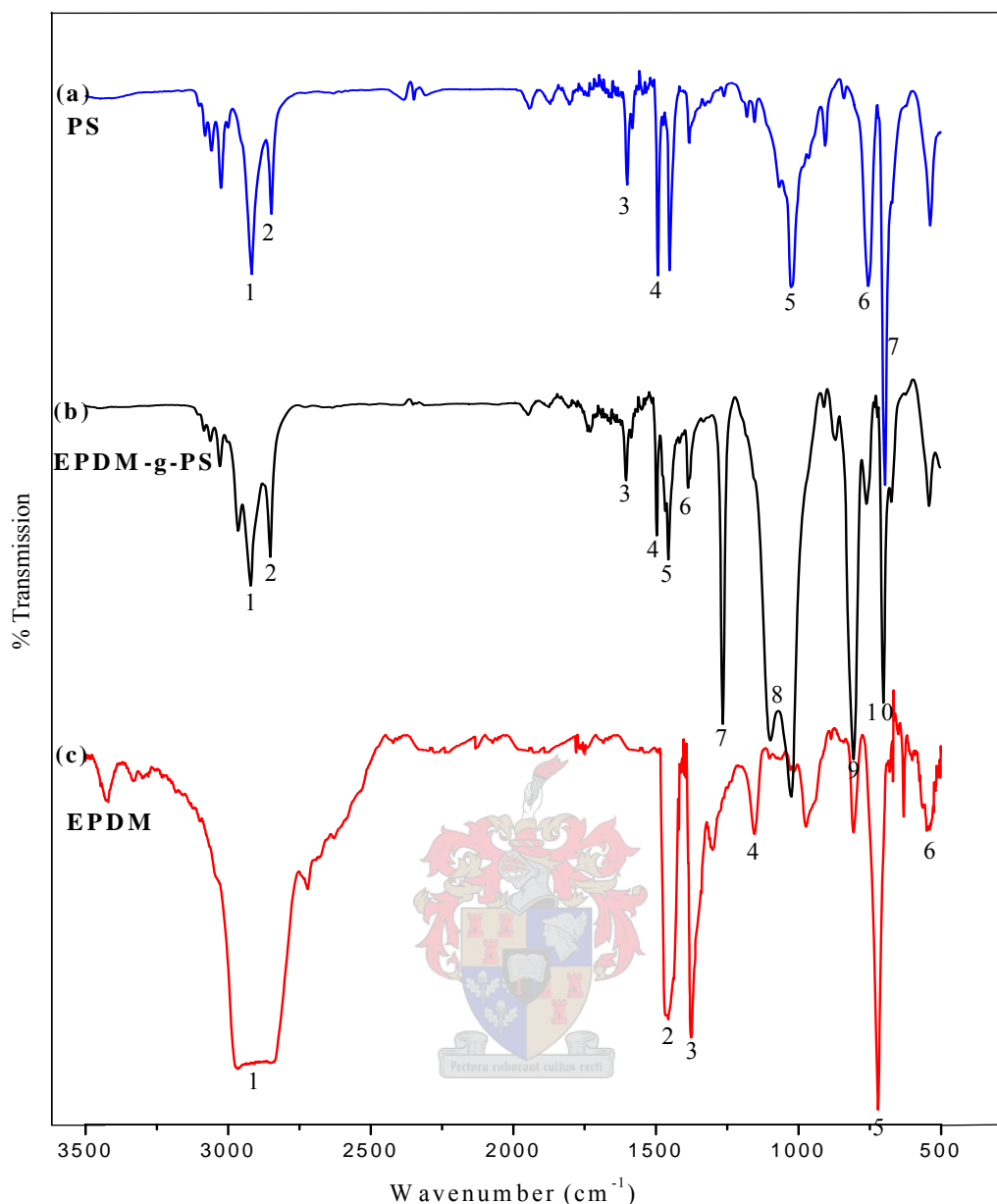


The FTIR spectra of an example of the EPDM-g-PS after extracting, EPDM, and PS are illustrated in Figure 4.20, and a complete list of EPDM-g-PS, EPDM, and PS structure assignments is given in Table 4.12.<sup>14,15</sup>

Indications are that a change in chemical structure of the EPDM occurred during the grafting reaction. The FTIR spectrum of EPDM-g-PS confirms that the PS was “grafted from” the EPDM through the double bond during free-radical copolymerization. Overall results obtained from FTIR analysis are in agreement with those obtained from <sup>1</sup>H-NMR.

**Table 4.12: Characteristic infrared peaks of EPDM, EPDM-g-PMMA and PMMA homopolymer**

peak number (see Fig 4.20)	peak intensity	wave number (cm-1)	absorption group	assignment
EPDM				
1 and 2	strong	2925, 2850	CH	stretching vibration
3	medium	1453	CH <sub>2</sub>	angular deformation
4	medium	1377	CH <sub>3</sub>	angular deformation
5	strong	727	CH <sub>2</sub>	angular deformation
EPDM-g-PS				
1 and 2	strong	2950, 2850	CH	stretching vibration
3	medium	1600	ring	stretching
4	medium	1493	ring	stretching
5	medium	1450	CH <sub>2</sub>	angular deformation
6	medium	1384	CH <sub>3</sub>	angular deformation
7	strong	1265	CH	stretching vibration
8	strong	1000-1100	O-CH-C	stretching
9	strong	790	CH (5 adjacent)	deformation
10	strong	720	ring	deformation
PS				
1 and 2	medium	3025-2923	CH	stretching vibration
3	strong	1600	ring	stretching
4	strong	1492	ring	stretching
5	weak	1030-1024	CH	stretching vibration
6	strong	770-730	CH (5 adjacent)	deformation
7	strong	710-690	ring	deformation



**Figure 4.20:** FTIR spectra of (a) PMMA, (b) EPDM-g-PMMA after extraction, and (c) EPDM starting material (peak assignments given in Table 4.12).

#### 4.6.3 Characterization of EPDM-g-PMMA and EPDM-g-PS graft copolymers by size-exclusion chromatography (SEC)

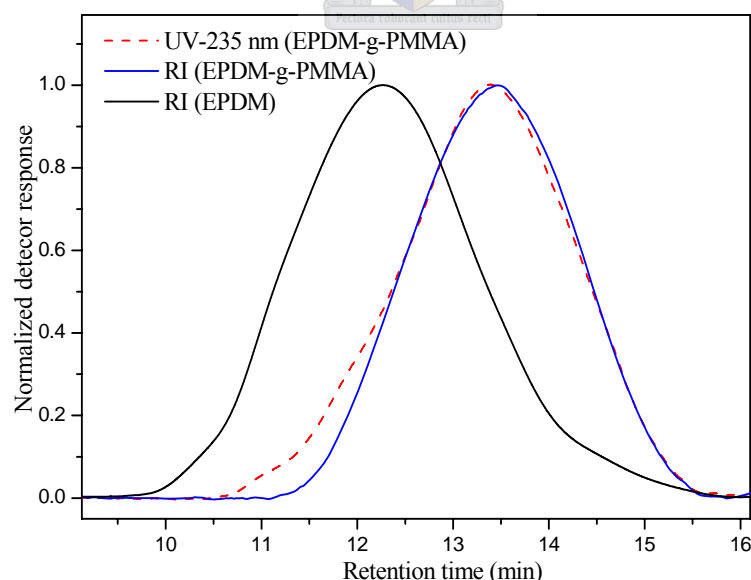
The respective graft copolymers as well as the extracted homopolymers EPDM, PMMA and PS were characterized by SEC, and molar masses were determined using a dual detector (UV and RI) setup. The UV detector was used to analyse the graft copolymers at  $\lambda=254$  nm for EPDM-g-PS, PS absorbs UV light at 254 nm, and  $\lambda=235$  nm for EPDM-g-PMMA, only PMMA absorbs UV light at 235 nm, with no response from EPDM at 254 and 235 nm.

The molar masses values of graft copolymers (branch polymers), which are obtained by SEC measurements, are generally lower than they should be because linear polymers have a much larger hydrodynamic volume than the corresponding branched polymers (graft copolymer) of the same molar mass. Obviously, the SEC measurements obtained by simply comparing elution volumes (or times) between branched and linear structures alone cannot offer an accurate molar mass result for the graft polymer. There are three different main reasons for the increase of the molecular mass (refer to Section 4.4.4 where the reasons were first discussed).

#### 4.6.3.1 EPDM-g-PMMA

Figure 4.21 shows an example of the SEC results of the EPDM-g-PMMA graft copolymer after extraction. The maximum graft copolymer peak was shifted towards a high retention time compared to the maximum peak of EPDM starting material, SEC results also show the molar mass distribution in the graft copolymer.

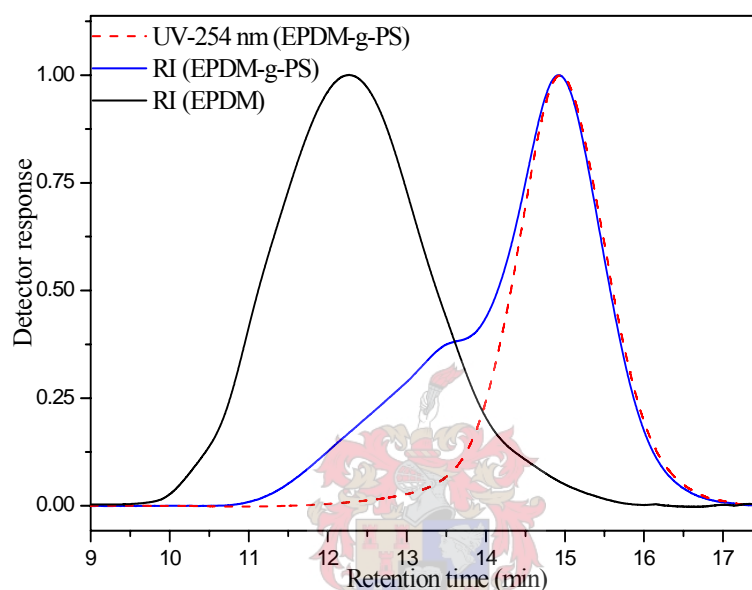
Figure 4.21 compares the RI and UV ( $\lambda = 235$  nm) detector curves. The high retention time peak in the UV curve matches well with the corresponding RI peak of the graft copolymer, which indicates a homogeneous distribution of PMMA in the graft copolymer. The low-retention time of the graft copolymer the high UV response indicates a high concentration of PMMA (in the high molar mass fraction).



**Figure 4.21: Comparison of the normalized RI signal of EPDM with the normalized RI and UV signals of the EPDM-g-PMMA copolymer.**

#### 4.6.3.2 EPDM-g-PS

Figure 4.22 shows an example of the SEC results of the EPDM-g-PS graft copolymer after extraction and compares the RI and UV ( $\lambda = 254$  nm) detector curves. At the wavelength of 254 nm, only PS absorbs UV light with no response from EPDM. The high retention time peak in the UV curve matches well with the corresponding RI peak of the graft copolymer, which indicates a homogeneous distribution of PS in the graft copolymer.



**Figure 4.22:** Comparison of the normalized RI signal of EPDM with the normalized RI and UV signals of the EPDM-g-PS copolymers after extraction.

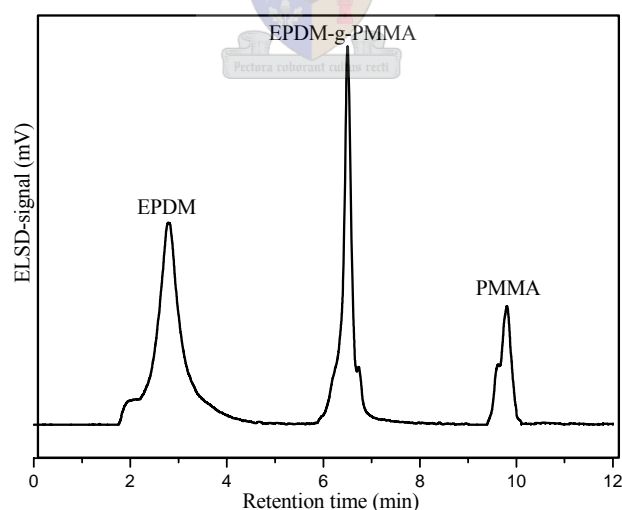
However, the low retention time peak with only very low UV response indicates quite low concentration of PS in the low retention time fraction. This indicates that some EPDM chains did not undergo grafting. HPLC was therefore used for further investigation.

#### 4.6.4 Characterization of EPDM-g-PMMA and EPDM-g-PS graft copolymers by high-performance liquid chromatography (HPLC)

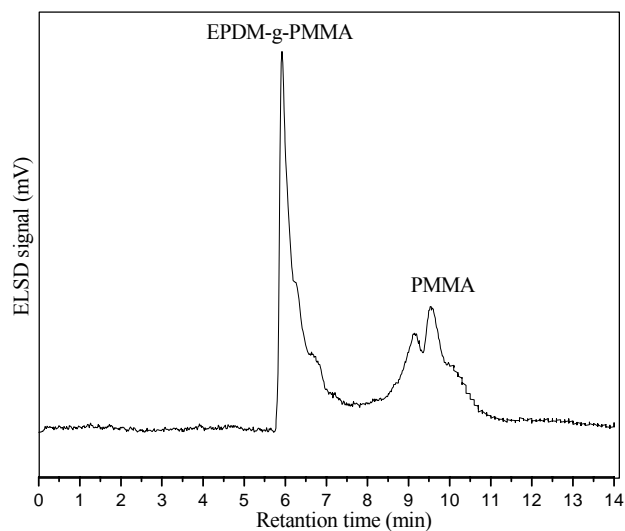
The grafting reaction of methyl methacrylate from EPDM was investigated by different chromatographic techniques, including HPLC. When EPDM is grafted with methyl methacrylate, the soluble fraction of the reaction product contains residual ungrafted EPDM, the graft copolymer EPDM-g-PMMA, or graft copolymer EPDM-g-PS and homopolymer PMMA or PS.

#### 4.6.4.1 Separation of EPDM-g-PMMA graft copolymer with HPLC

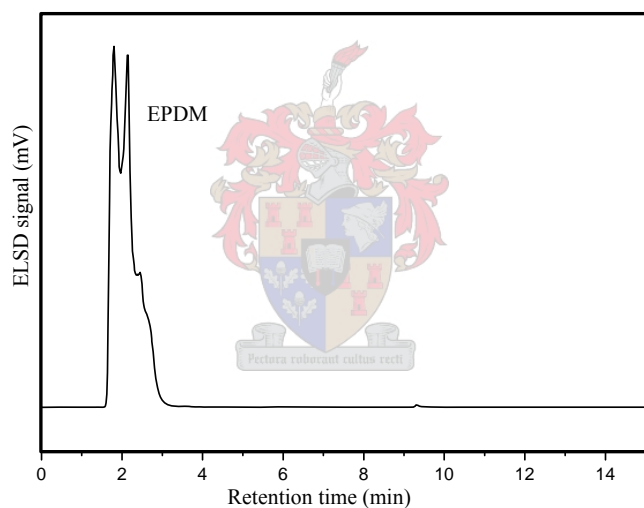
The resulting HPLC chromatogram of an example of the EPDM-g-PMMA graft copolymer before extractions is illustrated in Figure 4.23. The result shows that a very good separation into three fractions was obtained for all product samples. The assignment of the peaks was carried out by comparison the chromatographic behaviour of EPDM and PMMA using a reversed phase column (Nucleosil CN 100 Å). Separation is a function of component polarity. The polarity of EPDM is not as great as that of PMMA.<sup>16</sup> The less polar component consequently elutes first, followed by the graft copolymer EPDM-g-PMMA and the more polar PMMA homopolymer. The three elution peaks visible can be assigned to the sample constituents EPDM, PMMA and EPDM-g-PMMA. Based on the comparison with the starting material, the first peak can be EPDM. Accordingly, it is eluted quickly and leaves the column first. The second peak is significantly retained, indicating that it contains polar MMA units. Based on comparison with reference samples (model compound) of EPDM (Figure 4.25) and PMMA (Figure 4.26) homopolymers run under the same condition, and the third peak can be assigned to PMMA homopolymer. As was expected, it is retained most strongly on the stationary phase. Figure 4.24 shows the extracted product (EPDM-g-PMMA graft copolymer).



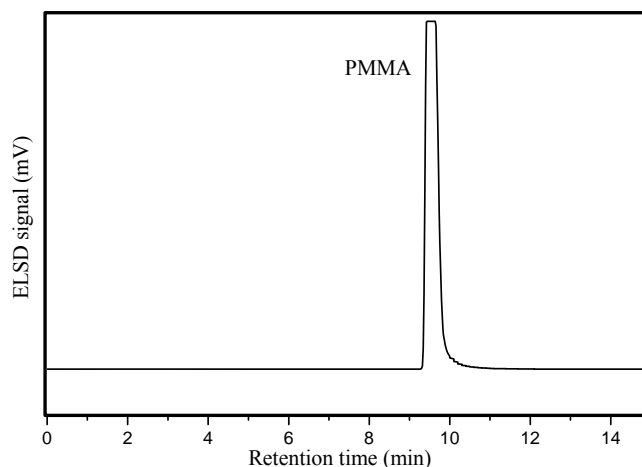
**Figure 4.23: Gradient HPLC chromatogram of the graft product and starting materials. (Stationary phase: Nucleosil CN 100Å; eluent: THF/i-octane; detector: ELSD).**



**Figure 4.24: Gradient HPLC chromatogram of the extracted graft product. (Stationary phase: Nucleosil CN 100Å; eluent: THF/i-octane; detector: ELSD).**



**Figure 4.25: EPDM starting materials analyzed by gradient HPLC. (Stationary phase: Nucleosil CN 100Å; eluent: THF/i-octane; detector: ELSD).**



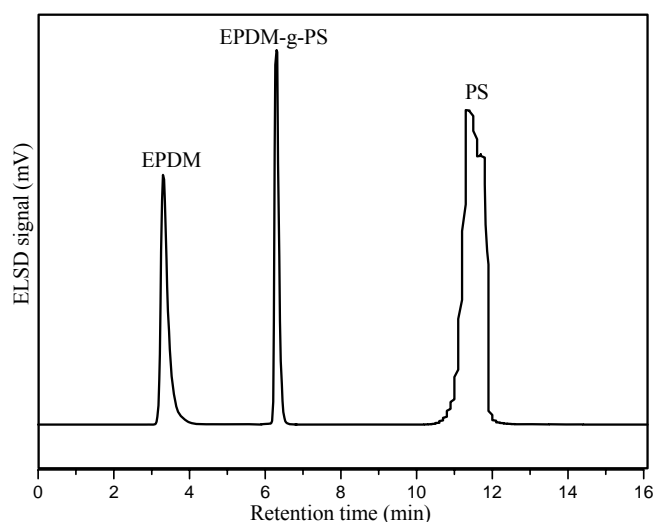
**Figure 4.26: PMMA standards analyzed by gradient HPLC. (Stationary phase: Nucleosil CN 100Å; eluent: THF/i-octane; detector: ELSD).**

Overall, the results obtained from HPLC analyses are in agreement with those presented in Table 4.9.

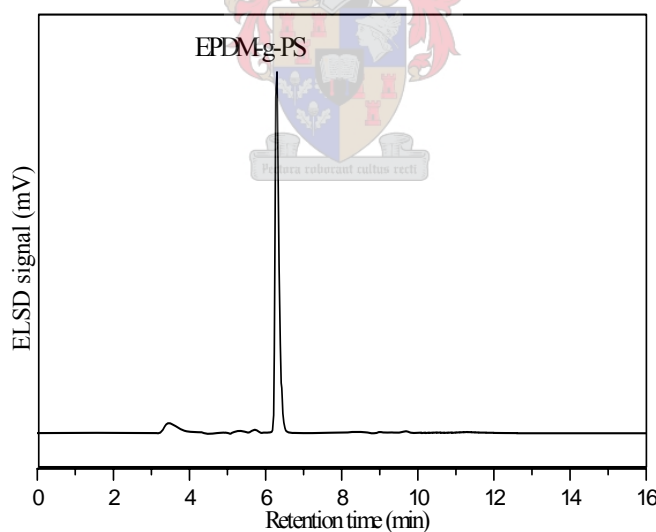
#### 4.6.4.2 Separation of EPDM-g-PS graft copolymer with HPLC

The resulting HPLC chromatograph of an example of the EPDM-g-PS graft copolymer before extraction is illustrated in Figure 4.27, showing a very good separation into three fractions for all product samples. The assignment of the peaks was carried out by comparison with the chromatographic behaviour of EPDM and PS, when using a reversed phase column (Nucleosil C<sub>18</sub> 300+500 Å), which is a function of component polarity. The polarity of EPDM and PS is low; the less polar component consequently eluted first, followed by the graft copolymer EPDM-g-PS and then PS homopolymer. There are three elution peaks visible that can be assigned to the sample constituents EPDM, PS and EPDM-g-PS. Based on the assumption of the elution order and comparison with the starting material, the first peak can be EPDM. Accordingly, it is eluted quickly and leaves the column first. The second peak is significantly retained, indicating that it contains EPDM and PS units (EPDM-g-PS graft copolymer). Based on comparison with reference samples (model compound) of EPDM and PS which was run under the same conditions, the third peak can be assigned to PS homopolymer. Figure 4.28 shows the extracted product (EPDM-g-PS graft copolymer)

The results obtained from HPLC analyse are in agreement with those presented in Table 4.10.



**Figure 4.27: Gradient HPLC chromatogram of the EPDM-g-PS graft product. (Stationary phase: Nucleosil C<sub>18</sub> 300+500 Å; eluent: THF/i-octane; detectors: ELSD The gradient was started at 99:1 (v/v) (THF:i-octane), held constant for 1 min, changed linearly to 34:66 (THF:i-octane) within 5 mins, held constant for 10 mins, and changed linearly to 100:0 (THF:i-octane) within 2 mins).**



**Figure 4.28: Gradient HPLC chromatogram of the extracted EPDM-g-PS graft product. (Stationary phase: Nucleosil C<sub>18</sub> 300+500 Å; eluent: THF/i-octane; detector: ELSD).**

The small peak observed at a retention time of about 3.1 min, shows that a small amount of EPDM homopolymer still remains after extraction.



#### 4.7 References

1. Chung, T. C.; Janvikul, W.; Bernard, R.; Hu, R.; Li, C. L.; Liu, S. L.; Jiang, G. J. *Polymer* **1995**, 36, 3565.
2. Pasch, H.; Trathnigg, B. *HPLC of Polymers*. Berlin: Springer, **1999**.
3. Mikhailov, B.; Bubnov, Y., *Organoboron Compounds in Organic Synthesis*. Harwood Academic Science: New York, **1984**.
4. Chung, T. C.; Janvikul, W.; Bernard, R.; Jiang, G. J. *Macromolecules* **1994**, 27, 26.
5. Dzunuzovic, E. *Prog. Org. Coat.* **2005**, 52, 136.
6. Wan, Q.; Schrickler, S. R.; Culbertson, B. M. *J. M. S.-Pure Appl. Chem.* **2000**, 37, 1301.
7. Degoulet, C.; Perrinaud, R.; Ajdari, A.; Prost, J.; Benoit, H.; Bourrel, M. *Macromolecules* **2001**, 34, 2667.
8. Pinazzi, C.; Brosse, J.; Pleureaux, A. *Appl. Polym. Symp.* **1975**, 26, 73.
9. Flory, P. J.; Rehner, J. *J. Chem. Phys.* **1943**, 11, 512.
10. Kraus, G. *Rubber Chem. Technol.* **1957**, 30, 928.
11. Mark, H. F.; M. Bikales, N.; G. Overberger, C.; Menges, G., Wiley & Sons : New York, 1986; Vol. 6, 522.
12. Augenstein, M.; Stickler, M. *Makromol. Chem.* **1990**, 191, 415.
13. Lin-Vien, D.; Colthup, N. B.; Fateley, W. G.; Grasselli, J. G., *Handbook of Infrared and Raman Characteristics of Organic Molecules*. New York, 1991.
14. Sheng, J.; Hu, J. *J. Appl. Polym. Sci.* **1996**, 60, 1499.
15. Ptiček, A.; Hrnjak-Murgić, Z.; Jelenčić, J.; Kovačić, T. *Polym. Degrad. Stab.* **2005**, 90, 319.
16. Siewing, A.; Schierholz, J.; Braun, D.; Hellmann, G.; Pasch, H. *Macromol. Chem. Phys.* **2001**, 202 (14), 2890.

## Chapter 5

### Conclusions and recommendations

#### 5.1 Conclusions

The synthesis of a model compound 2-hexene-9-BBN was successfully carried out, as confirmed by  $^1\text{H-NMR}$  spectroscopy.

The determination of the conditions for the hydroboration reaction using the above model compound was successfully carried out. The best results for a heterogeneous reaction of an autoxidation system are realized when the  $\text{O}_2$  is introduced slowly (the ratio of oxygen should be less than 10%, added hourly) so that at any time  $\text{O} \ll \text{B}$ , even though the final stoichiometry of oxygen to boron is found to be 0.5:1. Subsequently, the model compound was used as a macroinitiator and facilitated initiation and polymerization of MMA. Finally, the produced PMMA- 2-hexenyl was characterized by  $^1\text{H-NMR}$

The same borane chemistry was extended to the synthesis of polystyrene block copolymers. The chain-end unsaturated PS (macromonomers) synthesized by anionic polymerization was effectively hydroborated and then polymerized to produce PS-b-PMMA block copolymers.  $\text{O}_2$  was used as initiator. The molecular structures of the PS macromonomers were confirmed by  $^1\text{H-NMR}$  and SEC. In addition, the PS-b-PMMA block copolymers were fully characterized by means of SEC,  $^1\text{H-NMR}$  and FTIR. Complete separation of all components was achieved by HPLC at the critical point of polystyrene as well as at the critical point of the PMMA. The quantitative evaluation of the PS-b-PMMA block was successfully carried out by  $^1\text{H-NMR}$ .

The synthesis of polyolefin graft copolymers was achieved by the hydroboration reaction. Several commercial rubbers with different levels of unsaturated segments were efficiently grafted with the vinyl monomers MMA and St, by means of this method. The grafting reactions were carried out under various reaction conditions to determine the effect of the following factors: concentration of oxygen, amounts of boranes and monomer concentration. By controlling these factors, different graft

densities were achieved with high graft efficiencies. All reactions produced mixed products including unreacted (non-functional) macroinitiator, homopolymer, and graft copolymer.

The poly(isobutylene-co-isoprene) with 1.6 mol% of double bonds graft PMMA was synthesized. This graft reaction was difficult due to the relatively small number of monomer molecules incorporated into the rubber. This is due to the small number of double bonds present in the polymer backbone. To increase the number of incorporated monomer molecules into the rubber, highly unsaturated polyisoprene (98% cis 1,4 content) was used instead of polyisobutylene. The polyisoprene graft PMMA was synthesized but formed the predominately cross-linked product with a PMMA. This cross-linking is due to the abundance of double bonds that is present in the polyisoprene backbone.

To overcome these problems (i.e. small numbers of incorporated monomer molecules into the rubber in the case of polyisobutylene, and cross-linking in the case of polyisoprene), standard grade ethylene-propylene-5-ethylidene-2-norbornene rubber (EPDM) with 9.2 mol% of double bonds was used as intermediate unsaturated polymer. The EPDM grafts of PMMA and PS were successfully synthesized.

The polyolefin graft copolymers were fully characterized by various chromatographic techniques. The molar mass of polyolefin copolymers were measured using SEC calibrated with linear polystyrene standards. <sup>1</sup>H-NMR and FTIR were used to confirm the structures of these copolymers. Gradient HPLC profiles were developed to fully characterize the graft products by performing gradient HPLC. It was found that through correct solvent composition selection it is possible to separate homopolymers from the grafted products. This was done by using different columns, and changing the injection volumes of the grafted material and gradient profiles of the applied gradient.

The effects of the oxygen and monomer concentration on the grafting reaction were determined. It was found that an excess of O<sub>2</sub> is not only a poison for free-radical polymerizations but also leads to overoxidation of boranes to boronates and borates, both of which are poor free-radical initiators for polymerization at room temperature. It was also found that an increase in the mass of 9-BBN used during the hydroboration reaction led to a decrease in the ungrafted starting materials, with an increase in the

amounts of homopolymers. The higher initial monomer concentration resulted in higher grafted monomer content in the copolymers. This could be due to an increase in the grafted polymer (PMMA, PS) molecular mass in the side chains.

The results of the grafting efficiency evaluation were successfully determined by  $^1\text{H-NMR}$ , and showed that grafting efficiency varied with different reaction conditions.

## **5.2 Recommendations**

Although the chemistry of hydroboration has been known for more than a decade, little has been done in the last few years to escalate the value of this particular chemistry in the field of polymers. Despite the fact that hydroboration is not the easiest synthetic method to cope with, its use to function as a chain extender and macroinitiator is still extremely interesting and important to investigate. Some observations were made during this study, which ultimately lead to recommendations for additional studies. The author can mention at this stage that at least one recommendation has already been investigated to evaluate the feasibility of these claims, and can duly report that further actions are planned to continue work in this field.

Recommendations are:

- Investigate the possibilities of using PDMS as rubber alternative in the hydroboration studies.
- Investigate the possibility of using RAFT agents in the hydroboration method.

